research report

Design of Bearing Stiffeners in Cold Formed Steel C-Sections

RESEARCH REPORT RP01-1

JULY 2001
REVISION 2006

Committee on Specifications
for the Design of Cold-Formed
Steel Structural Members

American Iron and Steel Institute

The material contained herein has been developed by researchers based on their research findings. The material has also been reviewed by the American Iron and Steel Institute Committee on Specifications for the Design of Cold-Formed Steel Structural Members. The Committee acknowledges and is grateful for the contributions of such researchers.

The material herein is for general information only. The information in it should not be used without first securing competent advice with respect to its suitability for any given application. The publication of the information is not intended as a representation or warranty on the part of the American Iron and Steel Institute, or of any other person named herein, that the information is suitable for any general or particular use or of freedom from infringement of any patent or patents. Anyone making use of the information assumes all liability arising from such use.

Design of Bearing Stiffeners in Cold Formed Steel C-Sections

by

Steven R. Fox
Research Assistant

Prof. Reinhold M. Schuster
Project Director

SUMMARY

This research project was initiated by the *American Iron and Steel Institute* to investigating the capacity of bearing stiffeners used in cold formed steel joists. These joists are often C-sections, and depending on the sheet thickness, can be susceptible to web crippling when subjected to concentrated loads. Bearing stiffeners are normally added to avoid the capacity reductions associated with this type of failure. Cold formed steel structural members are becoming more widely used in residential and light commercial construction. Consequently, there is an increased interest from industry in developing appropriate and economical design rules. The current design provisions for transverse stiffeners in the AISI *Specification for the Design of Cold-Formed Steel Structural Members* [1] and the CSA-S136 Standard *Cold Formed Steel Structural Members* [2] do not apply to the common types of bearing stiffeners being used today in lightweight steel framing. Consequently, research was needed to develop design rules for these stiffener types.

Presented in this report are the results of the experimental and analytical investigations into the behavior of cold formed steel bearing stiffeners, as well as proposed design provisions.

The AISI and CSA design documents require a bearing stiffener when h/t of the web of a flexural member exceeds 200, and design provisions are provided. However, there are some practical problems with the current requirements. The most significant issue is the stipulation that the flat width of any element in the bearing stiffener shall not exceed the limit for local buckling. This means that no element in the stiffener can be subject to effective width reductions up to the design stress level. This condition is not met by any of the bearing stiffeners in common use today. A stud or track section as a bearing stiffener will be subject to effective width reductions at modest stress levels and fall outside the provisions of the specification.

A total of 263 end and interior two-flange-loading tests were carried out on different stiffened C-section assemblies. The following conclusions have been reached:

(a) The current design provisions in the AISI and CSA specifications can be unconservative if applied to the types of bearing stiffeners commonly used in lightweight steel framing.

(b) For the stud and track stiffener types, the failure mode is local buckling of the stiffener acting as a short beam-column member. Overall column buckling can be a failure mode for deeper joists with stiffeners made from smaller sections such as bridging channels.

(c) The capacity of the assembly is influenced by the following parameters:
   - stiffener type and material properties
   - bearing width

- joist size and material properties
- number and pattern of fasteners connecting the stiffener to the joist
- location of the stiffener on the joist (i.e. end or intermediate, inside or outside)
- gap between the stiffener and the joist flanges

(d) The capacity of the stiffened joist assembly is a combination of the web crippling capacity of the joist plus the axial capacity of the stiffener, times a reduction factor.

(e) The web crippling capacity of the joist is influenced by the presence of the bearing stiffener and the connection of the stiffener to the joist web. Web crippling of the joist should be considered as the serviceability limit sate for the assembly.

(f) The design of the stiffener must take into account the eccentric axial loads and lateral loads transferred from the fasteners.

(g) This project has only considered the stiffener and joist assembly. No recognition was made of the other components also commonly present in a floor (e.g. rim joist, sub-floor) that add to the strength of the assembly.

(h) A simplified design approach is proposed for those stiffeners not subject to column-type buckling.

TABLE OF CONTENTS

LIST OF FIGURES

LIST OF TABLES

1   BACKGROUND

1.1   GROWING APPLICATIONS OF COLD FORMED STEEL IN RESIDENTIAL CONSTRUCTION

Cold formed steel has been used for the manufacture of structural sections for many years. Historically, the majority of these applications have been in the commercial and industrial types of buildings. Typical examples would include secondary structural members such as purlins and girts, roof and floor deck, as well as exterior wall and roof cladding. The commercial/industrial construction industry is familiar with steel products and there are many experienced designers.

In recent years, the low-rise residential construction market has been faced with a decreasing supply of quality lumber at an increasing cost. Consequently, home builders have started to look for alternative building materials, and cold formed steel is a natural option. Cold formed steel offers the home builder the advantages of a quality construction material at stable prices. Cold formed steel sections used for residential construction are made from relatively thin sheet steel material, 0.8 to 2.0 mm (0.03 to 0.10 in.) and are commonly referred to as "lightweight steel framing" or "LSF". LSF members are sized much the same as dimensional wood framing members, making it easy for the architects and builders to incorporate steel into existing house designs. An example of typical LSF residential platform construction is shown in the photograph in Figure 1.1.1 and the details are illustrated in Figure 1.1.2.

Figure 1.1.1: Photograph Showing LSF Residential Construction
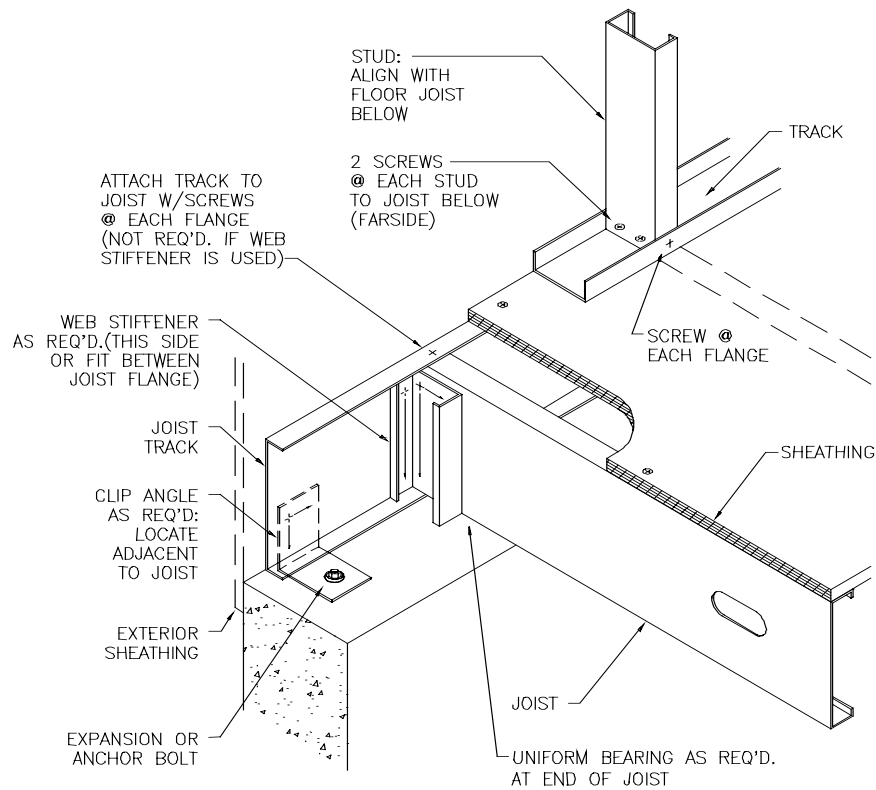
Figure 1.1.2: LSF Platform Construction Details

There is a tremendous business opportunity in residential construction that the North American steel industry is trying to capitalize upon. This expanded interest in utilizing LSF has raised a number of questions with engineers about the proper design procedures for these types of structures. One specific area of interest concerns the design of bearing stiffeners for LSF floor joists.

LSF floor joists are typically C-sections ranging in depth from 150 to 356 mm (6 to 14 in.). The thin sheet steel makes these sections prone to web buckling (or web crippling) under fairly low concentrated loads. Such concentrated loads occur at every support or every location where a floor joist supports a loadbearing wall above. To avoid the capacity reductions that the web crippling limit state would impose, bearing stiffeners (or web stiffeners) are attached to the joist to transfer these loads.

Typically, bearing stiffeners for LSF sections are made from short lengths of 89 mm (3-5/8 in.) wide stud or track sections. These stiffeners are either attached to the back of the joist web or cut to fit between the flanges of the joist, as shown in Figure 1.1.3. Connections are made between the stiffener and the joist with self-drilling screws.

2
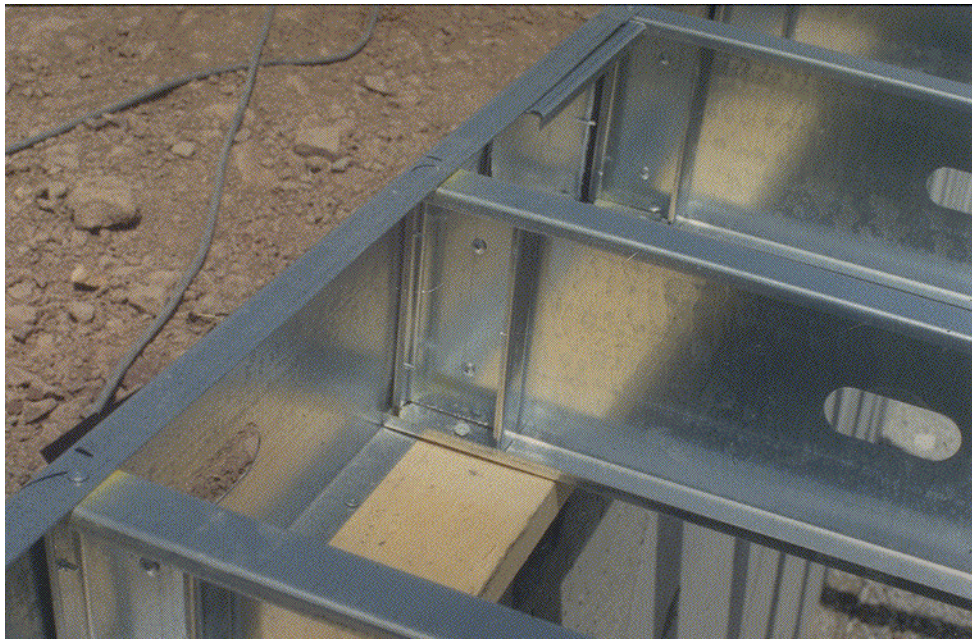
Figure 1.1.3: Photograph of Bearing Stiffeners

1.2 RESEARCH OBJECTIVE AND SCOPE

The objective of this work was to understand the behavior of cold formed steel C-sections with bearing stiffeners, and to develop design expressions for the end and interior two-flange loading of assemblies typically used in LSF construction. The resulting design expressions will be submitted to the AISI and CSA specification committees for consideration as new specification provisions. This objective has been met through a combination of experiment, finite element analysis and analytical work.

The experimental work has included a total of 263 tests of stiffened C-section joist assemblies subjected to end and interior two-flange loading. These tests have provided data on the following parameters:

- Joist depths up to 356 mm (14 in.) and web slenderness up to 300
- Stiffener type (stud, track, bridging channel)
- Location of the stiffener on the joist (between the flanges or on the back of the joist web)
- Position of the stiffener along the joist length (at the joist end or an intermediate position)
- Fastener pattern connecting the stiffener to the joist web
- Amount of gap between the end of the stiffener and the joist flanges
- Bearing width
- Web crippling capacity of the joist as a serviceability limit state

In addition to these assembly tests, additional tests were carried out to investigate the following parameters:

- Strain gauge measurements of the stiffener during the loading cycle

3

- Strain gauge and deflection measurements of the joist web during the loading cycle
- Measurements of the forces in the fasteners connecting the stiffener to the joist web

These measurements were used to develop the analytical model of the stiffened assembly and to calibrate a finite element model. The FE modeling was used to determine the forces in the fasteners for various fastener configurations as well as determine the web crippling capacity of the joist.

2   EARLIER WORK

2.1   NGUYEN & YU, 1978

2.1.1   Background

In 1973, a research project at the University of Missouri-Rolla was sponsored by the American Iron and Steel Institute titled "Webs for Cold-Formed Steel Flexural Members". The purpose of this multi-phase project was to study the structural behavior of unreinforced and reinforced beam webs subjected to bending stress, shear stress, web crippling load and combinations thereof. At the time, neither the AISI Specification [1] nor CSA-S136 Standard [2] included any specific design provisions for reinforced webs. The results of this work are included in the following references: LaBoube & Yu [3, 4, 5], Hetrakul & Yu [6] and Nguyen & Yu [7,8]. The work by Nguyen & Yu [7] was the first to study transversely stiffened cold formed steel sections. This work will be described in more detail since it forms the basis of the current specification design provisions.

The objectives of the test program of Nguyen & Yu was to study the structural behavior of reinforced beam webs subjected to bending stress, shear stress, web crippling load and combinations thereof. This was important at the time since the governing AISI Specification did not include any specific design provisions for reinforced beam webs. Reinforced webs were necessary to extend the applicability of the specification beyond the h/t limit of 200. The investigation was directed toward the study of the load carrying capacity of transverse stiffeners located within the spans, or at the ends of the beam members, and subjected directly to concentrated loads or reactions.

The design practice of the time recognized that the load carrying capacity of transverse stiffeners, when provided at the locations of the applied loads or reactions, could be determined on the basis of column formulae that included an adjacent portion of the web as a part of the stiffener column. The determination of this effective portion of the web was very complicated for analytical analysis because it would involve the web crippling strength of a combination of beam web and stiffener, the elastic and inelastic instability of the stiffener, and the local buckling of the plate elements of the stiffener. For these reasons, Nguyen & Yu undertook an experimental study to provide the data needed to formulate design provisions for cold formed steel transverse stiffeners.

2.1.2   Summary of Test Specimens

The tests were carried out on C-section specimens tested in pairs back-to-back, separated by pieces of cold formed angles attached to the flanges. The specimens were also restrained from lateral movement to prevent lateral-torsional buckling. The load was located either directly over the interior stiffener or the

end stiffener depending on the test series. For all of these tests the stiffener was located on the back of the joist web and connected with either 19 mm (3/4 in.) bolts or #12x14 self-tapping Tek screws. The C-section joist members had web depth to thickness ratios *(h/t)* from 150 to 300 and depths from 150 to 535 mm (6 to 21 in.). The test set-up is shown in Figure 2.1.1. In total, 33 tests were carried out on intermediate stiffeners and 28 tests on end stiffeners.

The transverse stiffeners were proportioned so that there would be no local buckling of any sub-element. The stiffeners were unlipped C-sections with a flange width of 12.7 mm (0.5 in.), a web depth of 38 mm (1.5 in.) and thickness of 1.02 mm (0.040 in.). Strain gauges were attached to points on the stiffener as well as the beam web to measure the stress distribution, and were also used to ensure the loading was concentric on the stiffener.
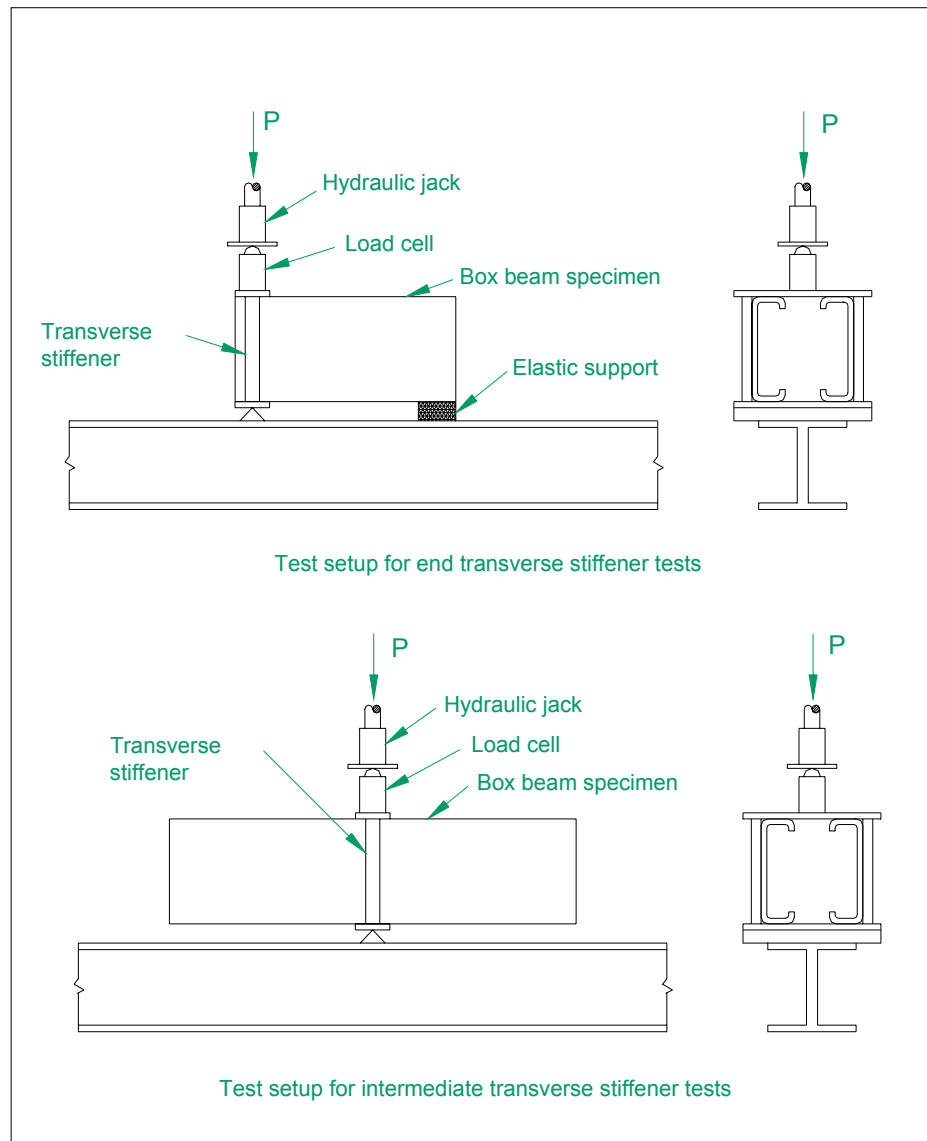
Figure 2.1.1: Nguyen & Yu Test Set-up

6

2.1.3   Failure Modes

There were two modes of failure observed for the stiffeners: (1) crushing of the stiffener in the specimens with *h/t* less than 250, and (2) column buckling for the specimens with *h/t* ratios greater than 250. In the tests were crushing was the failure mode, the ultimate load was less than that predicted by multiplying the gross stiffener area by its yield stress. During the testing, strain gauges were used to measure the stress in the stiffener. The measurements showed that the mean ratio of the measured stress to the yield stress was 0.86; however, the ultimate load was greater than the gross stiffener area times this reduced stress. Consequently, it was argued that a portion of the beam web was also mobilized by the stiffener and contributed to the overall capacity. Design recommendations were developed on this basis as follows:

$$P_{max} = 0.52F_{ya}A_c$$

Where,

F_{ya} = average yield point of web-stiffener section

A_c = $18t_w + A_s$ for intermediate stiffeners

   = $10t_w + A_s$ for end transverse stiffeners

t_w = thickness of beam web

A_s = area of stiffener

In those cases where the beam web was deep (i.e. h/t >250) the stiffeners failed by column buckling. As with the crushing failure mode, tests that failed by column buckling also did so at loads greater than predicted by considering the stiffener alone. The difference was also attributed to the mobilization of an effective portion of the beam web into the column cross-sectional area. The data also showed that this effective portion of the web increased as the web thickness increased and as the D/t_w increased. The design recommendations were given as follows:

$$P_{max} = F_{al}A_b$$

Where,

F_{al} = allowable column stress determined according to the current *AISI*

   Specification for the cross section A_b

A_b = $b_1t_w + A_s$ for intermediate stiffeners

   = $b_2t_w + A_s$ for end transverse stiffeners

b_1 = $25t_w[0.00241(D/t_w) + 0.720] \leq 42t_w$

b_2 = $12t_w[0.00437(D/t_w) + 0.833] \leq 30t_w$

D = length of transverse stiffener

One restriction placed on the application of these formulae is that the stiffened and unstiffened elements of cold formed steel transverse stiffeners shall not be subject to effective width reductions. The tests used

a stiffener section that was 38 mm (1-1/2 in.) wide with 12 mm (1/2 in.) flanges, which are sections used today for through-the-knockout bridging, but not normally considered as stiffeners.

2.1.4   Conclusions by Nguyen & Yu

(a) The strength of transverse stiffeners alone provide a very conservative result in predicting the load carrying capacity of beam webs loaded at the locations of the transverse stiffeners.

(b) A portion of the beam web contributes to the load carrying capacity of the web-stiffener column.

(c) Short stiffeners usually failed by end crushing at a stress less than that of the yield point of the stiffener steel.

(d) Stability failure occurred for long transverse stiffeners, and the effective width of beam webs depends on the web thickness and the D/t_w ratio of the steel beam.

(e) Connections between the beam webs and the transverse stiffeners have a significant effect on the behavior of the transverse stiffeners.

(f) On the basis of the experimental data obtained, design formulae were derived to compute the effective widths of beam webs for intermediate and end transverse stiffeners under end crushing and stability failure.

(g) The column design criteria in the AISI Specification can be used to predict the ultimate load of a web-stiffener assembly column.

As a recommendation of their work, Nguyen & Yu [7] proposed formulae (given above) for the design of transverse stiffeners when they are provided at the location of applied loads or reactions. These formulae, in a modified form, are currently in both the AISI Specification [1] and the CSA-S136 Standard [2], and are presented in Section 2.2.

2.2   CURRENT BEARING STIFFENER DESIGN PROVISIONS AND LIMITATIONS

The provisions of AISI Specification Section B6.1 *Transverse Stiffeners* are as follows:

"Transverse stiffeners attached to beam webs at points of concentrated loads or reactions shall be designed as compressive members. Concentrated loads or reactions shall be applied directly into the stiffeners or each stiffener shall be fitted accurately to the flat portion of the flange to provide direct load-bearing into the end of the stiffener. Means of shear transfer between the stiffener and the web shall be provided according to Chapter E. For concentrated loads or reactions the nominal strength equals P_n, where P_n is the smaller value given by (a) and (b) as follows:

    (a) $P_r = F_{wy}A_c$

    (b) P_n = Nominal axial strength evaluated according to Section C4(a), with A_e replaced by A_b

        $S_c = 2.0$ (ASD)

        $N_c = 0.86$ (LRFD)

Where,

A_c = $18t^2 + A_s$, *for transverse stiffeners at interior support and under concentrated load*

A_c = $10t^2 + A_s$, *for transverse stiffeners at end support*

F_{wy} = *Lower value of F_y for the beam web, or F_{ys} for the stiffener section*

A_b = $b_1t + A_s$, *for transverse stiffeners at interior support and under concentrated load*

A_b = $b_2t + A_s$, *for transverse stiffeners at end support*

A_s = *Cross-sectional area of transverse stiffener*

b_1 = *$25t[0.0024(L_{st}/t) + 0.72] \leq 25t$*

b_2 = *$12t[0.0044(L_{st}/t) + 0.83] \leq 12t$*

L_{st} = *total length of transverse stiffener*

t = *thickness of beam web*

The w/t_s ratio for the stiffened and unstiffened elements of cold-formed steel transverse stiffeners shall not exceed $1.28\sqrt{E/F_{ys}}$ and $0.37\sqrt{E/F_{ys}}$, respectively, where F_{ys} is the yield stress, and t_s is the thickness of the stiffener steel."

In AISI Specification [1] Chapter B1.2, it also specifies that $(h/t)_{max} = 200$ for unreinforced webs. This means that for the deeper LSF sections some type of web stiffener is a mandatory requirement of the Specification. The same provisions are also included in the CSA-S136 Standard [2].

2.3   NEED FOR ADDITIONAL RESEARCH

The requirements in the Specification are quite clear; when *h/t* exceeds 200 a stiffener is required for unreinforced webs and the design rules are given. However, there are two practical problems with these requirements. The most significant issue is the condition that the flat width of any element in the stiffener shall not exceed the limit for local buckling. This means that no element in the stiffener can be subject to effective width reductions. This condition is not met by any of the stiffeners in common use today. A LSF stud or track section as a bearing stiffener will be subject to effective width reductions at modest stress levels and fall outside the provisions of the Standard.

A second problem arises from the condition that the stiffener must be fitted accurately to the flange to provided direct load bearing. It is common practice to cut the stiffener shorter than the inside dimension between the flanges to facilitate construction: a condition that would not satisfy the Specification requirement that the stiffener is to be fitted accurately.

The designer, therefore, must use engineering judgment or tests to arrive at an appropriate design method if the thin LSF stiffener sections are being used. Common engineering practice is to consider these members not as transverse stiffeners, but as short concentrically loaded columns transferring point loads

across the member. This column member also happens to be connected to the joist web, which stiffens the web to prevent web crippling. It could be argued, however, that the requirements of the Specification are not being met. This ambiguity was one of the reasons the AISI and CSSBI technical committees were interested in a research project to develop design procedures applicable to the types of stiffeners being used in LSF construction today.

3 GENERAL DESCRIPTION OF TEST PROCEDURES

3.1 TEST SET-UP

The basic test procedure involved conducting a series of two-flange loading tests on transversely stiffened joist specimens of different configurations. For the stiffeners at the end of the joist, end-two flange tests were conducted. When the stiffener was at an intermediate location, interior-two-flange tests were done. The test set-up is shown in the photograph in Figure 3.1.1 and the drawing in Figure 3.1.2. The testing machine in the University of Waterloo Civil Engineering Structures Lab was set for stroke control such that the load was applied at a steady rate of 5 kN/min (1000 lb/min). The load and deflection were both recorded along with the deflected shape of the specimen at failure.

Figure 3.1.1: Photograph of a Typical Stud-End-Inside Test

The test specimens were constructed as shown in Figure 3.1.3. Two joist members were connected by short angles to restrain the torsional forces in the C-sections. The stiffeners were attached to the joist web with #10 sheet metal screws and care was taken to ensure the specimen was aligned and square prior to testing. The load was applied to the top flange of the joist through a steel bearing plate positioned on top of the joist. The point of application of the load was centered between the two stiffeners. No other means were used to ensure that the load was distributed exactly evenly between the two members except in some cases were an additional load cell was positioned under one of the joist ends.
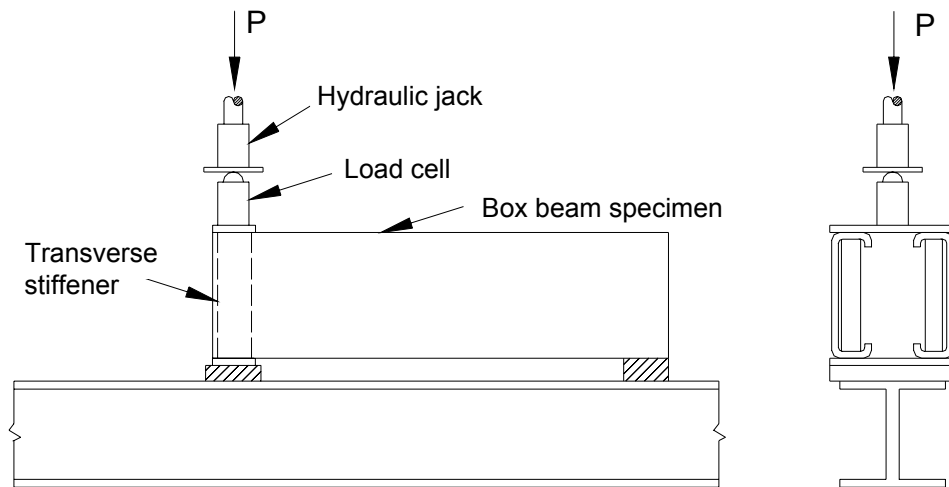
Test setup for end transverse stiffener tests
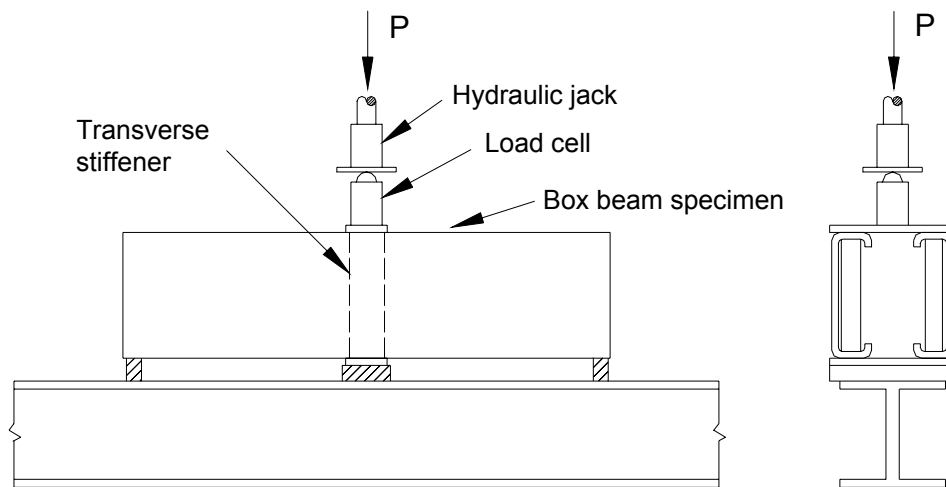
Test setup for intermediate transverse stiffener tests

Figure 3.1.2: Test Set-Up

The stud and track stiffeners were positioned 5 mm (1/4 in.) in from the end of the joist to ensure that the stiffener flanges were in complete contact with the inside of the joist flanges. The bridging channel stiffeners were located 50 mm (2 in.) in from the joist end such that their center line was at the same location relative to the joist as the stud and track stiffeners. The width of the bearing plate varied between 89 and 100 mm (3-1/2 to 4 in.) to simulate the loading that would be transferred through a track section typical in platform construction. For the tests with the stiffener positioned on the outside of the joist, a 100 mm (4 in.) bearing plate was used to completely cover the end of the stiffener for full bearing.
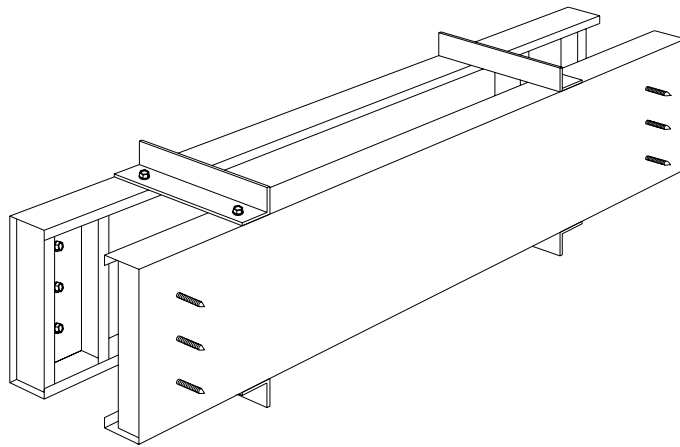
Figure 3.1.3: Typical Test Specimen

The joist specimens for the end location tests were cut to a length at least twice their depth. This was consistent with the specimens used in the Nguyen & Yu test series. This length also allowed a test to be carried out on each end of the specimen. The tests of the intermediate stiffeners used a joist length of at least three times the depth, which was also consistent with the Nguyen & Yu tests.

3.2   STIFFENER CONFIGURATIONS

There are four configurations for the stiffened assembly as illustrated in Figure 3.2.1. Throughout this report the distinction is made between end and intermediate locations along the joist length, as well as inside and outside locations relative to the joist flanges.

Intermediate, Outside

End, Outside

Intermediate, Inside

End, Inside
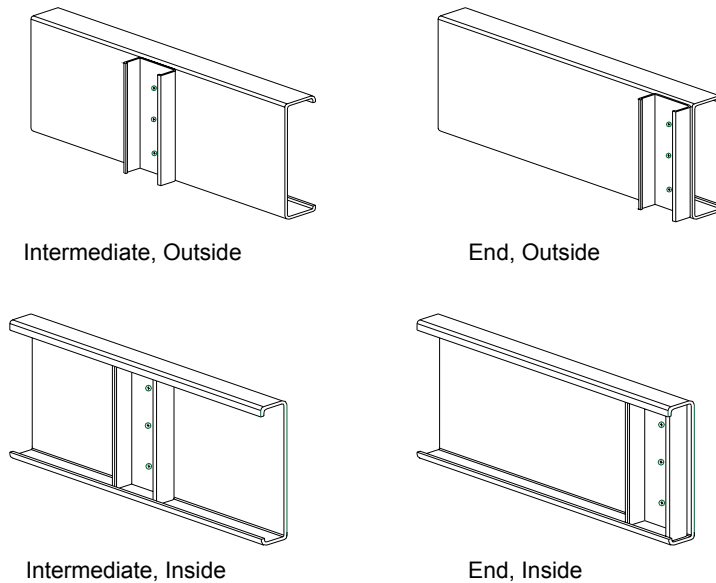
Figure 3.2.1: Stiffener Configurations

4   EXPERIMENTAL TEST RESULTS AND ANALYSIS

4.1   INTRODUCTION

Described in the following sections are the general failure modes and findings arising from observations of the different test series conducted.

4.2   GENERAL FAILURE DEFORMATION

Many of the tests were conducted on bearing stiffeners attached to the joist web between the joist flanges. This location forces the applied load to be transferred to the stiffener through bearing on the underside of the joist flange. A key factor in the behavior of this assembly is the gap between the end of the stiffener and the joist.

Figure 4.2.1 illustrates the stages in the loading cycle. Initially the stiffener is not in contact with the joist flange (Figure 4.2.1(a)). Since the cold forming process used to fabricate these members creates rounded corners, when the load is applied it first contacts the edge of the flange corner radius and does not transfer directly into the joist web. Consequently, the flanges will immediately start to rotate (Figure 4.2.1(b)). The flange rotation will also create moments at the top and bottom of the joist web that will start to curve the web outward.

(a) Before loading   (b) Initial flange rotation   (c) Web collapse
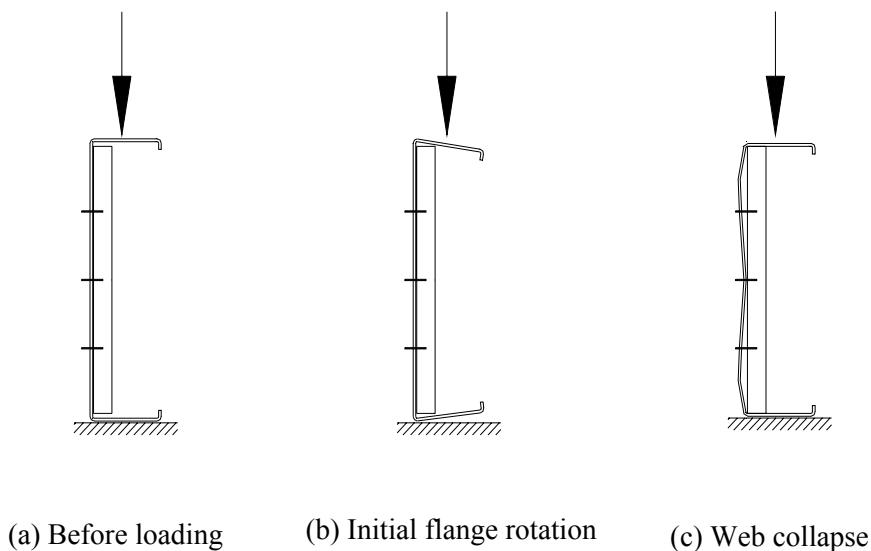
Figure 4.2.1: Stiffener Deformation Stages

As the joist flanges rotate, they will eventually contact the edge of the bearing stiffener as shown in Figure 4.2.1(b). At this point the load is still being transferred largely through the joist flange corner

radius into the web. There comes a point, however, when the compressive force in the web, combined with the bending moment caused by loading the corner radius, causes the web to buckle. Once the web buckles (i.e. web crippling) it has little post-buckling strength and the assembly will not carry any significant extra load until the flange comes in full contact with the end of the stiffener (Figure 4.2.1 (c)). From this point onward the additional load is transferred directly into the stiffener through end bearing.

This mechanism is also illustrated in the load-deflection curve shown in Figure 4.2.2. The first upward sloping region corresponds to the initial flange rotation and loading the stiffener at the contact points. The next flatter region corresponds to the web buckling, and the following stiff region is where the load is bearing directly on the stiffener. The final buckled shape of the joist web is shown in the photograph in Figure 4.2.3.
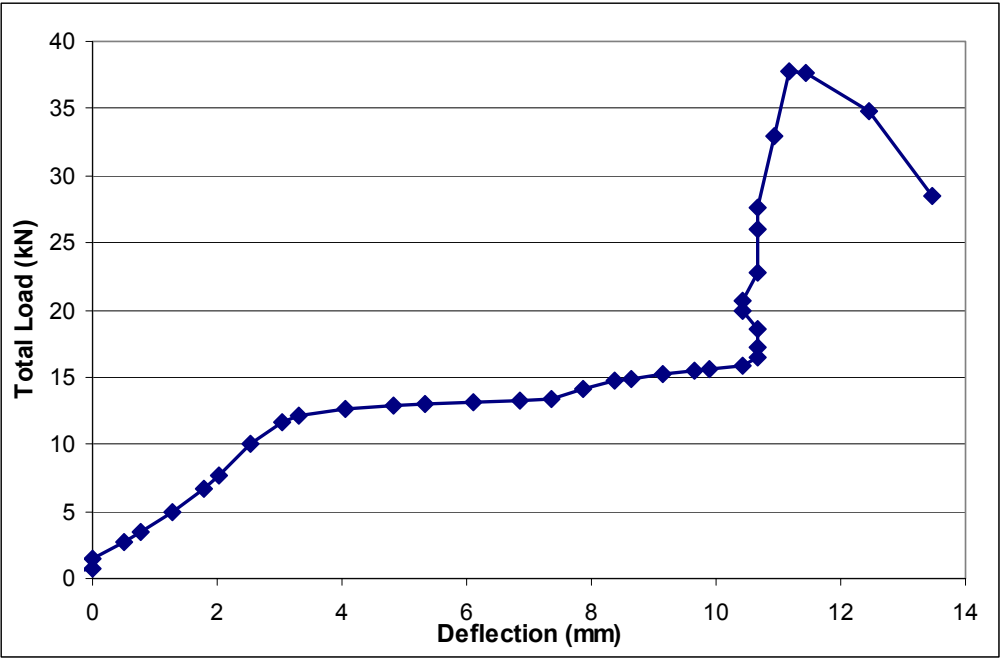
Figure 4.2.2: Web Buckling Load-Deflection

This deformation mechanism has implications for the forces that develop in the assembly and is influenced by parameters such as the stiffener length, location and screw pattern. These different factors are discussed in subsequent sections.
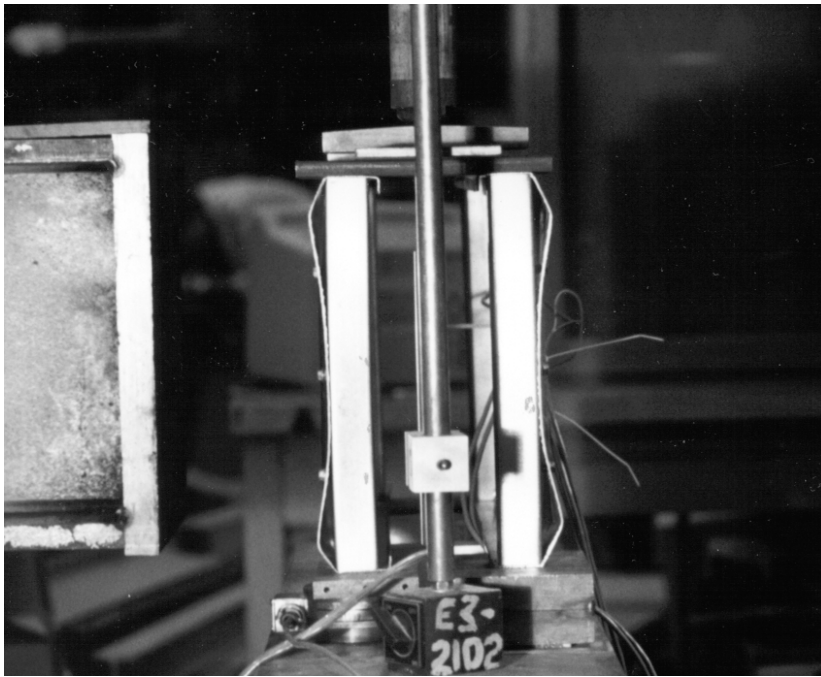
Figure 4.2.3: Photograph Showing Buckled Webs

4.3   TEST RESULTS

4.3.1   *Summary of the Parameters Investigated*

The stiffened joist assembly was made up of components that could be combined in a number of ways. Each of these variations may have an influence on the behaviour of the assembly and have been studied individually. The following is a general discussion about the parameters that were investigated during this study.

(a) *Joist depth and thickness:* The depth and thickness of the joist will influence the web crippling capacity, post-buckling behaviour and the forces exerted on the stiffener by the joist during the loading cycle. Joist samples were selected to provide a range of h/t ratios (100 to 300), depths (203 to 356 mm, 8 to 14 in.) and thicknesses (0.84 to 1.91 mm, 0.033 to 0.075 in.) that were representative of typical cold formed steel sections in current usage.

(b) *Stiffener type and size:* The bearing stiffener is the principal load-carrying member in the assembly, and the stiffener type and size will significantly influence the capacity. Three types of stiffeners were tested: stud, track and channels. These were selected as being representative of products in common usage. Thicknesses ranged from 0.80 to 1.52 mm (0.031 to 0.060 in.)

(c) *Fastener pattern*: The fasteners connecting the stiffener to the joist web will influence the buckled shape of the joist, and in turn apply different loads on the stiffener. Common variations in fastener pattern were investigated.

16

(d) *End gap between stiffener and joist flange*: When the stiffener is positioned between the joist flanges, it is commonly cut short to facilitate installation. The effect of this gap between the stiffener and the joist was investigated to determine what affect it had on the capacity of the assembly.

(e) *Bearing width*: The stiffened assembly was subjected to two-flange loading and the stiffener was acting as a short column. If the bearing width is less then the width of the stiffener, the capacity of the stiffener will be affected.

(f) *Fastening joist flange to the support*: In other web crippling studies it has been determined that fastening the flanges of the specimen to the supports can have a measurable affect on the capacity of the section. Tests were carried out to compare the influence of fastening the joist flange to the support in a stiffened assembly.

(g) *Reaction at the free end of the test specimen*: During the tests the specimen rested on two bearing supports but loaded only at one end. Measurements were taken of the load at the unloaded support to determine whether two load cells would be needed to determine the failure load.

(h) *Web crippling capacity of the joist*: One of the serviceability limit states of these type of assemblies would be the web crippling capacity of the joist. This would be significant for those assemblies with the stiffener positioned between the joist flanges and cut shorted than the depth of the joist.

(i) *Fastener forces*: The buckling of the joist web is restrained by the fasteners connecting the joist to the stiffener. The number and location of the fasteners, the size of the joist web, and size of the stiffener will determine what forces are developed and transferred to the stiffener. The capacity of the stiffener will in turn be affected by these added lateral forces.

4.3.2   Material properties and Dimensions

Tables A1 through A9 list the material properties and the stiffener dimensions for all of the tests. The joist sections varied in depth (as indicated in Tables B1 through B8) but in each case had a nominal flange width of 41 mm (1-5/8 in.) with 12 mm (1/2 in.) lips.

4.3.3   Tested Bearing Capacities\

Tables B1 through B8 provide all of the tested capacities. These tables will be referred to in the following sections as various specific studies are discussed. The tested capacities are analyzed in more detail in Section 9 were the various prediction methods are considered.

4.4 EFFECTS OF STIFFENER END GAP AND FASTENER PATTERNS

4.4.1 Test Parameters and Specimen Dimensions

4.4.1.1 End Gap

It is common in residential steel framed construction for the bearing stiffener to be installed between the joist flanges. To facilitate this type of construction, the stiffener is cut shorter than the inside dimension between the flanges. Typically the total gap between the stiffener and the joist is approximately 5 mm (3/16 in.). This gap is illustrated in Figure 4.4.1. A test series was carried out to investigate the effects of increasing this gap. The difference in length between the bearing stiffener and the joist depth was incrementally changed from having zero gap up to a gap of 15 mm (5/8 in.).
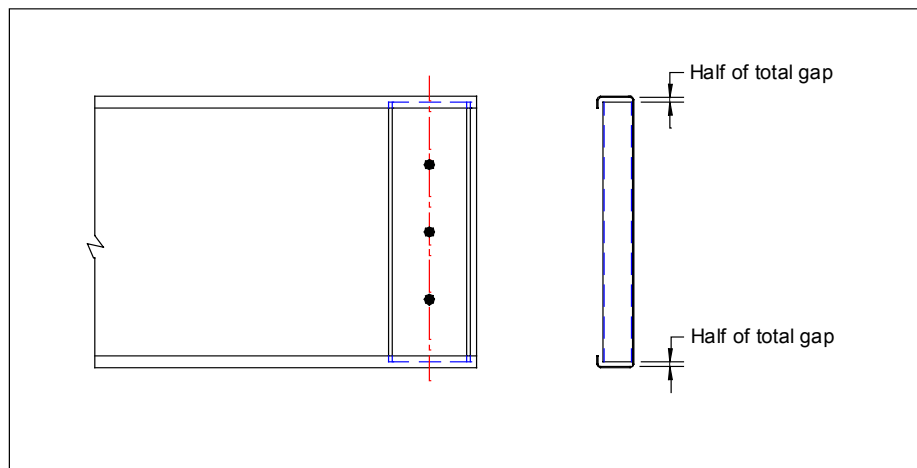
Figure 4.4.1: Stiffener End Gap

4.4.1.2 Fastener Pattern

There are a number of common fastener patterns used to connect the stiffener to the joist web. Since unnecessary screws are an added cost that might be avoided, there is an incentive to prove the acceptability of using fewer fasteners. A series of tests was carried out to investigate four common fastener arrangements as illustrated in Figure 4.4.2. The objective was to determine whether these fastener patterns had any measurable effect on the ultimate capacity of the bearing stiffener assembly.
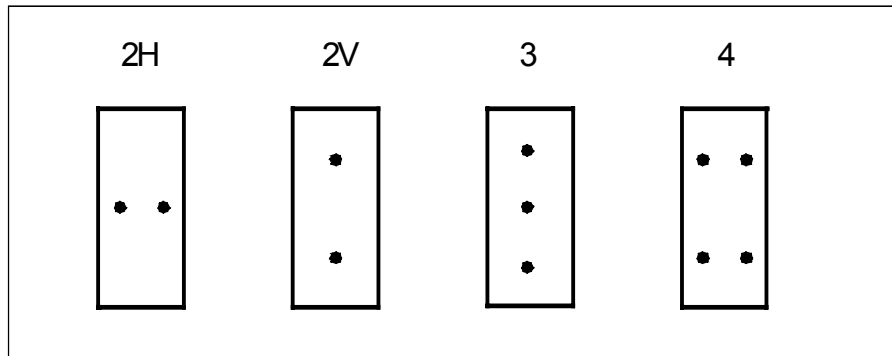
Figure 4.4.2: Fastener Pattern

4.4.1.3 Intermediate and End Locations

As illustrated in Figure 3.2.1, there are four locations for the stiffener on the joist: intermediate, end, inside and outside. Tests were carried with stiffeners at both the intermediate and end locations to compare the effects of the stiffener end gap on the ultimate capacity of these different configurations.

4.4.1.4 Joist Depth

In this particular test series two joist depths were used: 203 mm (8 in.) and 254 mm (10 in.). These two depth are representative of the majority of cold formed steel C-sections currently being used in North American residential construction.

4.4.1.5 Material Properties and Dimensions

The dimensions of each joist and stiffener tested were measured and recorded. These values are provided in Appendices A and B for the specific test designation reported in Table 4.4.1.

4.4.1.6 Specimen Assembly

The test specimens consisted of two C-section joist pieces connected together as illustrated in Figure 3.1.2. Specimens of the 254 mm (10 in.) joists were cut to a length of 600 mm (2 ft.) to allow a test to be conducted on each end. The 203 mm (8 in.) joists were cut to a length of 915 mm (3 ft.), which allowed one test to be conducted at each joist end and an intermediate test at the centre. When assembling the specimens, the centreline of the stiffeners were located 50 mm (2 in.) from the end of the joist to line up with the centre of the 100 mm (4 in.) bearing plate. A piece of 38 mm (1-1/2 in.) angle was attached to the top and bottom flanges of the joists to act as bridging. A 100 mm (4 in.) bearing plate was used to provide full end bearing for the stiffener.

4.4.2 Test Results

Data from the load cell and the LVDT recorded by the Labview® data acquisition system were used to determined the failure loads. Additional details of the tests are provided in Reference 16. The ultimate

19

capacities for all of the tests are presented in Table 4.4.1 and in Figure 4.4.3. The horizontal solid line in Figure 4.4.3 is the mean of all the end location tests, which is 19.45 kN (4,370 lbs.), and the two dashed lines represent +/- 20% limits. The test description identifies the length of the stiffener and the fastener pattern. For example, test 199-2H has a stiffener 199 mm long and the fastener pattern is 2H as depicted in Figure 4.4.2. The test designation corresponds to the tests as listed in Appendices A and B. The joist sections for these tests were either 203 mm or 254 mm deep; therefore, the 199 mm and 251 mm long stiffeners would have no end gap.

Table 4.4.1: Results for Stiffener End Gap Tests (Capacity per Stiffener)

Test Description	Test Designation	Tested Capacity (kN)
199-2H	Stud-E/I-31	19.29
196-2H	Stud-E/I-32	19.59
193-2H	Stud-E/I-33	18.27
190-2H	Stud-E/I-34	17.73
187-2H	Stud-E/I-35	17.76
184-2H	Stud-E/I-36	15.72
	Mean	18.06
	COV	0.077
199-2V	Stud-E/I-37	17.31
196-2V	Stud-E/I-38	18.81
193-2V	Stud-E/I-39	19.74
190-2V	Stud-E/I-40	17.46
187-2V	Stud-E/I-41	17.79
184-2V	Stud-E/I-42	17.58
	Mean	18.12
	COV	0.053
251-3	Stud-E/I-19	21.3
249-3	Stud-E/I-20	20.16
246-3	Stud-E/I-21	23.13
244-3	Stud-E/I-22	21.96
241-3	Stud-E/I-23	19.29
239-3	Stud-E/I-24	17.32
	Mean	20.53
	COV	0.101
251-4	Stud-E/I-25	19.2
249-4	Stud-E/I-26	24.15
246-4	Stud-E/I-27	20.79
244-4	Stud-E/I-28	24.54
241-4	Stud-E/I-29	19.77
239-4	Stud-E/I-30	18.03

	Mean	21.08
	COV	0.127
199I-3	Stud-I/I-63	22.23
196I-3	Stud-I/I-64	29.76
193I-3	Stud-I/I-65	23.58
190I-3	Stud-I/I-66	22.14
187I-3	Stud-I/I-67	22.23
184I-3	Stud-I/I-68	23.73
	Mean	23.95
	COV	0.123

Note: The capacity per stiffener is taken as one half of the maximum recorded test load.
1 kN = 224.8 lbs, 1 mm = 0.0394 in.
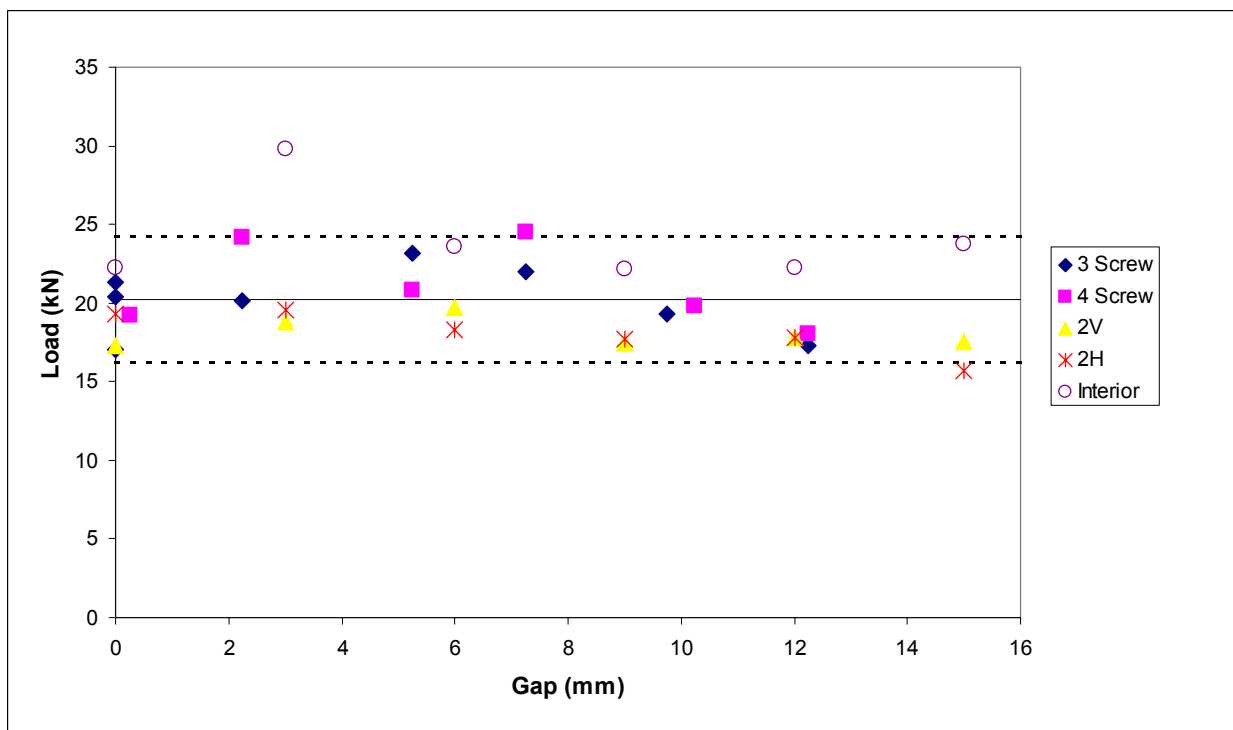
Figure 4.4.3: Results of Stiffener End Gap Tests (Load per Stiffener)

4.4.3   Analysis of Results

4.4.3.1   Effect of Stiffener End Gap

Considering all of the data plotted in Figure 4.4.3, the stiffener end gap does not appear to have a significant effect on the ultimate capacity of the assembly for an end gap up to 8 mm (1/4 in.). The load versus deflection plots provided in Ref. 16 also show that the behavior does not vary if the end gap increases. The gap only extends the region where web crippling of the joist has occurred and the joist flanges are collapsing onto the stiffener. An 8 mm (1/4 in.) gap is quite sufficient to allow for the easy construction of these assemblies.

4.4.3.2 Effect of Screw Spacing

One of the objectives of this work was to determine if the screw pattern had an effect on the strength of the stiffened joist assembly. The results have been separated into two plots shown in Figures 4.4.4 and 4.4.5. These plots show that there is no significant difference between the three and four screw pattern, and similarly for the 2V and 2H patterns. There is, however, a difference between the assemblies with two screws and those with three or four screws. The horizontal solid line is the mean of all end location tests. It is apparent from the two plots that the ultimate capacity of the two-screw tests were consistently lower than the mean.

The two screw tests were conducted on 203 mm (8 in.) joist specimens, while the three and four screw tests used 254 mm (10 in.) joist sections. It other tests (Ref. 14) it was determined that the joist depth did not have a significant influence on the ultimate capacity of assemblies with stud stiffeners. Taking this into consideration would indicate that the fastener pattern does have some significance. The stiffener sections for all of the tests came from the same lot of material, so there is no variation caused by material strength. The joist material is different (both in thickness and yield strength) as presented in Tables B1 and B3. It might be reasonable to assume that the capacity of the assembly is the addition of the web crippling capacity of the joist web plus the axial capacity of the stiffener. This hypothesis is investigated in more detail and discussed in a later section.
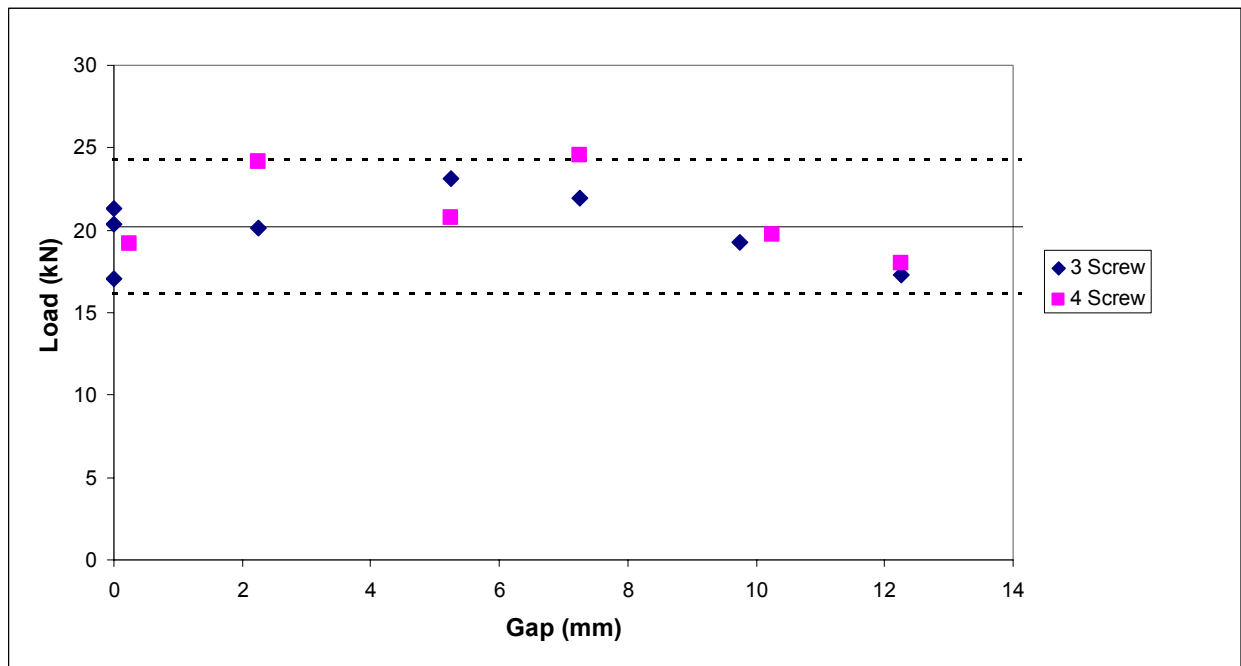
Figure 4.4.4: Ultimate Tested Capacities of 3 & 4 Screw Assemblies
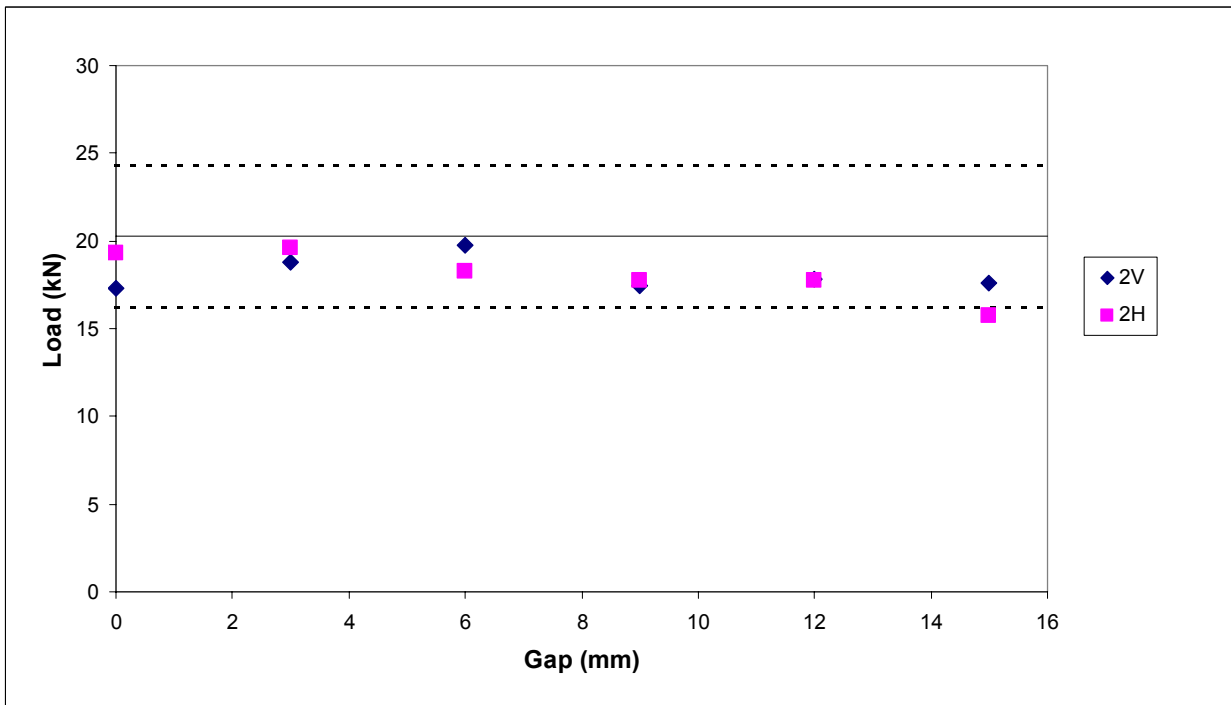
Figure 4.4.5: Ultimate Tested Capacities of 2H & 2V Screw Assemblies

4.4.3.3 *Intermediate Versus End Location*

Figure 4.4.6 shows a plot of the ultimate capacity of the stiffeners located at an intermediate position on the joist. This location has a consistently higher tested capacity than the end location, with a mean increase of 23%. This result is expected given the extra supporting joist web material around the stiffener.
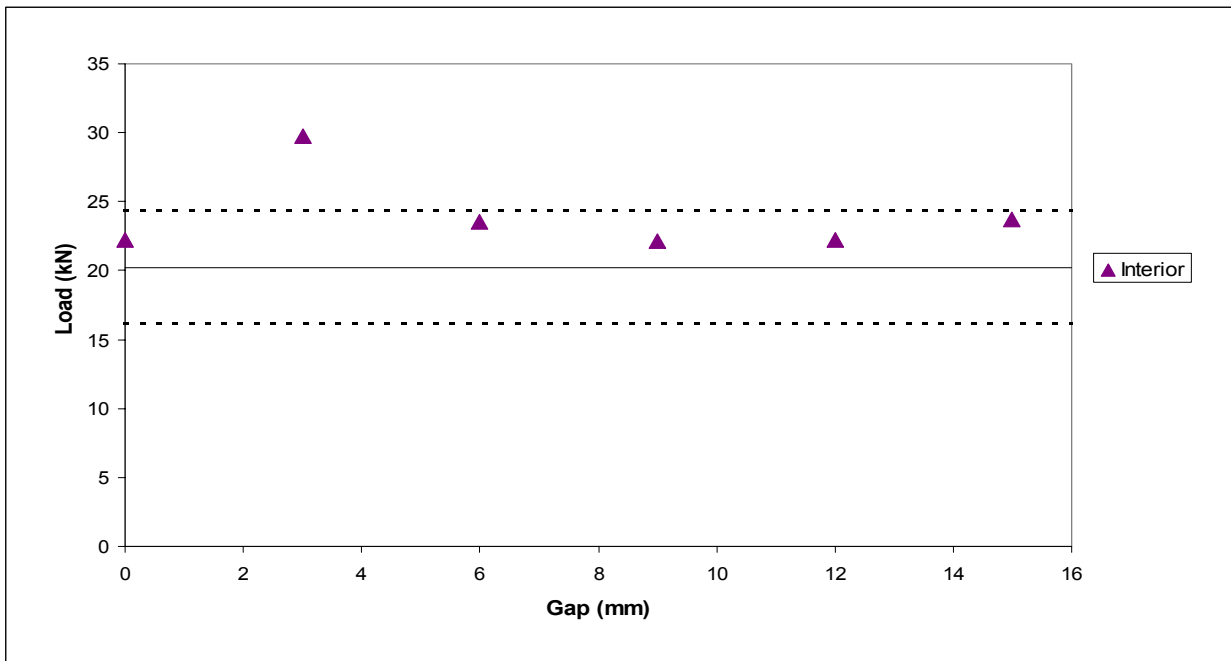
Figure 4.4.6: Ultimate Tested Capacity for Intermediate Stiffeners

4.4.4 Conclusions Related to the Effects of End Gap and Fastener Pattern

The following summarizes the conclusions of this phase of the work:

- The fastener pattern has some effect on the ultimate capacity of the stiffened sections. Those sections with more fasteners near the joist flange have a higher ultimate capacity that can be attributed to an increased web crippling resistance of the joist.

- Increasing the total end gap to 15 mm does not significantly affect the ultimate capacity, however, there could be serviceability problems with the resulting deformations.

- The web crippling capacity of the joist is an important serviceability limit state.

- The ultimate capacity of the interior-two-flange loading case was measured to be 23% on average higher than the end-two-flange case.

4.5 EFFECTS OF BEARING WIDTH

4.5.1 Objective and Scope

The objective of this phase of the project was to investigate the effects of the bearing width on the ultimate capacity of a stiffened cold formed steel C-section. The loading is both end-two-flange and interior-two-flange as illustrated in Figure 4.5.1. The resulting failure mechanism is discussed and a preliminary design method is presented.

Interior-Two-Flange   End-Two-Flange
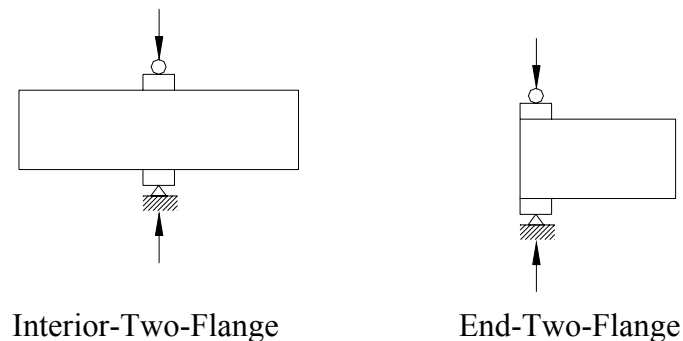
Figure 4.5.1: Loading Conditions

The scope of this work is experimental. A series of tests were conducted on stiffened assemblies with four different bearing widths: 25, 50, 75 and 100 mm (1, 2, 3 and 4 in.). For each of the different bearing widths, three different stiffener configurations were tested: end-inside, end-outside, and intermediate-inside. These configurations are illustrated in Figure 4.5.2.

End, Outside

Intermediate, Inside   End, Inside
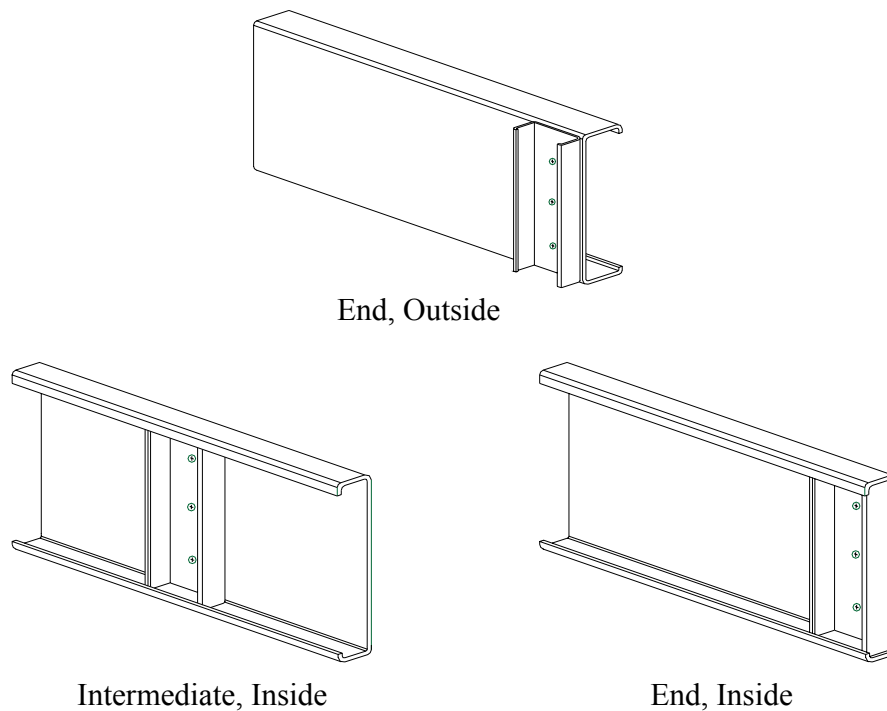
Figure 4.5.2: Test Specimen Configurations

4.5.2   Material Properties

The dimensions of each joist and stiffener tested were measured and recorded. These values are provided in Appendices A and B for the specific test designations reported in Table 4.5.1, and Reference 17 for the other assemblies. The tests with a bearing width less than the stiffener width were not used in the overall analysis discussed later in the this report, therefore were not included in the summary of assemblies provided in the Appendices.

4.5.3   Tested Loads

The ultimate capacities for all of the tests are listed in Table 4.5.1, and plotted in Figures 4.5.3, 4.5.4, and 4.5.5. The test descriptions used are as follows:

    End = stiffener located at the end of the joist

    Intermediate = stiffener located at the middle of the joist length

    Outside = stiffener positioned of the back of the joist web

    Inside = stiffener positioned between the joist flanges

    25, 50, 75, 100 = bearing widths (mm)

    1, 2 = test number for that assembly type

Table 4.5.1: Test Results (for a 2 stiffener assembly)

Test Description	Test Designation	Tested Capacity (kN)
End-25-Inside-1	N/A	27.54
End-25-Inside-2	N/A	24.54
End-50-Inside-1	N/A	27.96
End-50-Inside-2	N/A	27.00
End-75-Inside-1	N/A	33.72
End-75-Inside-2	N/A	28.80
End-100-Inside-1	Stud-E/I-45	44.22
End-100-Inside-2	Stud-E/I-46	45.12
End-25-Outside-1	N/A	23.88
End-25-Outside-2	N/A	20.88
End-50-Outside-1	N/A	27.78
End-50-Outside-2	N/A	28.08
End-75-Outside-1	N/A	21.90
End-75-Outside-2	N/A	25.98
End-100-Outside-1	Stud-E/O-3	49.14
End-100-Outside-2	Stud-E/O-4	43.38
Intermediate-25-Inside-1	N/A	25.02
Intermediate-25-Inside-2	N/A	27.60
Intermediate-50-Inside-1	N/A	28.98
Intermediate-50-Inside-2	N/A	28.32
Intermediate-75-Inside-1	N/A	35.52
Intermediate-75-Inside-2	N/A	34.80
Intermediate-100-Inside-1	Stud-I/I-9	40.80
Intermediate-100-Inside-2	Stud-I/I-10	50.64

Note: 1 kN = 224.8 lbs, 1 mm = 0.0394 in.

4.5.4   *Discussion of the End-Outside Location Tests*

The test results for the end-outside configurations are shown in Figure 4.5.3. This plot shows two regions: for bearing widths 75 mm (3 in.) and less, and for a bearing width of 100 mm (4 in.). This discontinuity is expected since the width of the stud stiffener was 90 mm (3-5/8 in.), and therefore only the 100 mm (4 in.) wide bearing plate completely covered the end of the stiffener. Two linear line segments could be used to model these results. One line segment would fit the 25 to 75 mm (1 to 3 in.) bearing width data and another for the 75 to 100 mm (3 to 4 in.) bearing widths.

The webs of the stud stiffeners used in these tests have a flat width ratio of 105 and will be subject to local buckling at the ultimate loads. As a consequence, only the one flange area and a portion of the web

will be effective in carrying any load when the bearing width is less than 100 mm (4 in.). When the bearing width is increased from 25 mm to 75 mm (1 to 3 in.) the stiffener will not contribute any additional capacity because the centre portion of the web is subject to local buckling. The webs of the stiffeners in the end-outside assemblies do not have the support of the joist flanges and are less influenced by bearing width than the inside location.
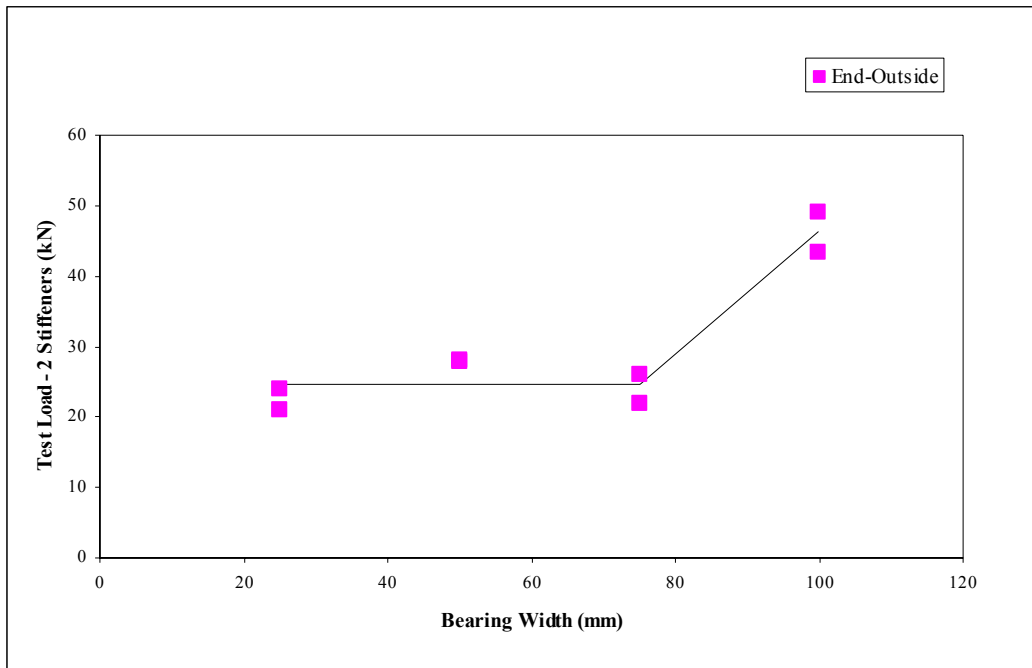
Figure 4.5.3: End-Outside Bearing

When the bearing width reaches 100 mm (4 in.), both flanges of the stiffener are covered and there is full bearing. No tests were carried out on stiffened assemblies with a bearing width larger than 100 mm (4 in.).

4.5.5   *Discussion of the End-Inside Location Tests*

The plot in Figure 4.5.4 shows a general increase in capacity from the 25 to 100 mm (1 to 4 in.) bearing width for the end-inside bearing. This is due to the increased web crippling capacity provided by the joist web and the load distribution caused by the joist flanges onto the end of the stiffener. The polynomial curve is fitted to the data to illustrate the general shape. For the end-inside assemblies the joist flange provides added support to the stiffener; therefore, the discontinuity seen in the end-outside assemblies is not as pronounced. The interesting result of these tests is the similarity of the inside and outside locations as shown in Figures 4.5.3 and 4.5.4. It was expected that the inside location would be much stronger since the joist flanges provide additional support to the stiffener that does not bear over its entire width. This may be the case for the 75 mm (3 in.) bearing width tests, but does not appear to be true for the narrower

width tests. This result is important since it is common to assume a minimum bearing width of 38 mm (1-1/2 in.), with the stiffener located on either side of the joist. These tests show that the location does not affect the capacity as significantly as the bearing width.
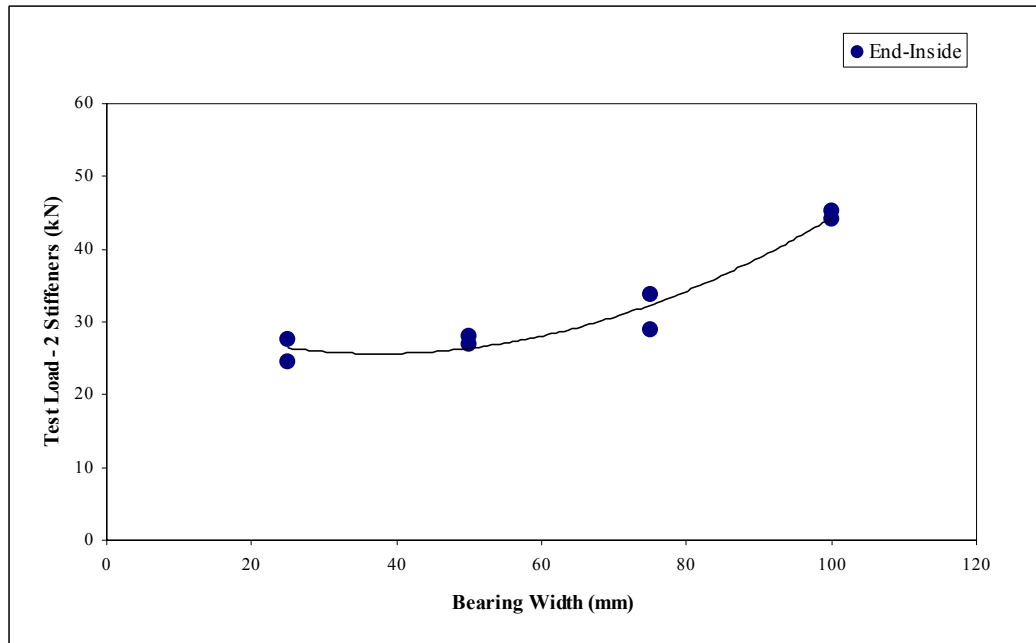
Figure 4.5.4: End-Inside Bearing

4.5.6   Discussion of the Intermediate-Inside Location Tests

The plot of the results of the intermediate-inside location tests shows a trend similar to the end-inside tests. A polynomial trend line is included with the data shown in Figure 4.5.5. In these tests the bearing plate was positioned at the centre of the stiffener. The support provided by the joist flanges to the stiffener was sufficient to transfer the bearing load, which increased as the bearing width got wider.

It is interesting to note that for the 25 mm (1 in.) bearing width the end-inside and intermediate-inside average test capacities were almost the same (26.04 and 26.31 kN respectively). This is not readily explainable since the bearing plate for the end-inside test covers one of the stiffener flanges, while the bearing on the intermediate-inside test is centred on the stiffener web. It is possible that the increased web crippling capacity of the intermediate-two-flange joist offsets the decrease in capacity resulting from the bearing on the stiffener web.
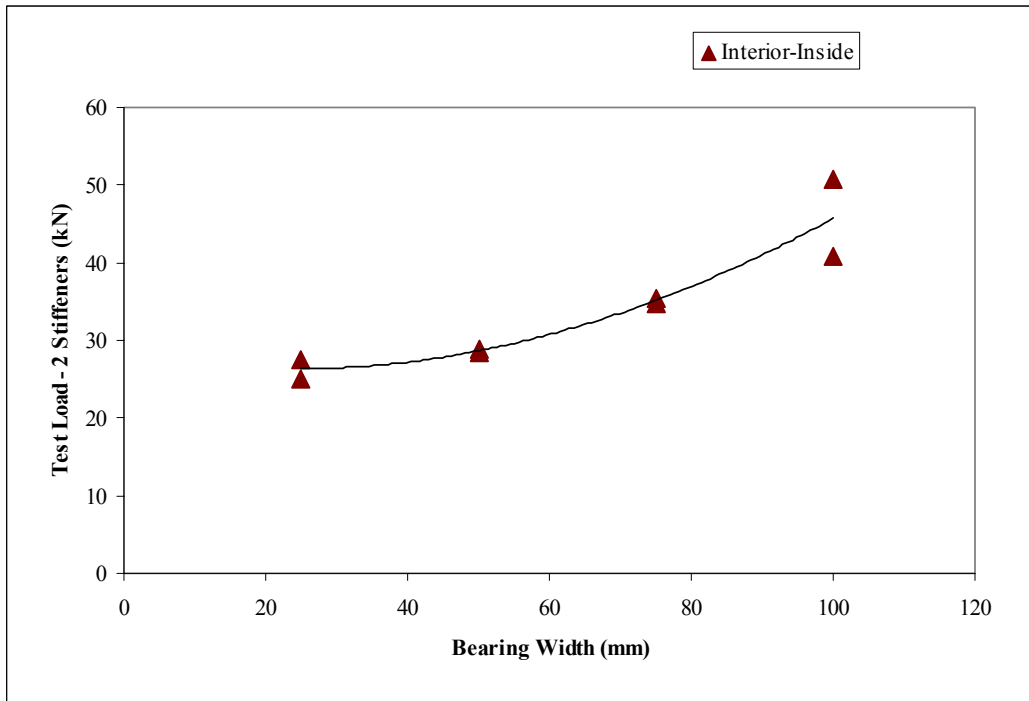
Figure 4.5.5: Intermediate-Inside Bearing

4.5.7   Conclusions and Recommendations for the Effects of Bearing Width

A method has been developed and presented in Reference 17 to predict the effects of bearing width on the bearing capacity of C-section joists stiffened with a 91 mm (3-5/8 in.) stud section. The method adds the web crippling capacity of the joist member to the axial capacity of the bearing stiffener. The capacity of the stiffener is taken as the effective area times the yield stress times a 0.8 reduction factor. The effective area changes with the bearing width. This design approach correlates well with the test data when the stiffener is located at the end of the joist, but less so for the stiffeners at an intermediate location. Additional work is needed to investigate the web crippling capacity of the C-sections in these types of assemblies. The presence of the stiffener changes the web crippling behavior of the joist and it can no longer be predicted using the resistance equations developed for single web members. Tests also need to be conducted on the intermediate-outside stiffener configuration, which was not tested in this series.

4.6   EFFECT OF FASTENING JOIST FLANGES TO BEARING SUPPORTS

4.6.1   Fastening Joist Flanges

A series of tests were carried out were the joist flanges were fastened to the bearing supports with #12 self drilling screws. A photo of the fastening arrangement is provided in Figure 4.6.1.

Figure 4.6.1: Fastening Joist Flanges to the Bearing Plate

The following Tables 4.6.1 through 4.6.5 give the predicted capacities for those tests used to investigate the effects of varying the joist thickness and fastening the joist flanges to the bearing support. The dimensions for the specimens and the material properties are available in the Appendix.

Table 4.6.1: Analyses of Fastening Joist to Bearing Supports
(Stud Stiffeners, End Location, Inside)

Test Designation	Fastened or Unfastened to Support	Tested Load, C_t (kN)	Yielding $C_y = F_y A_e$ (kN)	Test/Calc C_t / C_y	Test/Calc $C_t / 0.823C_y$
Stud-E/I-50	Unfastened	66.8	82.75	0.81	0.98
Stud-E/I-51	Unfastened	68.7	82.75	0.83	1.01
Stud-E/I-52	Unfastened	62.4	82.75	0.75	0.92
Stud-E/I-53	Unfastened	64.2	82.75	0.78	0.94
Stud-E/I-54	Fastened	71.4	82.75	0.86	1.05

30

Stud-E/I-55	Fastened	70.2	82.75	0.85	1.03
Stud-E/I-56	Fastened	74.9	83.17	0.90	1.09
Stud-E/I-57	Fastened	71.6	82.75	0.86	1.05
Stud-E/I-58	Unfastened	65.90	82.75	0.80	0.97
Stud-E/I-59	Unfastened	64.80	83.59	0.78	0.94
Stud-E/I-60	Fastened	71.40	83.17	0.86	1.04
Stud-E/I-61	Fastened	67.40	83.59	0.81	0.98
Average				**0.823**	**1.00**
COV					**0.054**
Average for Unfastened		**65.46**			**0.96**
COV		0.033			0.034
Average for Fastened		**71.13**			**1.04**
COV		0.034			0.035

Note: Calculated values are for 2 stiffeners. 1 kN = 224.8 lbs, 1 mm = 0.0394 in.

Table 4.6.2: Analyses of Fastening Joist to Bearing Supports
(Stud Stiffeners, End Location, Outside)

Test Designation	Fastened or Unfastened to Support	Tested Load, C_t (kN)	Yielding $C_y = F_y A_e$ (kN)	Test/Calc C_t / C_y	Test/Calc $C_t / 0.940C_y$
Stud-E/O-13	Unfastened	82.8	82.75	1.00	1.06
Stud-E/O-14	Unfastened	86.1	82.75	1.04	1.11
Stud-E/O-15	Unfastened	70.1	83.59	0.84	0.89
Stud-E/O-16	Unfastened	82.8	83.59	0.99	1.05
Stud-E/O-17	Fastened	81.9	82.75	0.99	1.05
Stud-E/O-18	Fastened	75.2	82.75	0.91	0.97
Stud-E/O-19	Fastened	69.2	83.59	0.83	0.88
Stud-E/O-20	Unfastened	76.50	82.75	0.92	0.98
Stud-E/O-21	Unfastened	78.50	83.59	0.94	1.00
Average				**0.940**	**1.00**
COV					**0.078**
Average for Unfastened		**79.46**			**1.02**
COV		0.072			0.075
Average for Fastened		**75.40**			**0.97**
COV		0.085			0.089

Note: Calculated values are for 2 stiffeners. 1 kN = 224.8 lbs, 1 mm = 0.0394 in.

Table 4.6.3: Analyses of Fastening Joist to Bearing Supports
(Stud Stiffeners, Intermediate Location, Inside)

Test Designation	Fastened or Unfastened to Support	Tested Load, C_t (kN)	Yielding $C_y = F_y A_e$ (kN)	Test/Calc C_t / C_y	Test/Calc $C_t / 1.098C_y$
Stud-I/I-11	Unfastened	79.1	82.75	0.96	0.87
Stud-I/I-12	Unfastened	95.7	82.75	1.16	1.05

Stud-I/I-13	Fastened	97.1	82.75	1.17	1.07
Stud-I/I-14	Fastened	91.5	82.75	1.11	1.01
Average				**1.098**	**1.00**
COV					**0.090**
Average for Unfastened		**87.38**			**0.96**
COV		0.135			0.135
Average for Fastened		**94.28**			**1.04**
COV		0.042			0.042

Note: Calculated values are for 2 stiffeners. 1 kN = 224.8 lbs, 1 mm = 0.0394 in.

Table 4.6.4: Analyses of Fastening Joist to Bearing Supports
(Stud Stiffeners, Intermediate Location, Outside)

Test Designation	Fastened or Unfastened to Support	Tested Load, C_t (kN)	Yielding $C_y = F_y A_e$ (kN)	Test/Calc C_t / C_y	Test/Calc $C_t / 0.999 C_y$
Stud-I/O-5	Unfastened	79.2	82.75	0.96	0.96
Stud-I/O-6	Unfastened	75.9	82.75	0.92	0.92
Stud-I/O-7	Unfastened	83.9	83.59	1.00	1.00
Stud-I/O-8	Unfastened	79.2	83.59	0.95	0.95
Stud-I/O-9	Fastened	77.3	82.75	0.93	0.93
Stud-I/O-10	Fastened	79.5	82.75	0.96	0.96
Stud-I/O-11	Fastened	87.9	83.59	1.05	1.05
Stud-I/O-12	Fastened	87.8	83.59	1.05	1.05
Stud-I/O-13	Unfastened	89.9	83.59	1.08	1.08
Stud-I/O-14	Unfastened	91.1	83.59	1.09	1.09
Average				**0.999**	**1.00**
COV					**0.064**
Average for Unfastened		**83.19**			**1.00**
COV		0.075			0.036
Average for Fastened		**83.10**			**1.00**
COV		0.067			0.061

Note: Calculated values are for 2 stiffeners. 1 kN = 224.8 lbs, 1 mm = 0.0394 in.

Table 4.6.5: Analyses of Fastening Joist to Bearing Supports
(Track Stiffeners, Intermediate Location, Inside)

Test Designation	Fastened or Unfastened to Support	Tested Load, C_t (kN)	Yielding $C_y = F_y A_e$ (kN)	Test/Calc C_t / C_y	Test/Calc $C_t / 1.038 C_y$
Track-I/I-1	Unfastened	66.3	67.02	0.99	0.95
Track-I/I-2	Unfastened	74.85	67.02	1.12	1.08
Track-I/I-3	Fastened	62.55	67.07	0.93	0.90
Track-I/I-4	Fastened	73.65	67.07	1.10	1.06
Track-I/I-5	Unfastened	69.2	67.04	1.03	0.99

Track-I/I-6	Unfastened	66.5	67.02	0.99	0.96
Track-I/I-7	Fastened	71.9	67.02	1.07	1.03
Track-I/I-8	Fastened	71.9	67.02	1.07	1.03
Average				**1.038**	**1.00**
COV				0.061	0.061
Average for Unfastened		**69.21**			**0.99**
COV		0.058			0.058
Average for Fastened		**70.00**			**1.01**
COV		0.072			0.072

Note: Calculated values are for 2 stiffeners. 1 kN = 224.8 lbs, 1 mm = 0.0394 in.

4.6.2   Effect of Fastening the Joist to the Support

Investigations into web crippling [9] have shown that fastening the joist flanges to the bearing supports can have a measurable impact on the web crippling capacity, particularly for Z-sections and multiple web sections. For C-section, the impact is not as significant. Testing of unreinforced C-sections has shown that fastening the flanges to the supports generally increases the capacity, but not more than 10%. This behavior was also observed for the C-sections with bearing stiffeners, as summarized in Table 4.6.6.

Table 4.6.6: Comparison of Fastened and Unfastened Test Results

Test Configuration		Reduction Factor	Difference
Stud Stiffeners, End Location, Inside	Unfastened	0.96	+ 8%
	Fastened	1.04	
Stud Stiffeners, End Location, Outside	Unfastened	1.02	- 5%
	Fastened	0.97	
Stud Stiffeners, Intermediate Location, Inside	Unfastened	0.96	+ 8%
	Fastened	1.04	
Stud Stiffeners, Intermediate Location, Outside	Unfastened	1.00	0
	Fastened	1.00	
Track Stiffeners, Intermediate Location, Inside	Unfastened	0.99	+ 2%
	Fastened	1.01	

The results shown in Table 4.6.6 could support the theory that the capacity of a C-section with bearing stiffeners is a combination of both the web crippling capacity of the joist as well as the bearing capacity of the stiffener. If the bearing stiffener was carrying all of the load at the ultimate limit state, there should be no significant difference between the fastened and unfastened assemblies. Since tests show a difference, some load is being carried by the joist web. It could also be argued, however, that the results in Table 4.6.6 can be explained by experimental error.

The load carried by the joist is a function of the location of the bearing stiffener. When the stiffener is on the back of the joist, the load is transferred into the stiffener directly and immediately. Since the bearing stiffener subject to axial compression is much stiffer than the C-section subject to a two-flange-loading,

the majority of the load will be carried by the stiffener. This assumption appears to be borne out by results shown in Table 4.6.6. There is little or no effect of fastening the flanges when the stiffener is on the outside of the joist.

5   MEASURING THE FASTENER FORCES AND THE WEB CRIPPLING CAPACITY

5.1   OBJECTIVE

The objective of this phase of the work was to measure the web crippling capacity of the joist and the forces developed in the fasteners caused by the joist web buckling. The web crippling capacity is the serviceability limit state for the assembly, and the fastener forces are used in the calibration of the finite element model.

5.2   SPECIMEN CONFIGURATIONS

A total of 96 test specimens were constructed and tested covering the following range of variables:

- 203 and 305 mm (8 and 12 in.) deep joists of different thickness and material properties,
- 92 mm (3-5/8 in.) stud stiffeners with 38 mm (1-1/4 in.) wide flanges,
- 3V and 4H screw fastener patterns,
- variations in the location of the fastener(s) closest to the top flange (h/4, h/6 and h/12),
- end and intermediate locations for the stiffeners.

These assembly configurations are illustrated in Figure 5.2.1. The material properties and stiffener dimensions are provided in Appendix A.
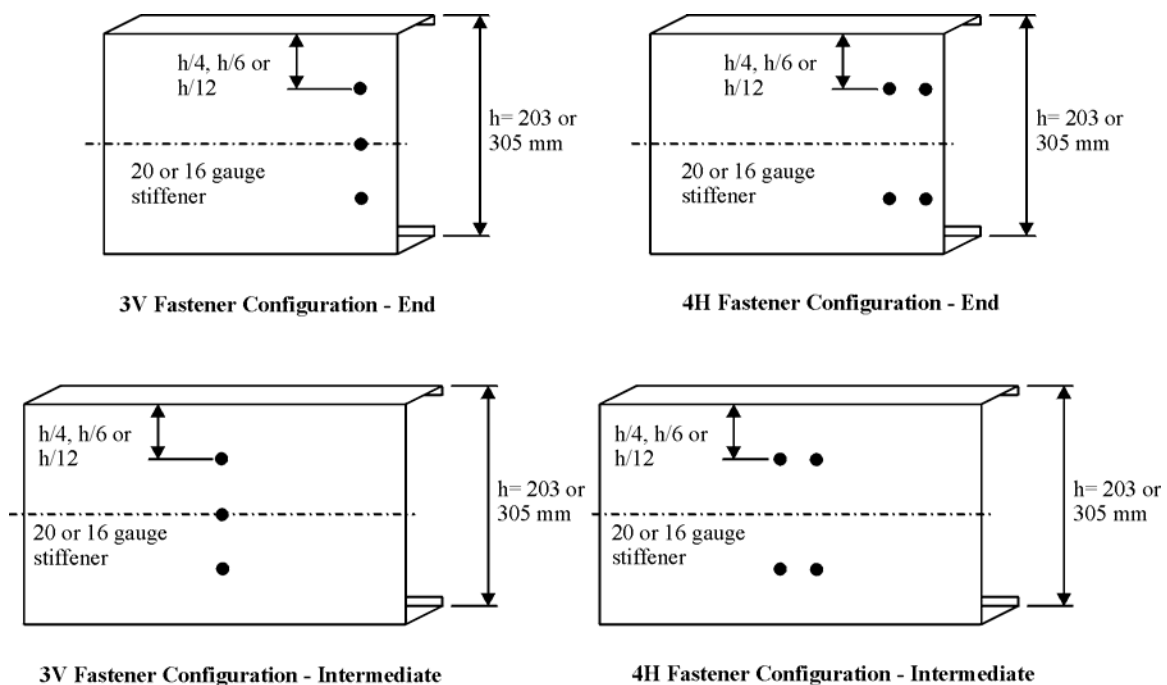
Figure 5.2.1 Configuration of the Assemblies Tested for Web Crippling and Fastener Forces

5.3 TEST PROCEDURES

A typical test assembly is shown in Figure 5.3.1. The test specimen was constructed such that four tests could be carried out on each specimen: two end and two intermediate locations. In all cases the bearing plates were 100 mm wide on top and bottom. The fasteners used to connect the joist to the stiffener were #10 self drilling screws. During the tests the following data was recorded: applied load, deflection of the upper bearing plate, loads at two of the fasteners, and deformed shape at failure.
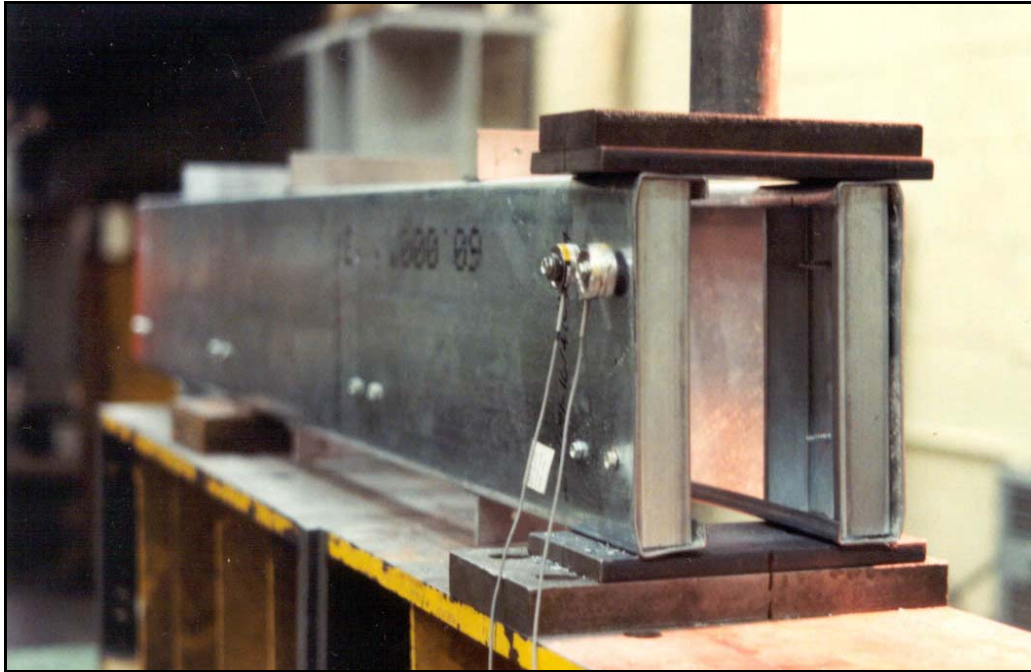
Figure 5.3.1: Typical Test Set-Up for Measuring Fastener Forces and Web Crippling

5.4 MEASURING THE WEB CRIPPLING LOADS

The test specimens were subjected to either end or interior two-flange loading. A typical load-deflection curve from one of these tests is shown in Figure 5.4.1. The initial curved portion corresponds to the flange rotation and web crippling of the joist as described in Figure 4.2.1. The final steeper portion of the curve corresponds to the condition where the joist flange has collapsed onto the end of the stiffener and the load is transferred into the stiffener through end bearing. The web crippling load was taken as the inflection point on the load deflection curve corresponding to the point where the joist flange has collapsed onto the end of the stiffener. This point was measured graphically from the load-deflection curves plotted for each of the tested assemblies.

36
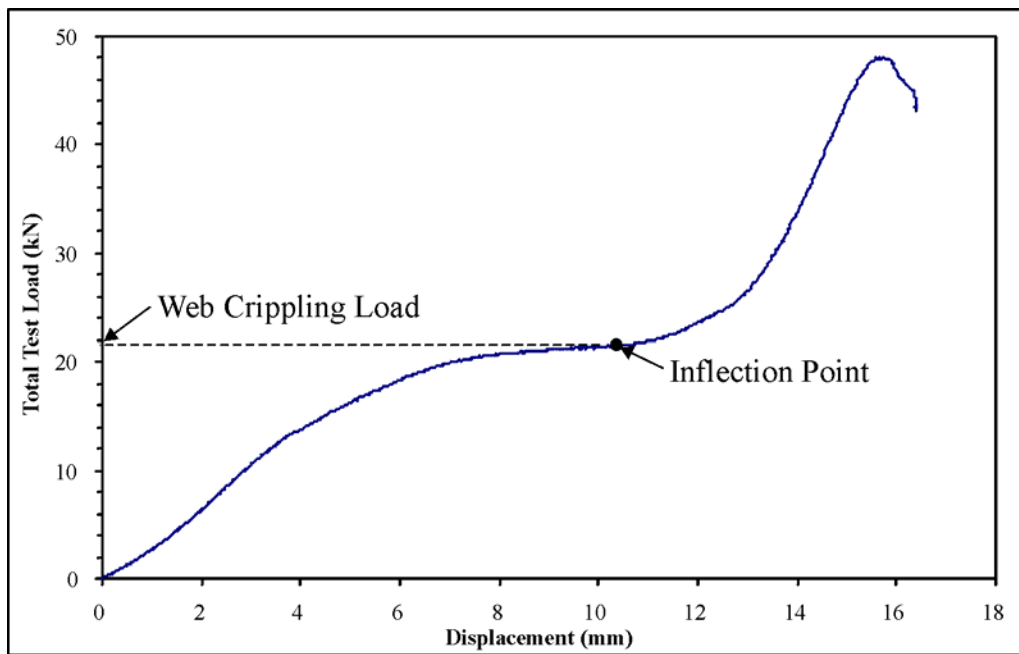
Figure 5.4.1: Determining the Web Crippling Capacity from a Load-Deflection Curve

5.5   MEASURING THE FASTENER FORCES

The second objective of this phase of the study was to measure the forces developed in the fasteners that connect the joist to the stiffener. The same series of tests described in the previous section that were used to determine the web crippling capacity were also instrumented to measure the fastener loads. A typical test set-up is illustrated in the photograph in Figure 5.5.1.

Small load cells were installed under the screws, which were able to measure the force exerted on the fastener caused by the joist web buckling. In order for the load cell under the screw head to measure any force, a pilot hole was drilled in the joist web that was larger than the diameter of the screw but smaller than the diameter of the load cell. This created a condition where the clamping action between the stiffener and the joist web was transferred through the load cell.

When the screws were installed they were given an initial pre-load that would correspond to the clamping force generated during the normal screw installation. The load-deflection curves for the fastener forces (see Figure 5.5.2) all start from a load corresponding to this pre-load. The attached load cell does not begin to record any additional load until the force generated in the fastener, as a result of web buckling, has exceeded the pre-load amount. In the three-screw configuration illustrated in Figure 5.5.2, the screw at the centre of the joist does not carry any additional load since the deformation of the joist web is towards the stiffener, not away from it.
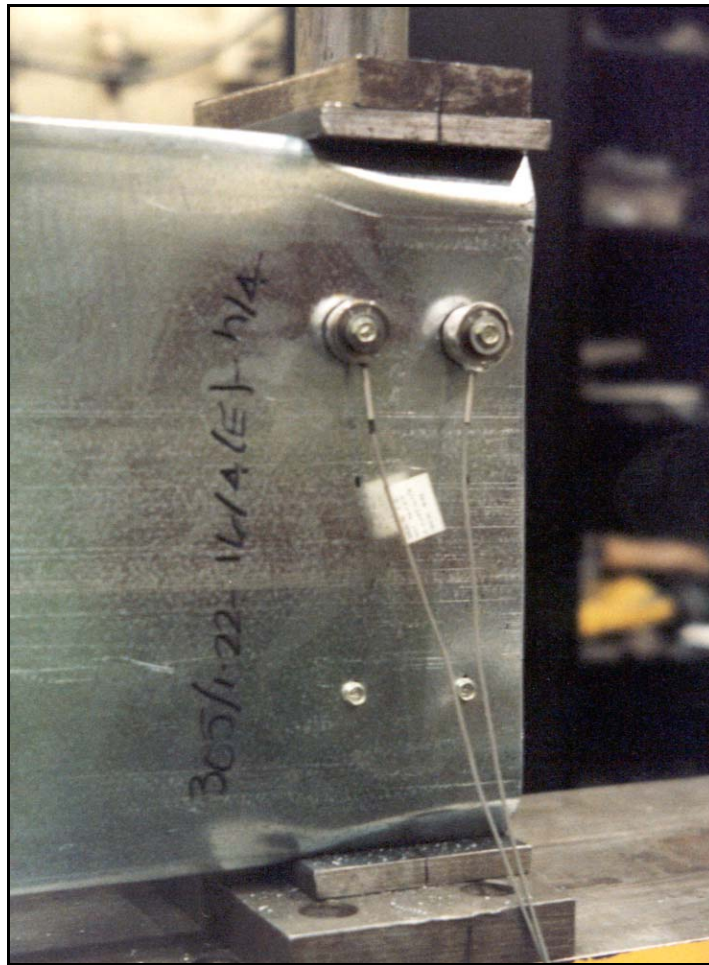
Figure 5.5.1: Photograph of Load Cells Used for Measuring Fastener Forces
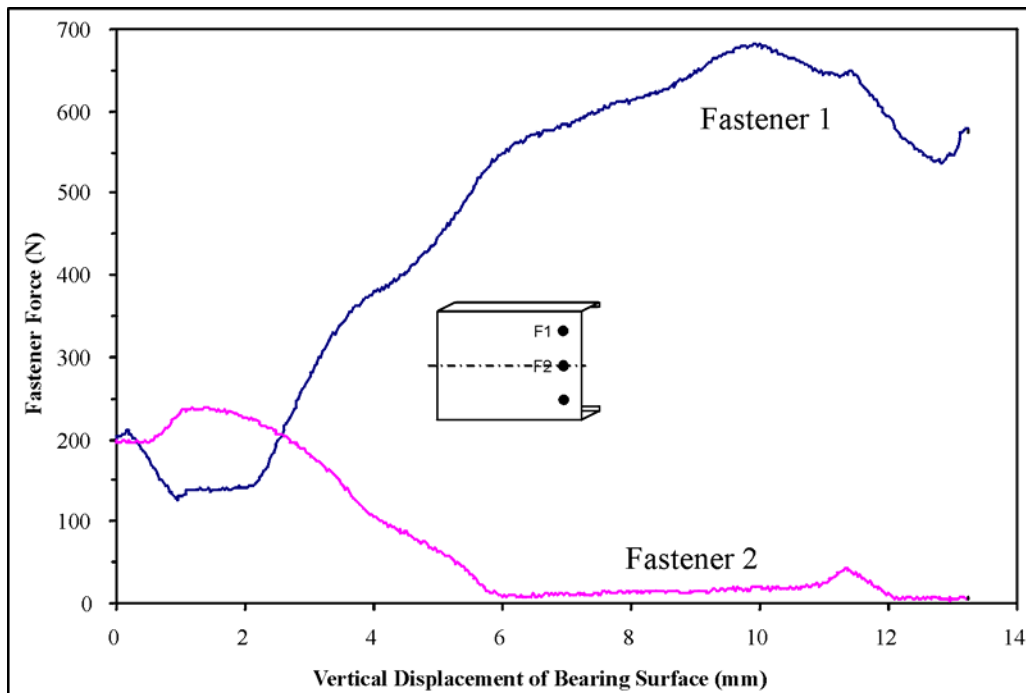
Figure 5.5.2: Measured Fastener Forces for Test Assembly Stud-E/I-67

5.6 TEST RESULTS

The material properties, component dimensions and test results are provided in Table 5.6.1 for the end-two-flange loading and in Table 5.6.2 for the interior-two-flange loading. The fastener pattern and numbering (F1 and F2) corresponds to the layouts shown in Figure 5.2.1. Where fastener force is recorded as being less than a particular values (e.g. F2 < 200) this indicates that the force in the fastener did not exceed the initial pre-load amount.

Table 5.6.1: Tested Web Crippling and Fastener Forces for Stud-End-Inside

| Test Designation | Fastener Pattern | Measured Fastener Forces | | Measured Web Crippling[1] (kN) | Joist | | | Stiffener | | Top Screw Location |
		F1 (N)	F2 (N)		Thickness (mm)	Yield F_y (MPa)	Depth d (mm)	Thickness (mm)	Yield (MPa)	
Stud-E/I-62	3V	1100	1170	11.6	1.21	332	305	1.50	399	h/12
Stud-E/I-63	3V	1270	1240	7.7	1.21	332	305	0.85	337	h/12
Stud-E/I-64	3V	1090	<200	8.7	1.21	332	305	1.50	399	h/6
Stud-E/I-65	3V	960	590	8.7	1.21	332	305	0.85	337	h/6
Stud-E/I-66	3V	970	<700	7.8	1.21	332	305	1.50	399	h/4
Stud-E/I-67	3V	680	<200	7.8	1.21	332	305	0.85	337	h/4
Stud-E/I-68	3V	1230	1050	10.9	1.21	323	203	1.50	399	h/12
Stud-E/I-69	3V	760	820	N/R	1.21	323	203	0.85	337	h/12
Stud-E/I-70	3V	830	<600	9.3	1.21	323	203	1.50	399	h/6
Stud-E/I-71	3V	<1260	<1260	9.5	1.21	323	203	0.85	337	h/6
Stud-E/I-72	3V	1020	<200	8.5	1.21	323	203	1.50	399	h/4
Stud-E/I-73	3V	970	<200	8.2	1.21	323	203	0.85	337	h/4
Stud-E/I-74	4H	1200	1030	14.5	1.21	323	203	1.50	399	h/12
Stud-E/I-75	4H	700	630	8.5	1.21	323	203	0.85	337	h/12
Stud-E/I-76	4H	1170	900	11.0	1.21	323	203	1.50	399	h/6
Stud-E/I-77	4H	610	590	9.8	1.21	323	203	0.85	337	h/6
Stud-E/I-78	4H	460	630	8.8	1.21	323	203	1.50	399	h/4
Stud-E/I-79	4H	680	450	8.1	1.21	323	203	0.85	337	h/4
Stud-E/I-80	4H	650	600	11.0	1.21	332	305	1.50	399	h/12
Stud-E/I-81	4H	740	300	7.0	1.21	332	305	0.85	337	h/12
Stud-E/I-82	4H	810	760	6.5	1.21	332	305	1.50	399	h/6
Stud-E/I-83	4H	850	540	7.5	1.21	332	305	0.85	337	h/6
Stud-E/I-84	4H	960	760	7.3	1.21	332	305	1.50	399	h/4
Stud-E/I-85	4H	610	600	7.3	1.21	332	305	0.85	337	h/4
Stud-E/I-86	4H	1030	1030	20.5	1.49	385	305	1.50	399	h/12
Stud-E/I-87	4H	590	490	10.0	1.49	385	305	0.85	337	h/12
Stud-E/I-88	4H	1220	820	15.5	1.49	385	305	1.50	399	h/6
Stud-E/I-89	4H	1020	720	11.5	1.49	385	305	0.85	337	h/6
Stud-E/I-90	4H	1260	1190	12.5	1.49	385	305	1.50	399	h/4
Stud-E/I-91	4H	660	470	12.0	1.49	385	305	0.85	337	h/4
Stud-E/I-92	3V	1000	2050	13.0	1.49	385	305	1.50	399	h/12
Stud-E/I-93	3V	550	1210	11.8	1.49	385	305	0.85	337	h/12

Stud-E/I-94	3V	1480	<370	13.8	1.49	385	305	1.50	399	h/6
Stud-E/I-95	3V	1540	<600	13.0	1.49	385	305	0.85	337	h/6
Stud-E/I-96	3V	1570	<630	12.8	1.49	385	305	1.50	399	h/4
Stud-E/I-97	3V	1000	<250	12.3	1.49	385	305	0.85	337	h/4
Stud-E/I-98	3V	1060	2010	24.0	1.83	413	203	1.50	399	h/12
Stud-E/I-99	3V	<830	1910	P/U	1.83	413	203	0.85	337	h/12
Stud-E/I-100	3V	2200	1130	20.5	1.83	413	203	1.50	399	h/6
Stud-E/I-101	3V	<750	1980	P/U	1.83	413	203	0.85	337	h/6
Stud-E/I-102	3V	1900	<900	21.0	1.83	413	203	1.50	399	h/4
Stud-E/I-103	3V	<1400	1760	19.0	1.83	413	203	0.85	337	h/4
Stud-E/I-104	4H	1760	1930	16.8	1.83	413	203	1.50	399	h/12
Stud-E/I-105	4H	890	950	16.3	1.83	413	203	0.85	337	h/12
Stud-E/I-106	4H	1650	1860	21.5	1.83	413	203	1.50	399	h/6
Stud-E/I-107	4H	1080	1590	16.5	1.83	413	203	0.85	337	h/6
Stud-E/I-108	4H	1350	1350	21.3	1.83	413	203	1.50	399	h/4
Stud-E/I-109	4H	1610	1380	17.0	1.83	413	203	0.85	337	h/4

Notes:
(1) Measured web crippling capacity is the average capacity for a single stiffener.
(2) N/R = value not recorded
(3) P/U = screw pull-out of fastener
(4) 1 kN = 224.8 lbs, 1 N = 0.2248 lbs, 1 mm = 0.0394 in., 1 MPa = 0.145 ksi

Table 5.6.2: Tested Web Crippling and Fastener Forces for Stud-Intermediate-Inside

Test Designation	Fastener Pattern	Measured Fastener Forces		Measured Web Crippling[1] (kN)	Joist			Stiffener		Top Screw Location
		F1 (N)	F2 (N)		Thickness (mm)	Yield F_y (MPa)	Depth d (mm)	Thickness (mm)	Yield (MPa)	
Stud-I/I-15	3V	<1510	<1510	12.5	1.21	332	305	1.50	399	h/12
Stud-I/I-16	3V	880	<830	12.0	1.21	332	305	0.85	337	h/12
Stud-I/I-17	3V	550	<200	11.6	1.21	332	305	1.50	399	h/6
Stud-I/I-18	3V	380	320	11.2	1.21	332	305	0.85	337	h/6
Stud-I/I-19	3V	1070	<870	10.9	1.21	332	305	1.50	399	h/4
Stud-I/I-20	3V	<850	<850	11.3	1.21	332	305	0.85	337	h/4
Stud-I/I-21	3V	1680	530	14.5	1.21	323	203	1.50	399	h/12
Stud-I/I-22	3V	930	550	12.3	1.21	323	203	0.85	337	h/12
Stud-I/I-23	3V	1060	<550	12.0	1.21	323	203	1.50	399	h/6
Stud-I/I-24	3V	<850	<850	11.0	1.21	323	203	0.85	337	h/6
Stud-I/I-25	3V	710	<200	11.8	1.21	323	203	1.50	399	h/4
Stud-I/I-26	3V	520	<200	11.4	1.21	323	203	0.85	337	h/4
Stud-I/I-27	4H	1150	1090	14.0	1.21	323	203	1.50	399	h/12
Stud-I/I-28	4H	420	350	12.5	1.21	323	203	0.85	337	h/12
Stud-I/I-29	4H	580	660	12.5	1.21	323	203	1.50	399	h/6
Stud-I/I-30	4H	370	560	12.3	1.21	323	203	0.85	337	h/6
Stud-I/I-31	4H	430	550	11.3	1.21	323	203	1.50	399	h/4
Stud-I/I-32	4H	280	450	11.3	1.21	323	203	0.85	337	h/4
Stud-I/I-33	4H	760	790	14.3	1.21	332	305	1.50	399	h/12
Stud-I/I-34	4H	310	480	12.8	1.21	332	305	0.85	337	h/12
Stud-I/I-35	4H	790	<570	12.0	1.21	332	305	1.50	399	h/6
Stud-I/I-36	4H	360	400	10.8	1.21	332	305	0.85	337	h/6

Stud-I/I-37	4H	760	<700	11.5	1.21	332	305	1.50	399	h/4
Stud-I/I-38	4H	<380	400	10.8	1.21	332	305	0.85	337	h/4
Stud-I/I-39	4H	930	950	24.0	1.49	385	305	1.50	399	h/12
Stud-I/I-40	4H	680	600	20.0	1.49	385	305	0.85	337	h/12
Stud-I/I-41	4H	830	860	20.8	1.49	385	305	1.50	399	h/6
Stud-I/I-42	4H	540	500	20.3	1.49	385	305	0.85	337	h/6
Stud-I/I-43	4H	540	700	18.5	1.49	385	305	1.50	399	h/4
Stud-I/I-44	4H	350	400	19.0	1.49	385	305	0.85	337	h/4
Stud-I/I-45	3V	1290	810	22.5	1.49	385	305	1.50	399	h/12
Stud-I/I-46	3V	430	230	20.5	1.49	385	305	0.85	337	h/12
Stud-I/I-47	3V	870	580	20.0	1.49	385	305	1.50	399	h/6
Stud-I/I-48	3V	<850	<850	19.0	1.49	385	305	0.85	337	h/6
Stud-I/I-49	3V	820	<520	18.8	1.49	385	305	1.50	399	h/4
Stud-I/I-50	3V	700	<650	18.8	1.49	385	305	0.85	337	h/4
Stud-I/I-51	3V	1870	1590	31.8	1.83	413	203	1.50	399	h/12
Stud-I/I-52	3V	1830	<1300	28.0	1.83	413	203	0.85	337	h/12
Stud-I/I-53	3V	2100	<700	29.3	1.83	413	203	1.50	399	h/6
Stud-I/I-54	3V	<1050	<1050	26.0	1.83	413	203	0.85	337	h/6
Stud-I/I-55	3V	1730	<650	26.8	1.83	413	203	1.50	399	h/4
Stud-I/I-56	3V	1350	<1180	26.8	1.83	413	203	0.85	337	h/4
Stud-I/I-57	4H	1780	1680	35.5	1.83	413	203	1.50	399	h/12
Stud-I/I-58	4H	1650	1350	28.3	1.83	413	203	0.85	337	h/12
Stud-I/I-59	4H	1800	1670	33.5	1.83	413	203	1.50	399	h/6
Stud-I/I-60	4H	<1990	<1990	29.0	1.83	413	203	0.85	337	h/6
Stud-I/I-61	4H	1390	1520	31.0	1.83	413	203	1.50	399	h/4
Stud-I/I-62	4H	1210	990	27.3	1.83	413	203	0.85	337	h/4

Notes:
   (1) Measured web crippling capacity is the average capacity for a single stiffener.
   (2) N/R = value not recorded
   (3) P/U = screw pull-out of fastener
   (4) 1 kN = 224.8 lbs, 1 N = 0.2248 lbs, 1 mm = 0.0394 in., 1 MPa = 0.145 ksi

5.7   APPLICATION OF TEST RESUTS

This section has presented the results of tests measuring the web crippling capacity and fastener forces for a range of assembly configurations. This data will be used in Chapter 8 to calibrate a finite element model. The tests have also provided additional data on the ultimate strength of the assemblies, which is included in the analyses described in Chapter 9.

6   STRAIN GAUGE MEASUREMENTS

6.1   OBJECTIVE

The principal objective of this phase of the work was to understand the behavior of the stiffener and the joist web buckling, as well as providing data that can be used to calibrate a finite element model. One of the most direct methods of investigation is with strain gauge measurements. The data from these gauges provides information to help determine the distribution of forces in the stiffener and the joist web. Three tests of this type have been conducted. With each additional test, the test procedures improved and more useful data was collected. The discussion that follows describes only one of the tests to illustrate the test procedures and the analysis.

6.2   SPECIMEN PROPERTIES

Joist and stiffener specimens representative of typical construction practice were used, the specific dimensions of which are shown in Figures 6.2.1 and 6.2.2. Coupons were taken from the stiffener and joist material and standard tensile tests were conducted. These material properties are recorded in Table 6.2.1.

Thickness (mm)	d1 (mm)	d2 (mm)	f1 (mm)	f2 (mm)	w1 (mm)	L (mm)
0.81	7	7	31	31	92	299

1 mm = 0.0394 in.
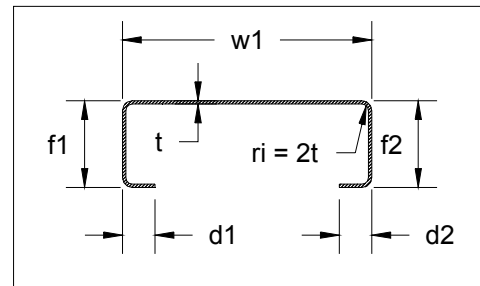
Figure 6.2.1: Stiffener Dimensions
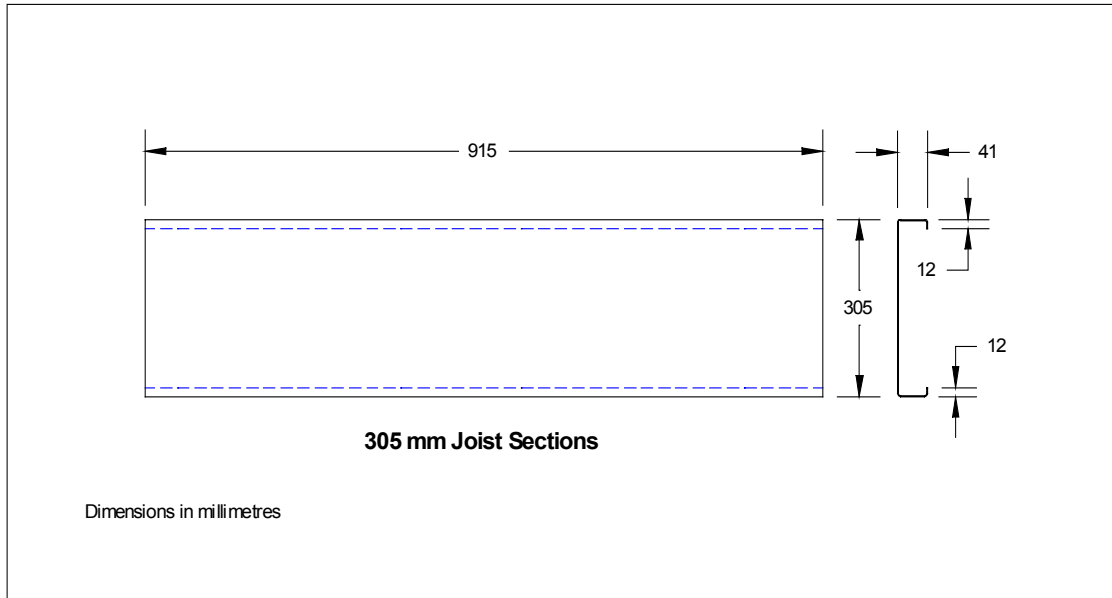
Figure 6.2.2: Joist Dimensions

Table 6.2.1: Material Properties

Specimen	Thickness (mm)	Yield Stress F_y (MPa)	Tensile Stress F_u (MPa)	% Elong.
305 mm C-Section Joist	1.24	307	360	35.3
92 mm C-Section Stiffener	0.81	349	372	31.3

Note: Reported values are the average of two tests, one from each specimen piece.
1 mm = 0.0394 in., 1 MPa = 0.145 ksi

Six pairs of strain gauges were positioned along the length of the stiffener as shown in Figure 6.2.3. By placing the gauges in these positions, the distribution of stresses along the two axes of the member could be calculated. The gauges were fixed close to the corner radii to avoid areas of possible local buckling. The pairs closest to the top of the stiffener were positioned 25 mm (1 in.) away from the end to avoid the area where local buckling has been observed to occur in previous tests. An additional six gauges are attached to the joist web, the results of which will be discussed in detail in section 6.4.
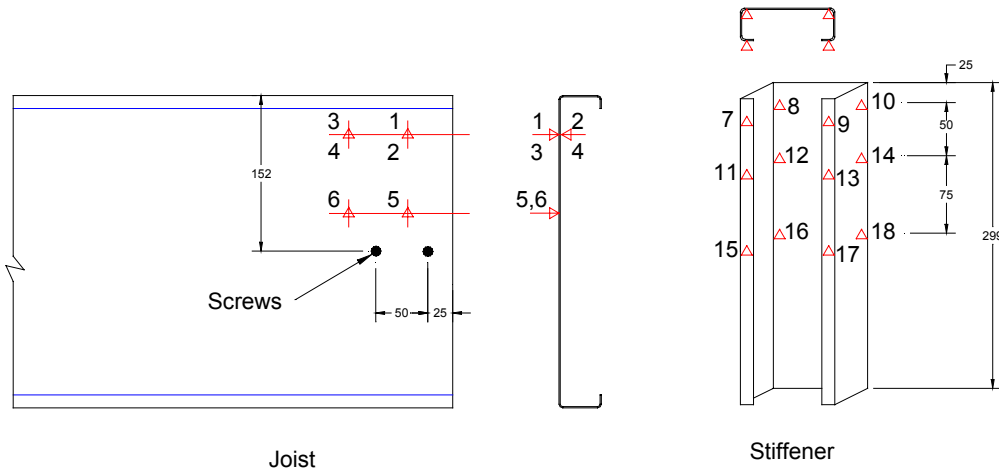
Figure 6.2.3: Strain Gauge Locations

6.3 STRAIN GAUGE RESULTS FOR THE STIFFENER

6.3.1 Strain Gauge Readings

Figures 6.3.1, 6.3.2 and 6.3.3 plot the strain gauge readings for the bearing stiffener during the loading cycle.
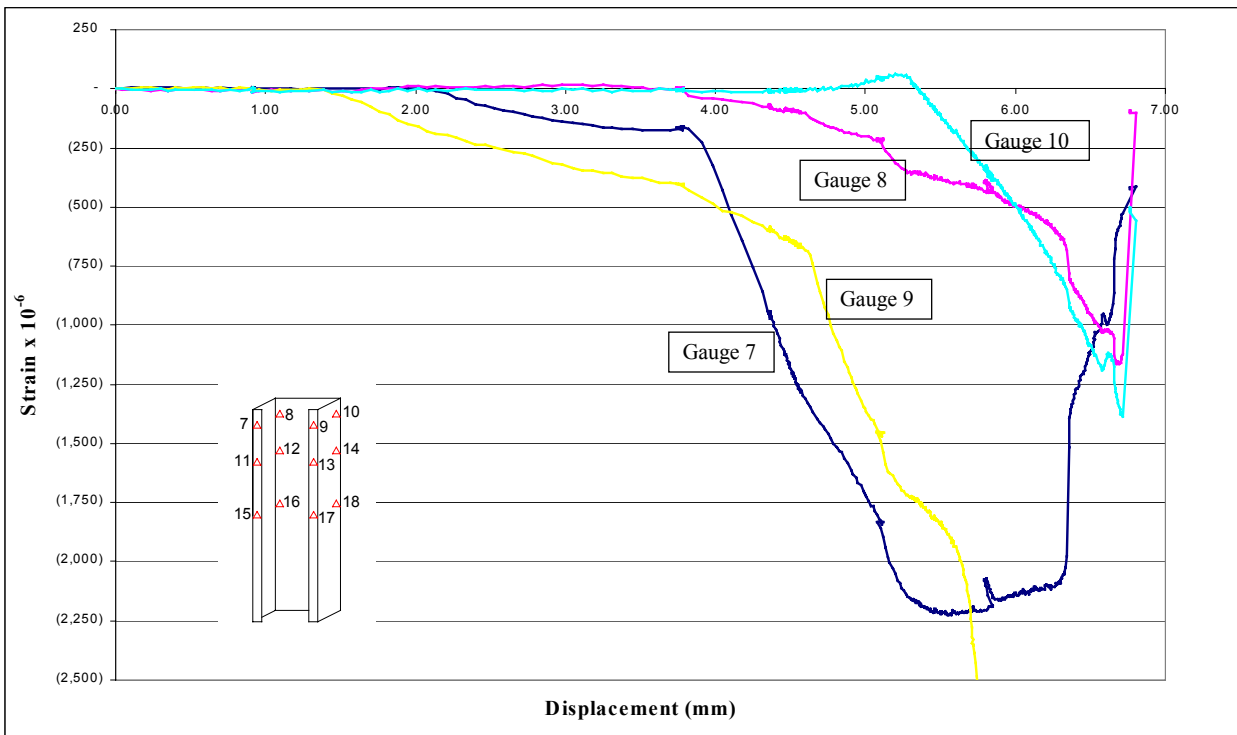
Figure 6.3.1: Strain Gauge Readings (Gauges 7 to 10) – 2H Screw Pattern

44
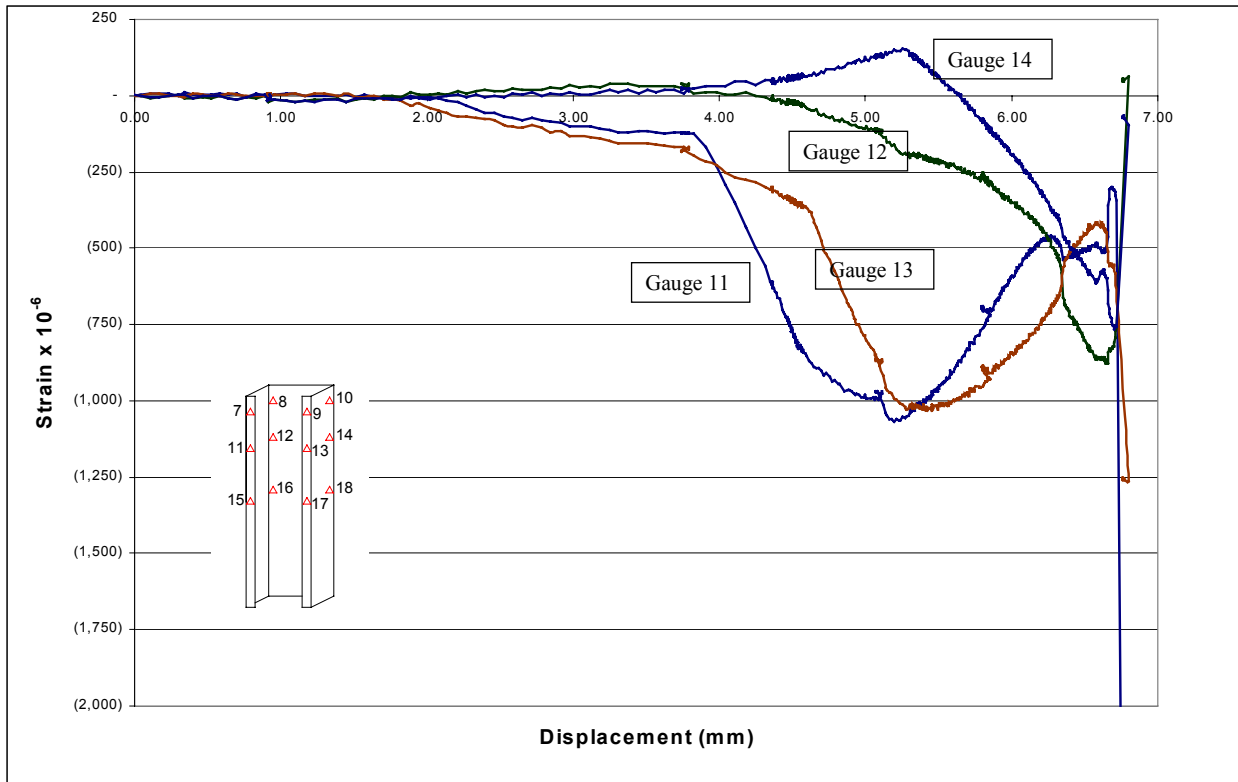
Figure 6.3.2: Strain Gauge Readings (Gauges 11 to 14) – 2H Screw Pattern
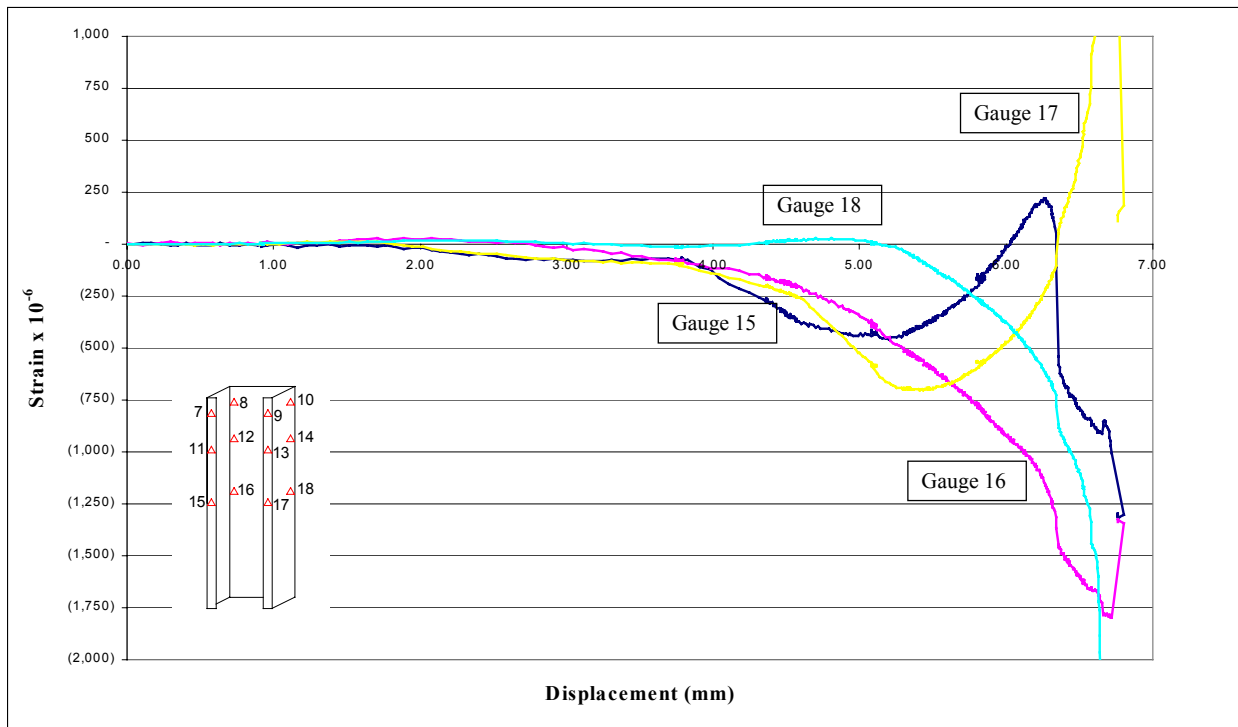
Figure 6.3.3: Strain Gauge Readings (Gauges 15 to 18) – 2H Screw Pattern

45

6.3.2   Discussion of the Results

The strain gauge readings for the stiffener are useful to help understand the general behavior of the stiffeners under load. The plot in Figure 6.3.1 for the gauges near the top of the stiffener show strains beginning in gauges 7 and 9 very early. This is caused by the initial rotation of the joist flanges under load. The flanges will first contact the lips of the stiffener flanges and start to transfer load eccentrically. Since the length of the stiffener is 6 mm (1/4 in.) shorter than the depth of the joist there is a gap between the stiffener and the joist flange, which affects the shape of the strain gauge plots. The stiffener does not become fully end bearing until the displacement has caused this gap to close. This is illustrated clearly in Figure 6.3.3 where there is very little strain until a displacement of 4 mm (5/32 in.) at which point the joist web would have buckled and collapsed the joist flange onto the end of the stiffener.

Once the stiffener is completely end bearing the strains increase rapidly. This is expected since the additional load at this point is being carried directly by the stiffener and no longer through the joist web. A point is reached at just over 5 mm (3/16) of displacement when the strains in the gauges 11, 13, 15, and 17 start to decrease. This corresponds to a distortional buckling mode of failure observed during the test. The flanges of the stiffener begin to rotate inward and redistribute the stress in the section. Near the failure load the strains again change radically due to local and then overall buckling of the stiffener.

6.4   STRAIN GAUGE RESULTS FOR THE JOIST

6.4.1   Strain Gauge Placement

Strain gauges were fixed to the joist web at the locations shown in Figure 6.4.1, and the gauge numbering is shown in Figure 6.2.3. These positions were selected based on observations of the deflected shape from previous tests. Strain gauges were attached to both sides of the web at the upper two locations, but only on the outside of the web at the two lower locations. Once the gauges were fixed in place and the leads soldered on, they were all checked to make sure there were no shorts and the gauge resistance was within specification. Uni-directional gauges were used orientated vertically to measure the principal stresses. Based on earlier tests, curvatures in the horizontal direction are relatively small and no large strain gauges were expected in this direction.
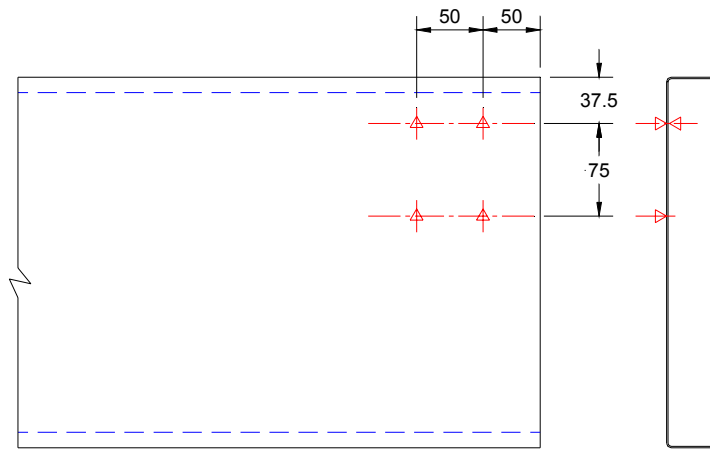
Dimensions in mm

Figure 6.4.1: Strain Gauge Locations

6.4.2 Strain Gauge Readings

Strain gauges were fixed to spots on the joist web as illustrated in Figures 6.4.1. Figure 6.4.2 shows the plot of these readings. Gauges 1,3,5 and 6 were on the outside of the joist web, and gauges 2 and 4 were on the inside of the web next to the stiffener.
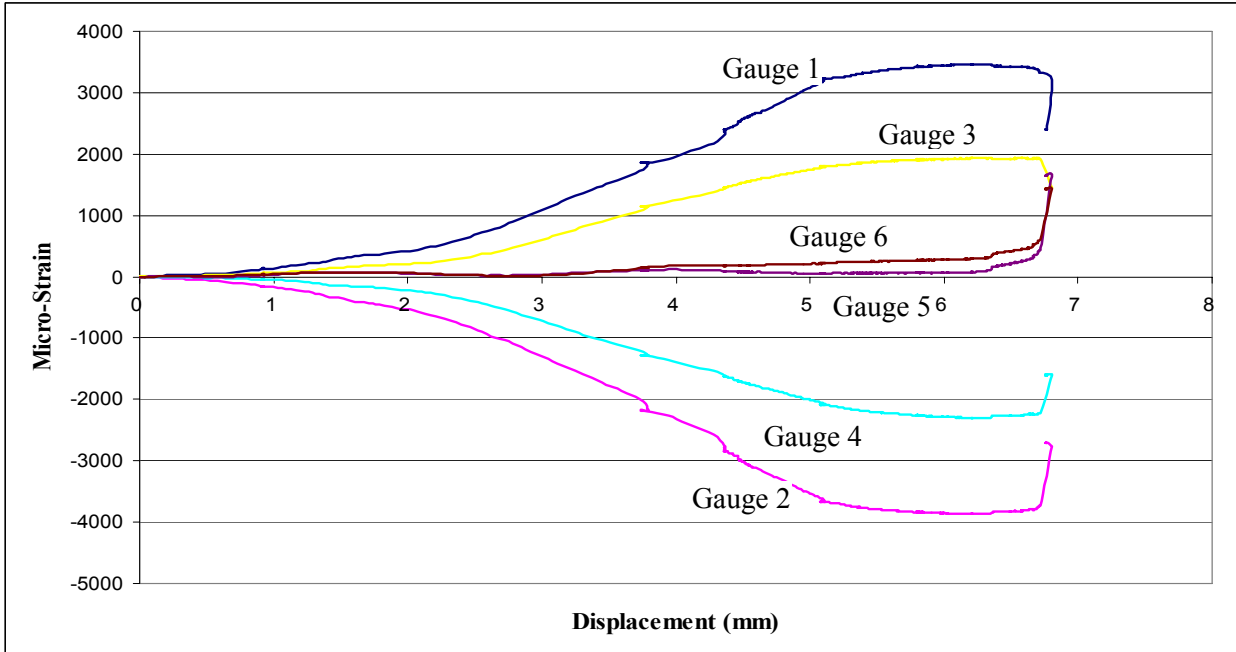
Figure 6.4.2: Joist Web Strain Gauge Readings

6.4.3   Discussion of the Results

The strain gauges for the joist readings confirms what would be expected based on the observed deformed shape. These results will be used in Section 7 in conjunction with the analysis of the measured web buckling, as well as being used in Section 8 to verify the finite element model.

7   WEB BUCKLING MEASUREMENTS AND ANALYSIS

7.1   OBJECTIVE AND SCOPE

The objective of this phase of the work was to provide physical data on the buckled shape of the joist web to determine the stresses in the joist web as well as verify the finite element model.

The scope of this work was as follows:

- Conduct a test of a C-section subjected to end-two-flange loading.
- Measure the deflected shape of the web at intervals during the load cycle.
- Mathematically model the deflected shape of the joist web and determine the in-plane strains due to bending.
- Determine the in-plane bending and axial stresses.

Three different web buckling tests were carried out. The following is a discussion of the last test conducted (which benefited from the experience gained in the first two tests) and presents the test methodology and analytical methods that are used.

7.2   SPECIMEN DIMENSIONS AND TEST SET-UP

7.2.1   Specimen Dimensions and Physical Properties

Figure 7.2.1 shows a photograph of the test specimen and test set-up. This is the same specimen used in the strain gauge measurement tests that was discussed in Section 6. The dimensions and material properties for the specimen are provided in Figures 6.2.1 and 6.2.1 and Table 6.2.1. Two fasteners were used to connect the joist web to the stiffener and were placed as indicated in Figure 7.2.2. The stiffener was positioned 5 mm (3/16 in.) in from the end of the joist to ensure bearing of the stiffener over its entire end area.
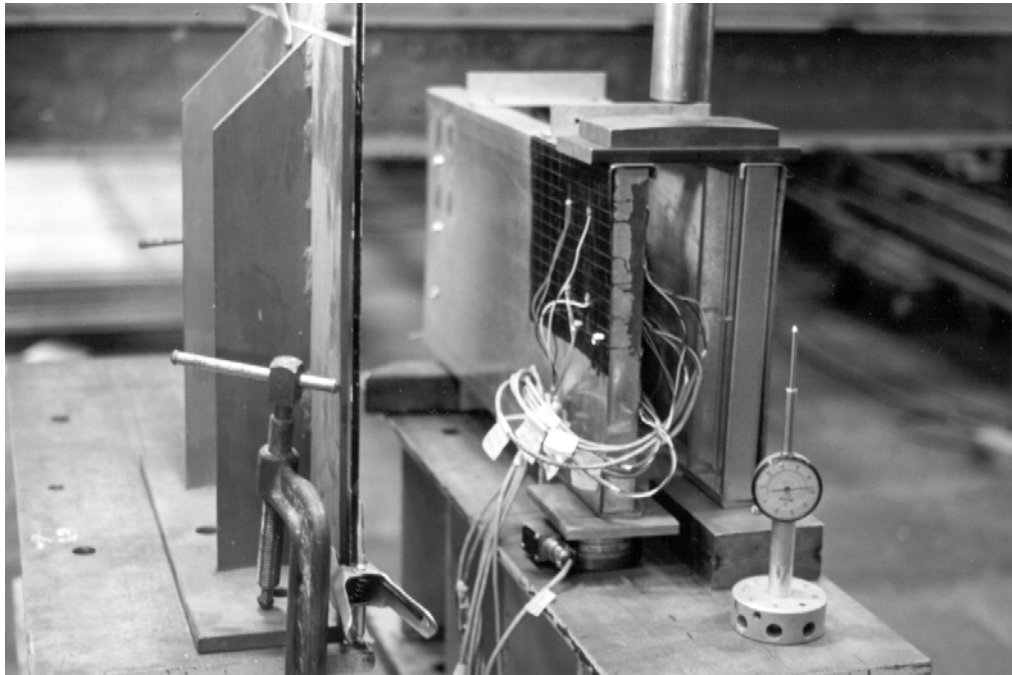
Figure 7.2.1: Photograph of Web Buckling Test Specimen
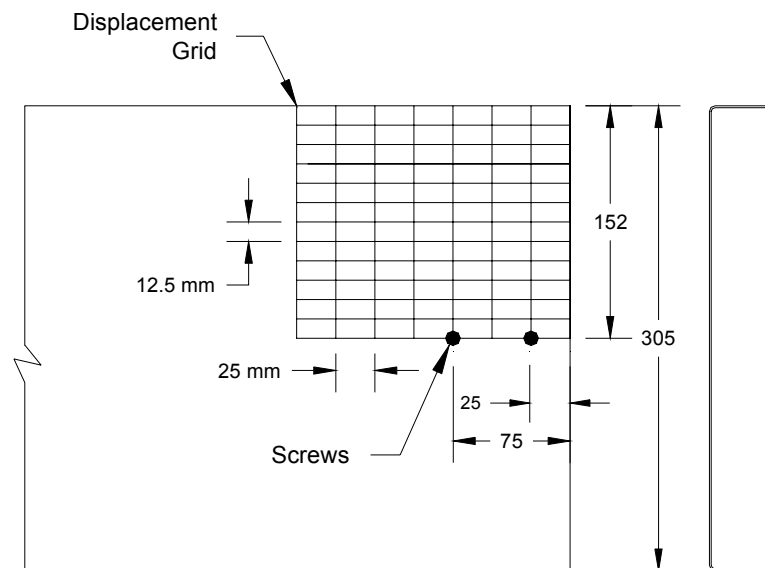
Figure 7.2.2: Displacement Grid and Fastener Location for Web Buckling Measurements

7.2.2   Marking the Displacement Grid

One objective of this experiment was to collect measurements of the deflected shape of the joist web. To do this, a grid was marked on the outside of the joist web as illustrated in Figure 7.2.2. The measurement points were selected to cover the entire area with a greater density in the vertical direction where the slope of the deflected shape would be greater. Increments of 12.5 mm (1/2 in.) were used vertically and 25 mm

(1 in.) increments horizontally. The grid covered only one half of the web depth since the deflected shape is typically symmetrical.

7.2.3   Measurement Devices

A dial gauge and an LVDT were used to measure the horizontal and vertical deflections. A rigid vertical reference plane was positioned to provide the necessary datum point on which a clean glass surface was mounted. A dial gauge was fixed to a movable base and positioned at each grid point sequentially and the distance measured between the joist web and the reference surface. Dial gauge measurements in 1/100 of a millimetre were recorded. An LVDT was used to measure the vertical deflection of the top bearing plate to give the overall shortening of the web. This device provided measurements in 1/10 of a millimetre.

In addition to measuring the deflected shape, two load cells were also used. One load cell was part of the hydraulic ram and recorded the total load applied to the entire specimen. The other load cell was positioned under the joist being measured to record its share of the total load. Each cell measured the load to within 1/100 of a kiloNewton.

7.2.4   Data Collection

Measurements were taken at five intervals: after an initial pre-load, and then at 25%, 50%, and 75% of the anticipated failure load and then finally at the failure load. Based on earlier tests, the failure load was predicted to be 40 kN. The load cell and strain gauge outputs were recorded with LabView, a computerized data collection system. Readings were taken at regular intervals during the load application and then paused during the time it took to measure the deflections with the dial gauge.

7.3   DATA COLLECTION

7.3.1   Deflected Shape of the Web

The data from the measurements of the web deflection at the five load increments are given in Appendix C. These measurements are relative to the deflected shape measured at the initial pre-load stage. The web profile at a load of 13.09 kN (2,940 lbs) (load on the single stiffener) is shown graphically in Figure 7.3.1. This represents only the upper half of the joist web. The load was applied over grid numbers A through E along row 0. The fasteners were located at grid points B13 and D13. At failure, the bearing stiffener was subject to local buckling in some elements and the forces exerted by the joist web caused the assembly to buckle out of plane. The deflected shape at the failure load is shown in Figure 7.3.2. The deflected shape prior to failure as shown in Figure 7.3.1 is typical of the types of failure modes most often observed, and subsequently was used for the analysis.
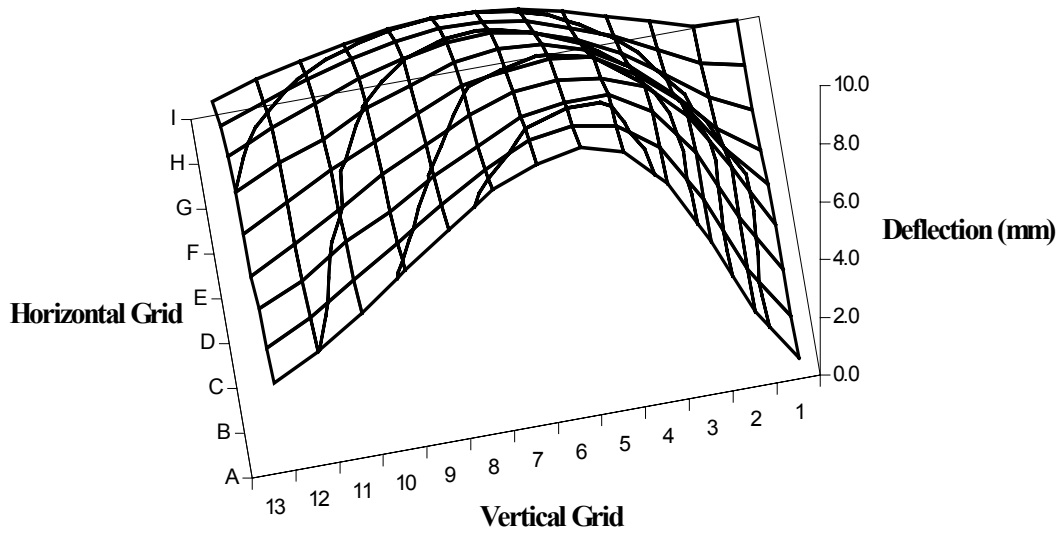
Figure 7.3.1: Measured Deflected Shape of the Joist Web at 13.09 kN
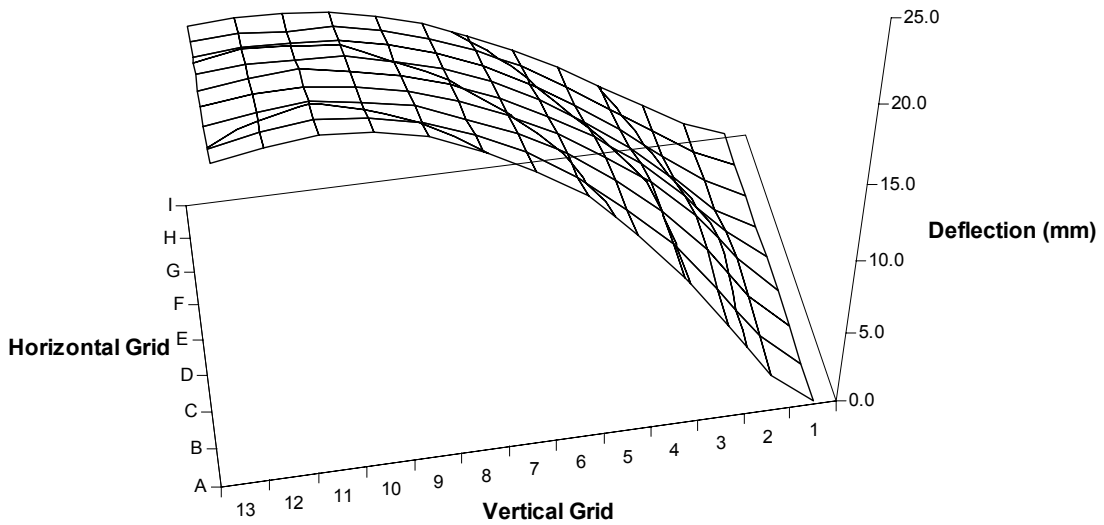
Figure 7.3.2: Measured Deflected Shape of the Joist Web at Failure Load of 15.80 kN

7.4   ANALYSIS

7.4.1   *Calculating the Plate Curvatures*

An equation fitting the deflected shape (at the 13.09 kN load level) was modeled using a polynomial trend line. The deflected shape and corresponding trend lines are shown in Figures 7.4.1 and 7.4.2. These curves plot the deflection along the vertical grid lines C and E, corresponding to the locations of the strain

gauges. Two additional curves are plotted in Figures 7.4.3 and 7.4.4 showing the deflected shapes along horizontal rows 3 and 10, also corresponding to the locations of the strain gauges.
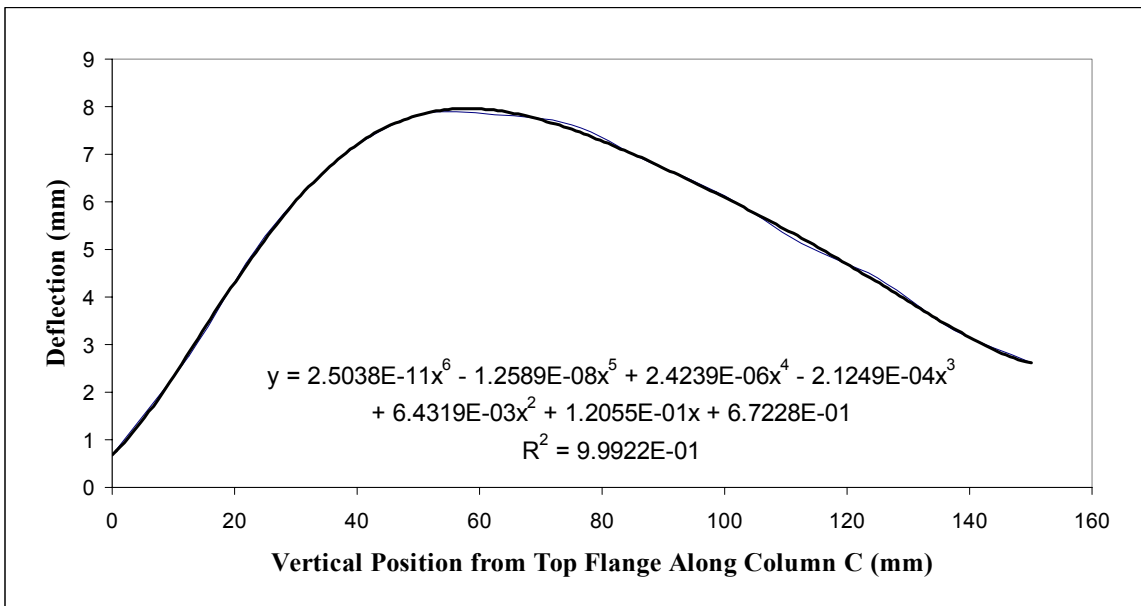
Figure 7.4.1: Deflected Shape Plot and Trend Line Along Column C
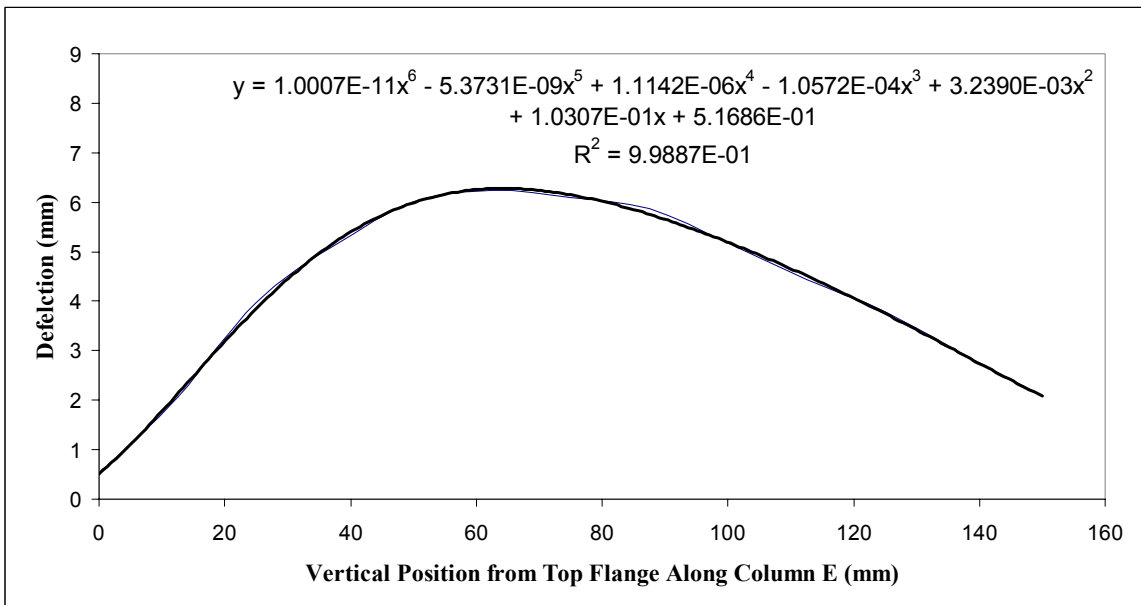
Figure 7.4.2: Deflected Shape Plot and Trend Line Along Column E

54
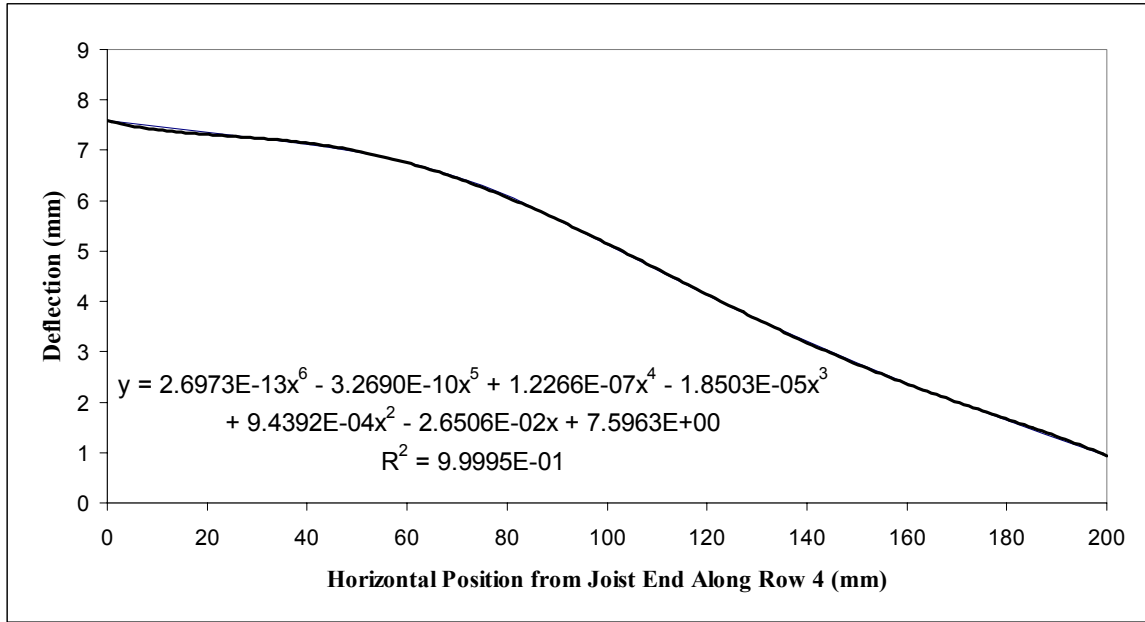
Figure 7.4.3: Deflected Shape Plot and Trend Line Along Row 4
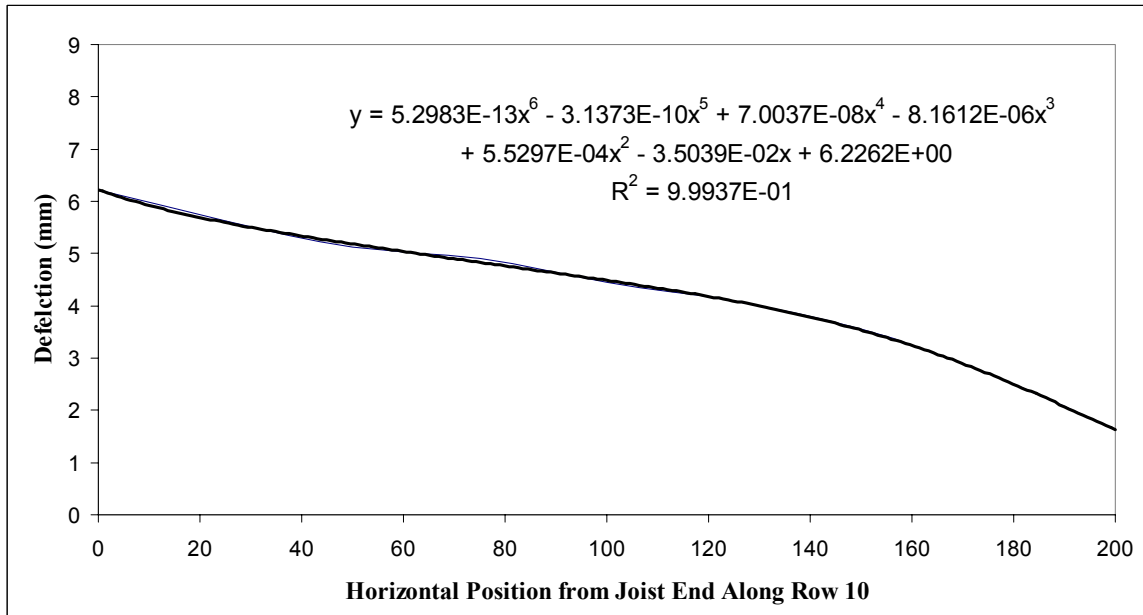
Figure 7.4.4: Deflected Shape Plot and Trend Line Along Row 10

7.4.2   Calculating the Bending Strains from the Deflected Shape

The Kirchhoff-Love hypothesis for the bending of plates states that plane sections remain plane after bending and the length of the neutral surface remains unchanged. This means that the strains due to bending will be linear across the plate thickness. Since the deflected shape is known, the curvature can be determined by integrating the trend lines and the strains calculated as follows:

$$\varepsilon_x = -\frac{z}{R_x} = -z\frac{\partial^2 w}{\partial x^2}$$

These calculations are presented in Table 5.2.2 for the principal strains in the vertical direction along the two rows C and E. The distance "z" is half the thickness of the web material, equal to 0.62 mm (0.024 in.). The horizontal strains along rows 3 and 10 were calculated in a similar manner and summarized in Table 7.4.2.

Table 7.4.1: Calculated Vertical Strains at Strain Gauge Locations

Vertical along Column C							
	x^6	x^5	x^4	x^3	x^2	x	C
y	2.5038E-11	-1.2589E-08	2.4239E-06	-2.1249E-04	6.4319E-03	1.2055E-01	6.7228E-01
dy/dx		1.5023E-10	-6.2945E-08	9.6956E-06	-6.3747E-04	1.2864E-02	1.2055E-01
d^2y/dx^2			7.5114E-10	-2.5178E-07	2.9087E-05	-1.2749E-03	1.2864E-02
x = 37.5			1.9775E+06	5.2734E+04	1.4063E+03	3.7500E+01	
d^2y/dx^2 =	-5.8352E-03						
Micro-strain =	" 3618	t = 0.62	**Compare to Gauges 1 and 2**				

Vertical along Column C							
	x^6	x^5	x^4	x^3	x^2	x	C
y	2.5038E-11	-1.2589E-08	2.4239E-06	-2.1249E-04	6.4319E-03	1.2055E-01	6.7228E-01
dy/dx		1.5023E-10	-6.2945E-08	9.6956E-06	-6.3747E-04	1.2864E-02	1.2055E-01
d^2y/dx^2			7.5114E-10	-2.5178E-07	2.9087E-05	-1.2749E-03	1.2864E-02
x = 112.5			1.6018E+08	1.4238E+06	1.2656E+04	1.1250E+02	
d^2y/dx^2 =	-6.1048E-04						
Micro-strain =	+378	t = 0.62	**Compare to Gauge 5**				

Vertical along Column E							
	x^6	x^5	x^4	x^3	x^2	x	C
y	1.0007E-11	-5.3731E-09	1.1142E-06	-1.0572E-04	3.2390E-03	1.0307E-01	5.1686E-01
dy/dx		6.0042E-11	-2.6866E-08	4.4568E-06	-3.1716E-04	6.4780E-03	1.0307E-01
d^2y/dx^2			3.0021E-10	-1.0746E-07	1.3370E-05	-6.3432E-04	6.4780E-03
x = 37.5			1.9775E+06	5.2734E+04	1.4063E+03	3.7500E+01	
d^2y/dx^2 =	-3.5801E-03						
Micro-strain =	" 2220	t = 0.62	**Compare to Gauges 3 and 4**				

Vertical along Column E							
	x^6	x^5	x^4	x^3	x^2	x	C
y	1.0007E-11	-5.3731E-09	1.1142E-06	-1.0572E-04	3.2390E-03	1.0307E-01	5.1686E-01
dy/dx		6.0042E-11	-2.6866E-08	4.4568E-06	-3.1716E-04	6.4780E-03	1.0307E-01
d^2y/dx^2			3.0021E-10	-1.0746E-07	1.3370E-05	-6.3432E-04	6.4780E-03
x = 112.5			1.6018E+08	1.4238E+06	1.2656E+04	1.1250E+02	

$d^2y/dx^2 =$	-5.8346E-04						
Micro-strain =	**+362**	t = 0.62	**Compare to Gauge 6**				

Table 7.4.2: Calculated Horizontal Strains at Strain Gauge Locations

Gauge Location	Micro-strain
Gauge 1 and 2	" 465
Gauge 3 and 4	" 139
Gauge 5	-46
Gauge 6	+44

7.4.3   Calculating the Stresses in the Web From the Balance of Internal Forces

The strains calculated in the preceding section can be attributed only to the bending component of the loads acting on the joist web, but there are also in-plane compressive forces. These in-plane stresses and strains can be determined in two ways. The first is to consider only the strain gauge readings. The sketches in Figure 7.4.5 show the strains across the web thickness as a linear distribution. The stresses are limited to the yield stress of the joist, $F_y = 307$ MPa. This yield stress corresponds to a yield strain of 1512×10^{-6}. The stresses across the web thickness can be determined from geometry and the resulting force components calculated.
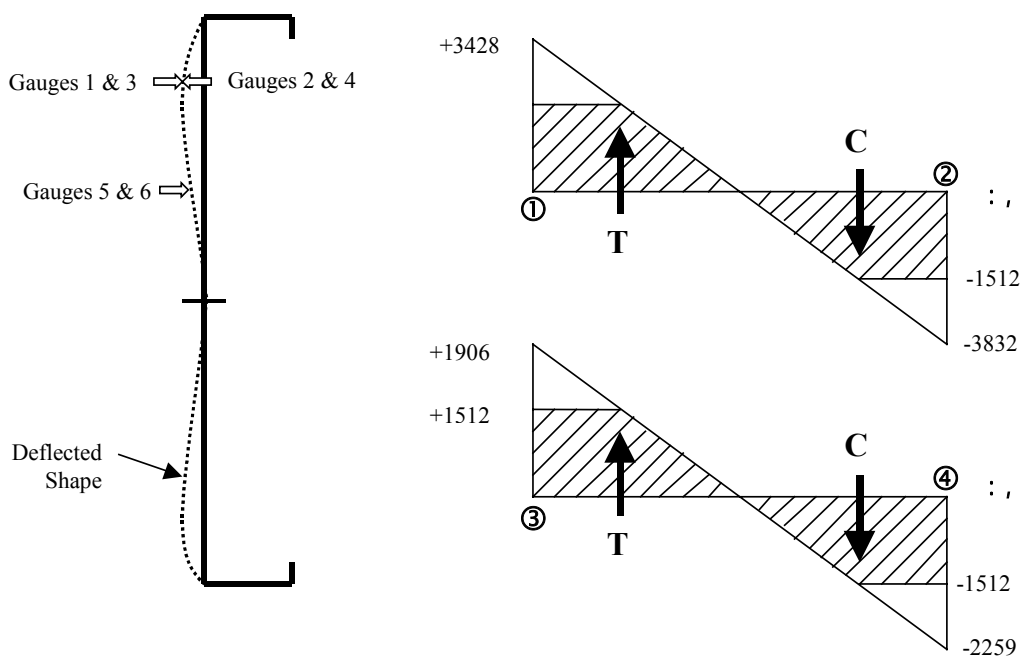
Figure 7.4.5: Calculated Vertical Stresses

57

At strain gauge locations 1 & 2:

        T = 140 N/mm of length   C = 161 N/mm of length

        Net compression = **21 N/mm = 17 MPa** (for 1.24 mm thick web)

At strain gauge locations 3 & 4:

        T = 105 N/mm of length   C = 137 N/mm of length

        Net compression = **32 N/mm = 26 MPa** (for 1.24 mm thick web)

7.4.4 Calculating the Stresses in the Web From Measured Curvatures

The in-plane stresses can also be determined using the strains calculated from the deflected shape along with the measured strains.

Table 7.4.3: Calculated In-Plane Strains and Stresses

	Gauge 1	**Gauge 2**	**Gauge 3**	**Gauge 4**
Measured micro-strain from strain gauges	+3428	-3832	+1906	-2259
Micro-strain from measured curvature	+3618	-3618	+2200	-2200
In-plane component of strain	-190	-214	-314	-39
Average in-plane compressive micro-strain	202		177	
Average in-plane compressive stress	**41 MPa**		**36 MPa**	

7.4.5 Calculating the Stresses in the Web From Web Crippling Calculations

One hypothesis about the behavior of a C-section with a bearing stiffener is that the capacity of the stiffened assembly is the addition of the web crippling capacity of the joist web and the axial capacity of the stiffener. Due to the restraint provided to the joist web by the stiffener, it can be argued that the web crippling of the stiffened joist behaves more like a built-up section than a single web member. This behavior can be also be used in the web buckling analysis. The web crippling capacity of a built-up I-section composed of two channels back-to-back, calculated according to the equation proposed by Beshara [9] is as follows:

$$P_r = Ct^2 F_y (\sin\theta)\left(1 - C_R \sqrt{R}\right)\left(1 + C_N \sqrt{N}\right)\left(1 - C_H \sqrt{H}\right)$$

Where,

        C   =   15.5

        C_R =   0.09

        C_N =   0.08

$$C_H \quad = \quad 0.04$$

$$h \quad = \quad 305 \text{ mm}$$

$$t \quad = \quad 1.24 \text{ mm}$$

$$F_y \quad = \quad 307 \text{ MPa}$$

$$\angle \quad = \quad 90E$$

$$R \quad = \quad 2$$

$$N \quad = \quad 100/1.24 = 81$$

$$H \quad = \quad 297/1.24 = 240 \text{ (this is over the maximum limit of 200 in the AISI Specification)}$$

$$P_r \quad = \quad (15.5)(1.24)^2(307)(1)(1 - 0.09\sqrt{2})(1 + 0.08\sqrt{81})(1 - 0.04\sqrt{240})$$
$$= \quad 4.18 \text{ kN}$$

This web crippling load corresponds to an in-plane stress in the web of **34 MPa** under the bearing plate.

7.4.6 Comparisons

When the three solutions are compared they show some similarity:

a) 17 MPa calculated from the balance of internal forces,

b) 41 MPa calculated from the measured deflected shape, and

c) 34 MPa calculated from the web crippling capacity.

Some caution needs to be used in inferring anything from these results. The stress determined from the web crippling expression assumes a uniform stress distribution under the applied load. While this may be a reasonable assumption directly under the bearing plate, the stress pattern will change at different locations through the joist web. There are also other errors associated with the measurement procedures as discussed in the next section.

7.4.7 Sources of Error

There are a number of sources of error inherent in this type of data collection.

a) *Error during the measurement of the deflected shape*. The dial gauge used to measure the deflected shape was capable of measuring to 1/1000 mm. However, the necessity of moving this gauge from one location to another introduced some variability in the repeatability of the measurements. To get an estimate of this error, a number of measurements were repeated and the two sets of data compared. The average difference between the two measurements (for 53 measurements) was 0.1%.

b) *Integration of the deflected shape*: The strains were determined through a double integration of the measured displacement field. The calculation of the gradients of the displacements will be subject to increasing errors. Any errors in the measurement of the deflected shape will be magnified through the process of integration.

c) *Experimental error*: 1% error in the gauge factor. 0.1% in the measurement of the load. 1% possible error in the strain gauge measurements.

d) *Bi-axial stress field*: An assumption has been made that the principal stresses are vertical in the orientation of the strain gauges. In fact, the orientation of the principal stresses is likely to vary over the web area. The deflected shape shows that there is some curvature in the longitudinal direction which were not included in the analysis.

7.5   CONCLUSIONS

The experimental method described in this section has arrived at an estimate of the in-plane stresses in the joist web due to the web crippling. While there is variability in the results, they are close enough to provide some confidence that using the measured deflected shape to determine the bending strains in the web is a viable means of providing data as input to the finite element program.

8   FINITE ELEMENT ANALYSIS

8.1   WHAT IS TO BE MODELED BY THE FINITE ELEMENT ANALYSIS AND WHY

8.1.1   *General Assembly Details*

The assembly to be modeled is a C-section joist with a bearing stiffener subjected to two-flange loading. The photograph in Figure 8.1.1 shows a test specimen consisting of two-C-section joists with bearing stiffeners fastened to the joist webs between the joist flanges. Two specimens were always tested in pairs to create a symmetrical assembly. The load was applied to the upper bearing plate, which was 100 mm wide. The assembly rested on a similar bearing plate to develop an end-two-flange loading condition. Self-drilling screws were used to connect the joist web to the stiffener. The photograph in Figure 8.1.1 also shows the location of the load cells used to measure the forces developed in the fasteners. Testing were carried out on assemblies of this type with a variety of fastener arrangements, joist sizes, stiffener types and stiffener locations.
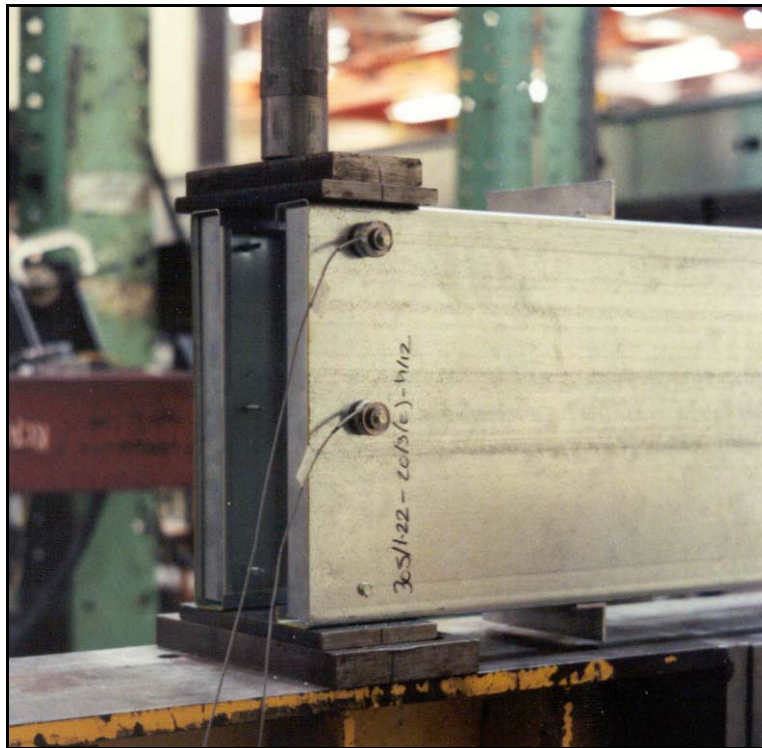
Figure 8.1.1: Photograph of a Pair of C-Sections with Bearing Stiffeners During Testing

Figure 8.1.2: Photograph of the Web Crippling of a Pair of C-Sections with Bearing Stiffeners

The photograph in Figure 8.1.2 was taken during a test, but before failure of the stiffener. In the unloaded state shown in Figure 8.1.1, the joist web is essentially flat, and there is normally a gap between the ends of the stiffener and the joist flanges. At the stage of the test shown in Figure 8.1.2, the joist web has buckled (web crippling) and the flanges of the joist are bearing directly on the ends of the stiffener.

The deformation of the joist web is restrained by the screws connecting the joist to the stiffener. This restraint in turn creates lateral loads on the bearing stiffener in addition to the applied axial loads. The stiffener acts as a beam-column and its ultimate capacity can be predicted with current design expressions if the magnitude of the fastener forces and the end eccentricity of the applied load are known.

The web crippling behavior of thin walled structural elements such as these C-sections is a very complicated interaction of large deformations and non-linear material behaviour. Consequently, the available design expressions provided in the design standards [1,2] for web crippling of individual members are empirical expressions based exclusively on test data. When the bearing stiffener is added to the C-section, the behavior becomes even more complicated, and beyond the practical possibility of developing an analytical solution. As a result, investigations have focused on experimental work to develop predictor equations. The finite element model discussed in this paper was developed to be used as a means of expanding the available data. The numerical results can be used in conjunction with the available laboratory test data to derive more comprehensive predictor equations for the capacity of cold formed steel C-sections with bearing stiffeners.

62

8.1.2 Key Characteristics and Behavior to be Numerically Modeled

The finite element model must capture a number of key characteristics of the assembly and its behaviour under load.

8.1.2.1 Deformed Shape

The results of the FEA must predict the basic deformed shape of the joist web in general agreement with that observed during the laboratory tests.

8.1.2.2 Stiffener End Gap

A certain amount of gap between the stiffener and the joist is necessary to accommodate manufacturing tolerances, and to make the assembly easier. The current industry standards for cold formed steel are the AISI *Standard for Cold-Formed Steel Framing - General Requirements* [20], and the CSSBI 55-99 *Residential Steel Framing Installation Manual* [21]. These documents stipulate that a bearing stiffener can only be 9 mm (3/8 in.) shorter than the joist depth. Taking into account the thickness of the joist material, this corresponds to a gap of approximately 3 mm (1/8 in.) at each end of the stiffener.

8.1.2.3 Contact Area

During the deformation of the assembly under load, the joist web buckles in a complicated shape (as illustrated in Figure 8.1.2). Typically, the area directly under the bearing plate will bulge outwards (away from the stiffener), and the area near the centre of the web will deflect towards the stiffener. The presence of the bearing stiffener, however, will restrict the inward deformation of the joist web. Since the web crippling capacity and fastener forces are influenced by the deformed shape, it is important that the FE model account for the possibility that these two elements (the joist web and the stiffener) may come into contact during the loading cycle.

8.1.2.4 Non-linearity

The FE model must also account for the geometric non-linearity resulting from large deformations, as well as the material non-linearity in those areas where the strains goes beyond the elastic limit.

8.1.2.5 Fastener Flexibility

The stiffness of the fasteners connecting the joist web to the bearing stiffener will restrain the deformation of the joist web, both locally and overall. The degree of restraint will be affected by the location of the fastener in the joist web, as well as the material strength and thickness of the bearing stiffener to which the fastener is connected.

8.1.3 Required Results/Output

The finite element model is primarily being used to supply only the following two results.

8.1.3.1 Web Crippling Capacity

Since there is a gap between the bearing stiffener and the joist flanges, the joist web will buckle (web crippling) at a load that can be significantly less than the ultimate load of the entire assembly. This condition would be a serviceability limit state for the assembly. In practice, the assembly should be designed to avoid web crippling at service loads for aesthetic reasons as well as the implications for accumulated deformations through multiple storeys, and the possible affects on brittle connected finishes. One of the required results from the FEA will be the web crippling capacity of the joist.

8.1.3.2 Fastener Forces

The capacity of the bearing stiffener is a function of the axial load, the end eccentricity and the lateral loads at the screw locations. The FEA must provide the fastener forces, which can be used in subsequent studies to determine the strength limit state for the stiffened assembly.

8.2 GENERAL FEATURES OF THE FINITE ELEMENT MODELING

8.2.1 FE Program

The finite element program used for this analysis was the ANSYS 5.6 program. This is a commercially available computer program that provides for a wide range of analyzes, including the features necessary for this study. No attempt was made to compare alternative programs. The ANSYS program was installed and run on a personal computer.

8.2.2 Element Types

8.2.2.1 Shell Elements

The basic behavior to be modeled was the deflected shape of thin sheet steel elements representing the joist. It was necessary to account for both the in-plane stresses and bending behavior, as well as model the curvature of the deflected shape with the fewest elements. *Shell93* elements were used, which have mid-side nodes (8 node quadrilateral) with six degrees of freedom at each node (3 displacement and 3 rotation). These elements were used to mesh all of the surface areas.

8.2.2.2 Contact Elements

The ANSYS 5.6 program is able to model contact between designated target and contact areas utilizing elements that are overlaid on the *Shell93* meshed areas. The contact pairs used were the *Targe170* for the area that is taken to be stationary, and *Conta174* elements for the area that changes its position. The target area represents the bearing stiffener and the contact area is an area of the joist web.

8.2.2.3 Link Elements

Link8 elements were used to represent the fasteners. These are 2-node 3D linear elements that have six degrees of freedom at each node (3 displacement and 3 rotation).

8.2.3 Boundary Conditions

The development of the model underwent a series of iterations to arrive at the boundary conditions and loading that best represented the restraints on the assembly and the nature of the load application. The model simulates a test specimen that is 600 mm long and has a bearing stiffener at the each end, although only the one end is loaded. An area 100 mm long on the top of the flange (Area A1 in Figure 8.2.1) is restrained against *ux* and *uy* displacement. This simulates the restraint caused by a bearing stiffener at the unloaded end of the specimen. A similar 100 mm long area (A2 in Figure 8.2.1) is restrained in *ux* and *uz*, but displaced -3 mm in *uy*. The 3 mm displacement simulates the collapse of the joist web onto the end of the bearing stiffener associated with web crippling.
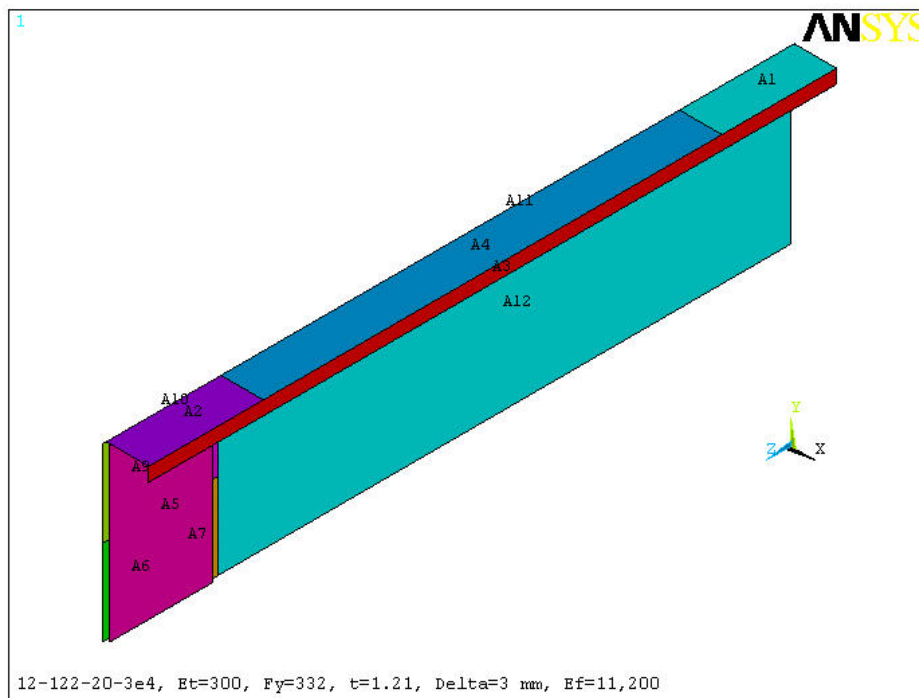
Figure 8.2.1: Typical Areas in Finite Element Model

Modeling of the full assembly would be inefficient since there is a line of symmetry that can be used to reduce the size of the model. A half model is shown in Figure 8.2.1. The symmetrical behaviour was introduced by restraining the vertical deflection, *uy*, and rotation about the longitudinal axis of the line

65

representing the middle of the joist web, *rotz*. This symmetrical model was shown to produce the same deformed shape and reactions as a full model.

8.2.4   Contact Analysis

An additional area was positioned 1 mm away from the area representing the joist web and designated as a contact area (Area A5 in Figure 8.2.1). Corresponding areas on the web (Areas A6, A7, A8, and A9) were designated as the target contact areas. These contact areas were incorporated to model the restraint of the stiffener.

8.2.5   Material Properties

The development of the FE model involved modeling actual test specimens. Included in the FE model are the material properties of the joist and stiffener sheet steel. The stress-strain curves of tensile coupons taken from the tested sheet steel material provided the yield and ultimate strengths of the material. A representation of the non-linear behaviour of the sheet steel was incorporated into the FE model by using bi-linear material properties. The initial linear range used a stiffness of 203 000 MPa (29 500 ksi), corresponding to Yonge's modulus. The second linear range corresponded to the tangent modulus of a line connecting the yield point to the ultimate tensile point. This bi-linear kinematic modeling is a feature of the ANSYS program. In addition to the material strength, the specific sheet thickness for each tested assembly was incorporated into FE model by specifying a thickness constant for the shell elements.

8.2.6   Representation of the Fasteners

One of the features of the actual assembly that needed to be included in the FE model was the restraint created by the screws connecting the joist web to the bearing stiffener. This was accomplished by including a link element perpendicular to the web areas and connected to the joist web mesh at nodes corresponding to the screw locations. The displacement of the free end of the link was fixed and only axial strains were allowed. The axial stiffness of these links was set to correspond to an equivalent stiffness based on the fastener location and stiffener material. Details of how this stiffness was determined is discussed in Section 8.3.7.

8.2.7   Load Steps

The loading on the assembly was applied in two stages that correspond to the construction and loading of the actual assembly. During a laboratory test, or a field application, the stiffener is connected to the joist web with self-drilling screws. When installed, the screws will clamp the joist web to the bearing stiffener. This action was modeled by applying a displacement of 1 mm *ux* to the free end of the links that represent the fasteners. This displacement simulated the initial clamping, but also allowed the link elements to deform in the subsequent load step.

The second load step was a –3 mm *uy* displacement of the area under the bearing surface. This corresponds to the application of the applied load above the bearing stiffener. Three millimetres of deflection was used to model the deformation exhibited in the laboratory tests. The two load steps were applied sequentially.

8.2.8 Meshing the Model

The model was meshed with the two contrary objectives: to create a sufficiently fine mesh to model the essential features of the deformed shape, and minimize the number of elements to reduce computation time. The shell elements with mid-side nodes can represent curved surfaces, but in areas where the curvature is higher, a finer mesh is warranted. The area under the bearing surface requires a finer mesh since this coincides with the area with the most out-of-plane web buckling (as illustrated in Figure 8.1.2).

8.2.9 Range of FE Models Developed

FE models were developed corresponding to assemblies with the following variables:

- 203 and 305 mm (8 and 12 in.) deep joists of different thickness and material properties,
- 3-screw and 4-screw fastener patterns,
- variations in the location of the fastener(s) closest to the top flange (h/4, h/6 and h/12).

In all there were 48 different assemblies modeled as illustrated in Figure 8.2.2.
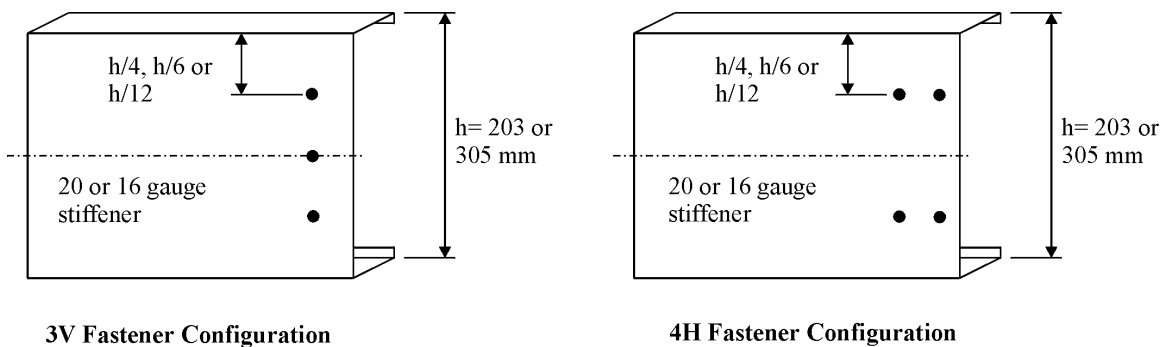
Figure 8.2.2 General Configuration of the Assemblies Modeled

8.2.10 Degree of Accuracy

An important criterion in the development and verification of the FE model will be the required accuracy of the results. In this application, accuracy is defined as the relationship between the tested results and the numerical results for the web crippling and fastener loads.

In cold formed steel research it is quite common to have results reported with coefficients of variation (COV) up to 20 percent. A COV less that 10 percent is considered very good. Variations will be caused

by many factors in a test program that will not necessarily be present in a FE analysis. If variations in the order of 10 percent are acceptable, then this influence how complicated or detailed the FE model must be.

8.3   DEVELOPMENT AND VERIFICATION OF THE FE MODEL

It is important to verify that the finite element program and the model developed adequately incorporates the essential features of the physical materials being investigated. A number of tests were carried out to confirm that validity of the model.

8.3.1   *Verification of Material Non-linearity*

The ability of the ANSYS program to incorporate bi-linear material properties was checked with a test of a strait bar subjected to uniaxial tension, and with Poisson's ratio equal to zero. The FE solution was confirmed since it matched the analytical solution.

8.3.2   *Verification of Geometric Non-linearity*

Large displacements are an important feature of the FE model. The ability of the ANSYS program to incorporate geometric non-linearity was confirmed by taking a thin column, fixed at the base and subjecting it to a moment at the free end. Under sufficient load, the resulting deflected shape was a portion of a circle. The FE solution was compared to the theoretical solution for the bending of flexible bars [13]. The results are given in Table 8.3.1, which shows acceptable agreement between the numerical and analytical solutions.

Table 8.3.1: Large Deflection Confirmation

	Configuration	X-displacement (mm)	Y-displacement (mm)	Rotation (degrees)
Example 1	2x25 FE shell mesh	84.20	47.67	140.9
	2x50 FE shell mesh	84.20	47.67	141.1
	Analytical solution	83.9	47.2	140.5
Example 2	2x25 FE shell mesh	70.95	60.62	164.1
	2x50 FE shell mesh	70.40	60.62	164.4
	Analytical solution	70.4	58.3	164.4

8.3.3   *Influence of the Number of Load Sub-Steps*

A FE model is an approximation of the true behavior both in the discretization of the physical object, but also the rate at which the loading is applied to the model. A Newton-Rapson analysis method was used by the ANSYS program to follow the non-linear behavior. The smaller the load step (i.e. the more load sub-steps) the closer should the FE solution model the actual behavior. In the practical application of a FE solution there is a trade-off between the increased accuracy associated with increased sub-steps, and the reduction in productivity caused by the increased computation time. To determine an appropriate number of load sub-steps, a FE model was developed and run a number of times with a different number of sub-

steps. The output that was collected were the forces in the fasteners, the deflection of the web at the fastener location and the equivalent web crippling load. The results of this study are provided in Table 8.3.2.

Table 8.3.2: Influence of Varying the Number of Loading Sub-Steps

Number of Sub-Steps	Force in Fastener 1 (N)	Displacement at Fastener 1 (mm)	Force in Fastener 2 (N)	Displacement at Fastener 2 (mm)	Web Crippling Load (N)
8	384.7	-1.452	-100.6	0.7591	7467
20	385.8	-1.456	-101.0	0.7620	7479
40	386.0	-1.457	-101.0	0.7624	7480
60	386.0	-1.457	-101.0	0.7625	7481
100	386.0	-1.457	-101.1	0.7626	7481

The objective of this FE analysis is to provide data on the fastener forces and web crippling capacity of the stiffened joist assembly. This FE data will be included with the results of laboratory tests to provide information with which to develop a general design model. Since the coefficient of variation of the test data can exceed 10 percent, the extra computation time needed to get the accuracy associated with 100 load steps is not justified. A value of 20 load sub-steps was taken to be a reasonable minimum number.

8.3.4   Repeatability of Results

The FE program was checked to ensure that it would give repeatable results when analyzing the same model. An analysis was carried out on a particular model and the results recorded. The same model was evaluated again and the results matched the first run to five significant digits.

8.3.5   Verifying the Web Crippling Reaction Load

One of the objectives is to determine the web crippling capacity of the assembly. Only half of the assembly is being modeled through symmetry to save on computation time. During the stages in developing the model, it was discovered that the best way of applying the load was as a displacement of the upper surface that would correspond to the bearing surface under the applied load. Using a pressure instead of a displacement area would have made the determination of the web crippling load easier; however, the post-buckling behaviour of the web is unstable. If a pressure load is applied that exceeded the web crippling (buckling) capacity of the member, the FE analysis would not converge. Therefore, the practical means of determining the web crippling load was to apply a displacement of the bearing area and add up the vertical reaction forces at all of the nodes along the line of symmetry. The validity of this method was verified by applying a pressure to the bearing area less than the web crippling capacity, running the FE analysis and adding up the nodal reactions. The test cases proved that the sum of the nodal reactions did equal the applied load.

8.3.6   Effect of Varying the Tangent Modulus

The non-linear material properties of the joist material is modeled by a bi-linear stress-strain curve. The initial elastic properties use a modulus of elasticity of 203 000 MPa, which is consistent with the current design standards for cold formed steel. The tangent modulus after the yield point was measured from the actual stress-strain curves of the material used in the laboratory tests, and with which the FE model was being verified. A typical value of the tangent modulus was measured from the stress-strain curve to be 300 MPa. A study was done to determine the sensitivity of the FE model results to a change in the tangent modulus. The results of this comparison are provided in Table 8.3.3.

Table 8.3.3: Influence of Varying the Tangent Modulus

Tangent Modulus (MPa)	Force in Fastener 1 (N)	Displacement at Fastener 1 (mm)	Force in Fastener 2 (N)	Displacement at Fastener 2 (mm)	Web Crippling Load (N)
300	306	-0.86	-120	0.67	8130
500	307	-0.86	-120	0.67	8160
1000	308	-0.86	-121	0.67	8260
2000	311	-0.87	-121	0.68	8440
5000	319	-0.89	-124	0.69	8930
10000	330	-0.92	-127	0.71	9614

Note: Model 12203e4, E=203000, E_f=14,800, t=1.21, F_y=332, Delta=0.5

The results show that a 10 times increase in the tangent modulus causes only a 10% increase in the web crippling load. These findings justify the simplification of using a tangent modulus of 300 MPa for all materials.

A similar study was carried out to determine if a multi-linear stress-strain model was warranted. An actual stress-strain curve is very non-linear beyond the yield stress. This curvature would be better described by a multi-linear model than a bi-linear model. A FEA was carried out on the same model but with the following two different material properties:

(1) bi-linear model with E = 203 000, F_y = 332, E_t = 300; and,

(2) multi-linear model with E = 203 000, F_y = 332, E_{t1} = 300, F_u = 400, E_{t2} = 10.

The results are provided in Table 8.3.4, and indicate that a multi-linear model is not necessary.

Table 8.3.4: Influence of a Multi-Linear Tangent Modulus

Tangent Modulus	Force in Fastener 1 (N)	Displacement at Fastener 1 (mm)	Force in Fastener 2 (N)	Displacement at Fastener 2 (mm)	Web Crippling Load (N)
Bi-linear	306	-0.86	-120	0.67	8130
Multi-linear	304	-0.85	-119	0.67	8000

8.3.7 Fastener Flexibility

In early studies, the fasteners connecting the joist web to the stiffener were modeled as fixed degrees of freedom at the nodes corresponding to the screw locations in the joist web. This assumption is not entirely correct since the deformation of the joist web will put tension on the fastener, which in turn is connected to the web of the stiffener. As the web buckles, the web deformation will be restrained by the fastener, but the degree of restraint depends on the thickness and strength of the stiffener material.

Two lengths of stiffeners were used in the laboratory testing (203 and 305 mm, 8 and 12 in.) in two thicknesses (0.85 and 1.50 mm, 0.033 and 0.059 in.). In addition, there were two types of fastener arrangements (3v and 4h) as well as three fastener spacings (h/4, h/6 and h/12). These configurations are illustrated in Figure 8.3.1. In all, 24 stiffener and fastener configurations were modeled.
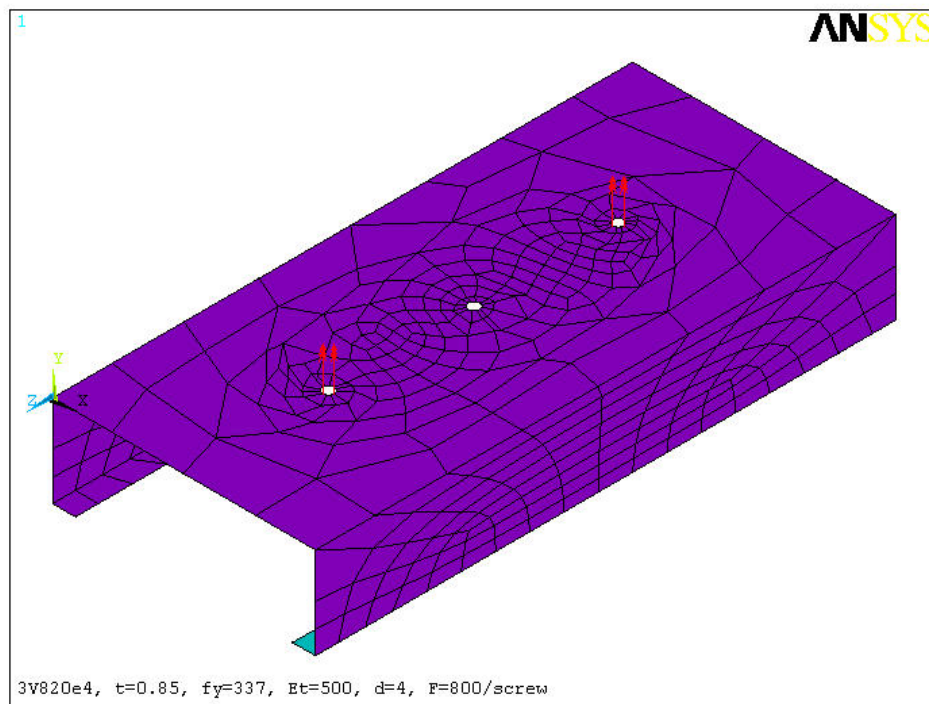
Figure 8.3.1: FE Model for Determining Fastener Stiffness

The FE model of a typical stiffener is shown in Figure 8.3.1. The holes are 4 mm (5/32 in.) in diameter corresponding to the size of a #10 self-drilling sheet metal screw. Loads were applied to the nodes around the holes and the resulting deflections determined.

The flexibility of the fastener restraining the web is incorporated into the FE model of the joist by including a link element perpendicular to the joist web, connected to the joist mesh at the node representing the fastener, and fixed at its other end. The modulus of elasticity of this link was set to correspond to the stiffness resulting from the load-deflection FE analysis.

The following example describes how this link stiffness was determined:

1) Apply a load at screw location in FE model of stiffener of 2,400 N (540 lbs) (see Figure 4.7.1).

2) From the FE analysis, determine the average deflection of nodes around screw hole at maximum load to be 8.1 mm (0.32 in.).

3) The length of FE link representing the screw is 50 mm and the area is 1 mm^2.

4) The strain in FE link corresponding to the average deflection would be 8.1/50 = 0.162.

5) The stress in FE link corresponding to maximum load would be 2,400/1 = 2,400 N/mm^2.

6) The equivalent stiffness of FE link would be 2,400/0.162 = 14,800 N/mm^2.

The equivalent elastic modulus for each of the 24 stiffener configurations were calculated in this manner, as summarized in Table 8.3.5.

Table 8.3.5: Equivalent Elastic Modulus Values for FE Links

Assembly Designation	Equivalent Modulus (MPa)	Assembly Designation	Equivalent Modulus (MPa)
3v1220e4	14,800	3v1216e4	29,600
3v820e4	13,900	3v816e4	38,500
4h1220e4	10,400	4h1216e4	32,000
4h820e4	13,800	4h816e4	49,500
3v1220e6	12,050	3v1216e6	32,920
3v820e6	14,800	3v816e6	41,240
4h1220e6	13,290	4h1216e6	41,030
4h820e6	16,260	4h816e6	52,290
3v1220e12	14,980	3v1216e12	42,330
3v820e12	17,320	3v816e12	53,330
4h1220e12	14,650	4h1216e12	49,690
4h820e12	16,060	4h816e12	57,140

1 MPa = 0.145 ksi

A series of laboratory tests were conducted to verify the FE model of the fastener stiffness. The basic test set-up is shown in Figure 8.3.2. A 305 mm (12 in.) length of stud representing the stiffener was clamping in a universal testing machine. A #10 self-drilling sheet metal screw was installed at a location corresponding to the location of a fastener in the FE model of the stiffened joist assembly. A bearing cap was fixed on the end of the screw against which the actuator could push. A load cell and LVDT measured the applied load and the resulting deflection of the screw. Three tests were conducted on two different thicknesses of stiffener (0.88 and 1.19 mm, 0.035 and 0.047 in.). The load-deflection curves for each test are given in Figure 8.3.3 and 8.3.4.

The purpose of doing these laboratory tests was to provide a comparison to the FE solution. Two FE models were developed of the stiffener corresponding to the tested configurations. The FE analysis was conducted and the resulting load-deflection relationship recorded. This data is also shown in Figures 8.3.3

and 8.3.4 along with the test results. These figures show that there is excellent correlation between the FE solution and the test results, which verifies the FE model of the fastener stiffness.
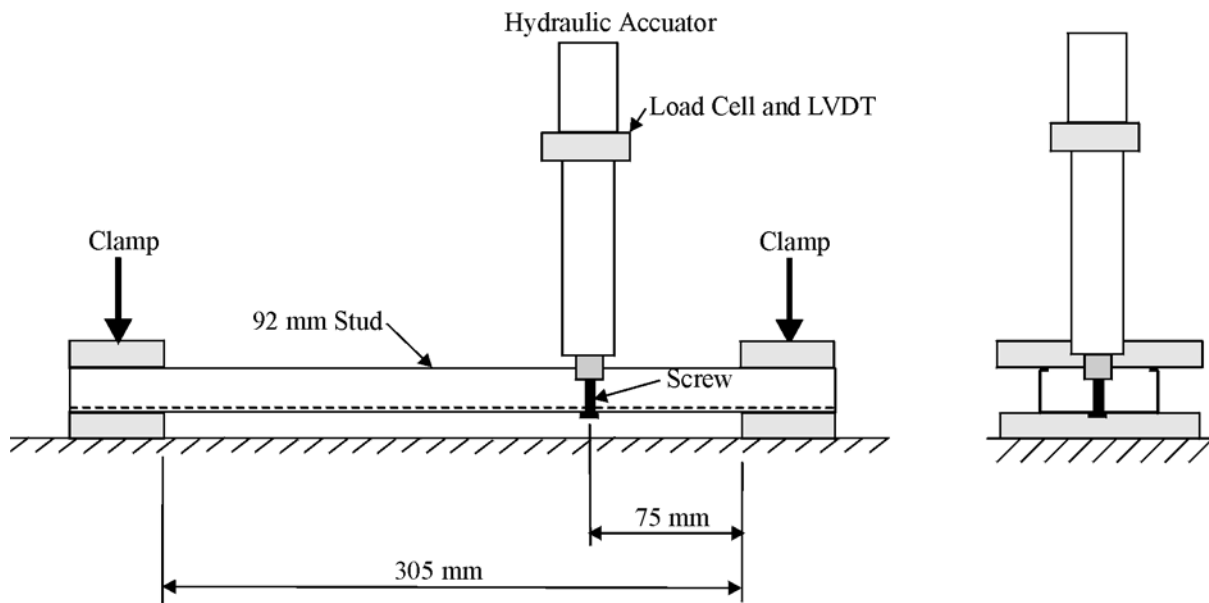
Figure 8.3.2: Test Set-Up for Screw Stiffness Measurements
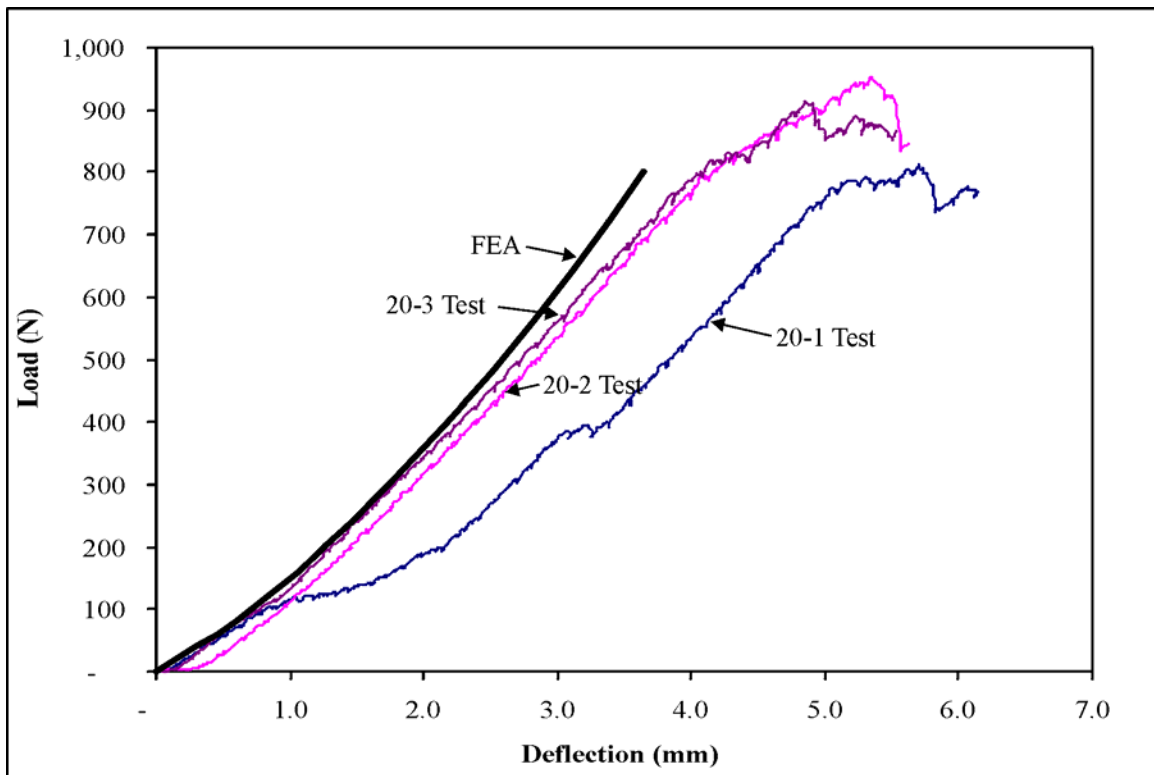
Figure 8.3.3: Load-Deflection Test for Screw in a 20 Ga. Stud
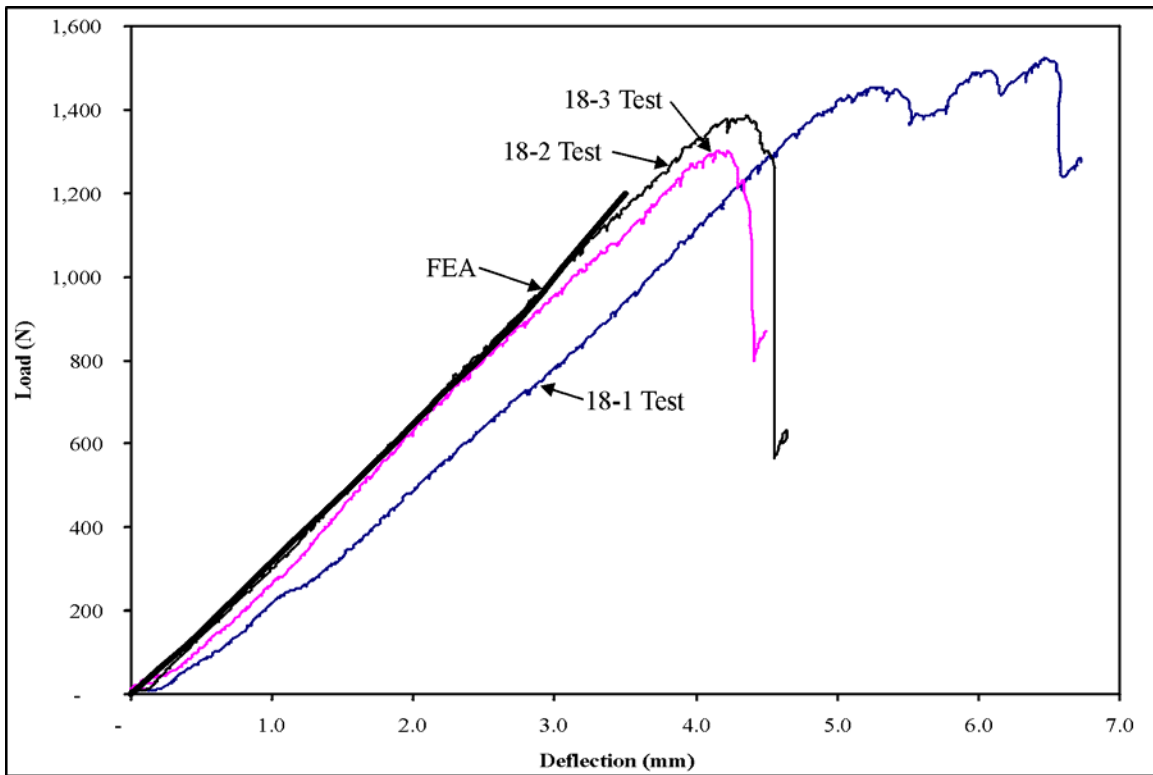
Figure 8.3.4: Load-Deflection Test for Screw in a 18 Ga. Stud

8.3.8 Refining the Mesh

The primary area of interest in the FE model is the location under the applied load, since this area exhibits the most deformation and is also the location of the fastener. Consequently, the mesh in this vicinity needs to be finer than the remainder of the model. The size of the elements under the load point were also made smaller in the vertical dimension than the horizontal, with an aspect ratio of approximately 1 to 2. This allowed the second order shape function used in the 8-node shell elements to better match the deformed shape. Various mesh options and configurations were tried and compared to come up with the general principals used to mesh all models.

8.3.9 Load Step Options

There are many possible means of applying loads to the FE model. The objective was to simulate the conditions of the tests. As discussed previously, the nature of the web buckling made the use of a pressure loading difficult for the FE program to converge. Consequently, displacement inputs were used, of which three options were investigated as illustrated in Figure 8.3.5.

74
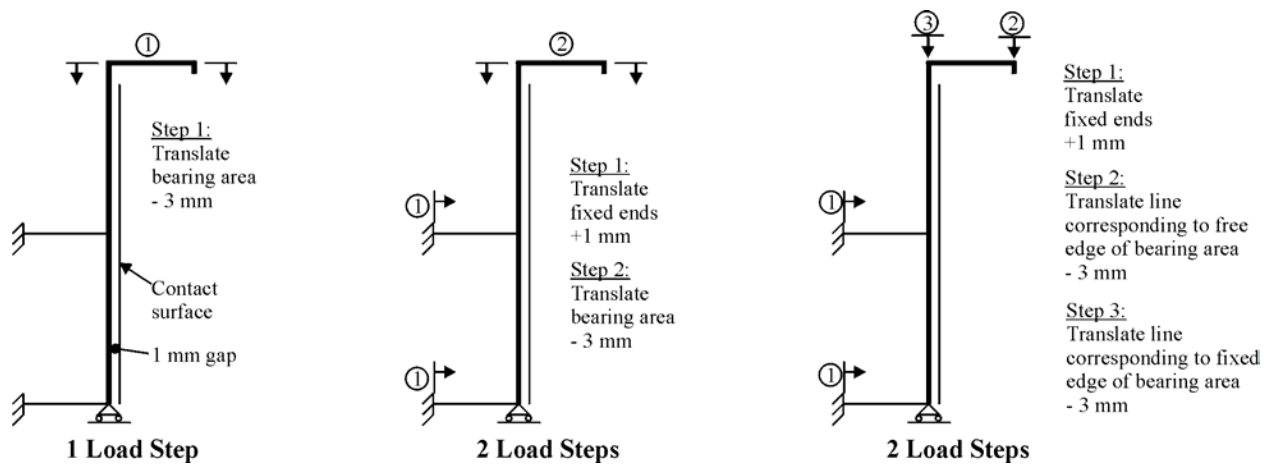
Figure 8.3.5: Description of Load Step Options

The first loading option is the "1 load step" where the upper bearing surface is restrained from translation in the *ux* and *uz* directions, and given a -3 mm *uy* displacement. The "2 load step" option first applied a +1 mm *ux* translation to the ends of the links to simulate installing the fasteners, followed by the vertical displacement of the bearing surface. The "3 load step" option applied the translation to the ends of the links, but followed with vertical translation of the lines that form the two longitudinal edges of the bearing surface area. This was done to simulate the behaviour joist flange rotation observed in the tests.

In the experimental assemblies, the joist flange was not fastened to the bearing surface. When the load was applied, initially the flange would tend to rotate about the corner radius until coming into contacted with the stiffener. During this portion of the cycle the load was primarily being transferred into the joist along the edge of the corner radius until web crippling occurred. After web crippling, the joist flange has collapsed to bear directly onto the stiffener and the load is then transferred through end bearing of the stiffener. This deformation sequence is illustrated in Figure 8.3.6.

(a) Prior to loading **(b) Initial flange rotation** **(c) Web crippling**
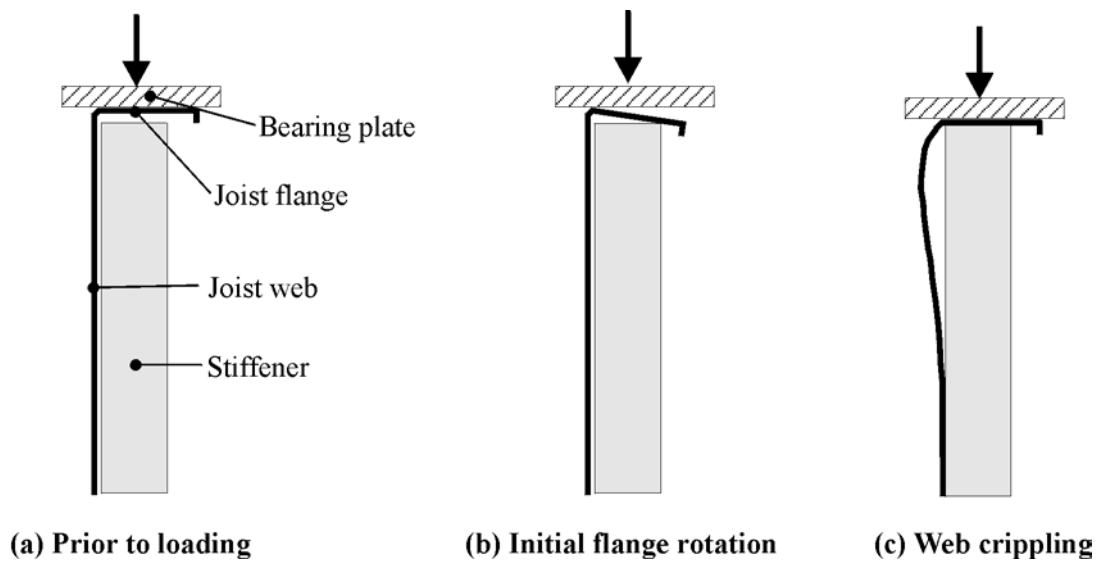
Figure 8.3.6: Joist Flange Deformation during the Loading Cycle

It is common practice in actual construction to fasten the joist flanges to the bearing support, which is not the way most of the laboratory tests were carried out. To check on the effects of this attachment, an experimental investigation was done [9]. This study concluded that fastening the joist flanges to the bearing surface had no significant effect on the ultimate capacity of the assembly; however, this study did not investigate if there was any the effect on the web crippling capacity.

A FEA was carried out on an assembly subjected to the three different load step option as discussed above. The objective was to determine if the load steps had a significant effect on the web crippling capacity and the fastener forces. The results of these analyzes are shown in Figure 8.3.7. Comparing the different load-displacement curves shows that for this assembly type the load step option does not have a significant effect on either the maximum web crippling load or the fastener force.

One disadvantage of increasing the number of load steps was an increased computational time. Each load step took the approximately same amount of time to run, and consequently, a 3 load step model took three times as long to run as the single load step. In was not unusual for a single load step analysis to take one to two hours. Therefore, the 3 load step option would add a considerable amount of computation time, especially when there are a larger number of configurations that need to be modeled. The 2 load step option was selected as the best compromise between computational efficiency and real-life modeling.
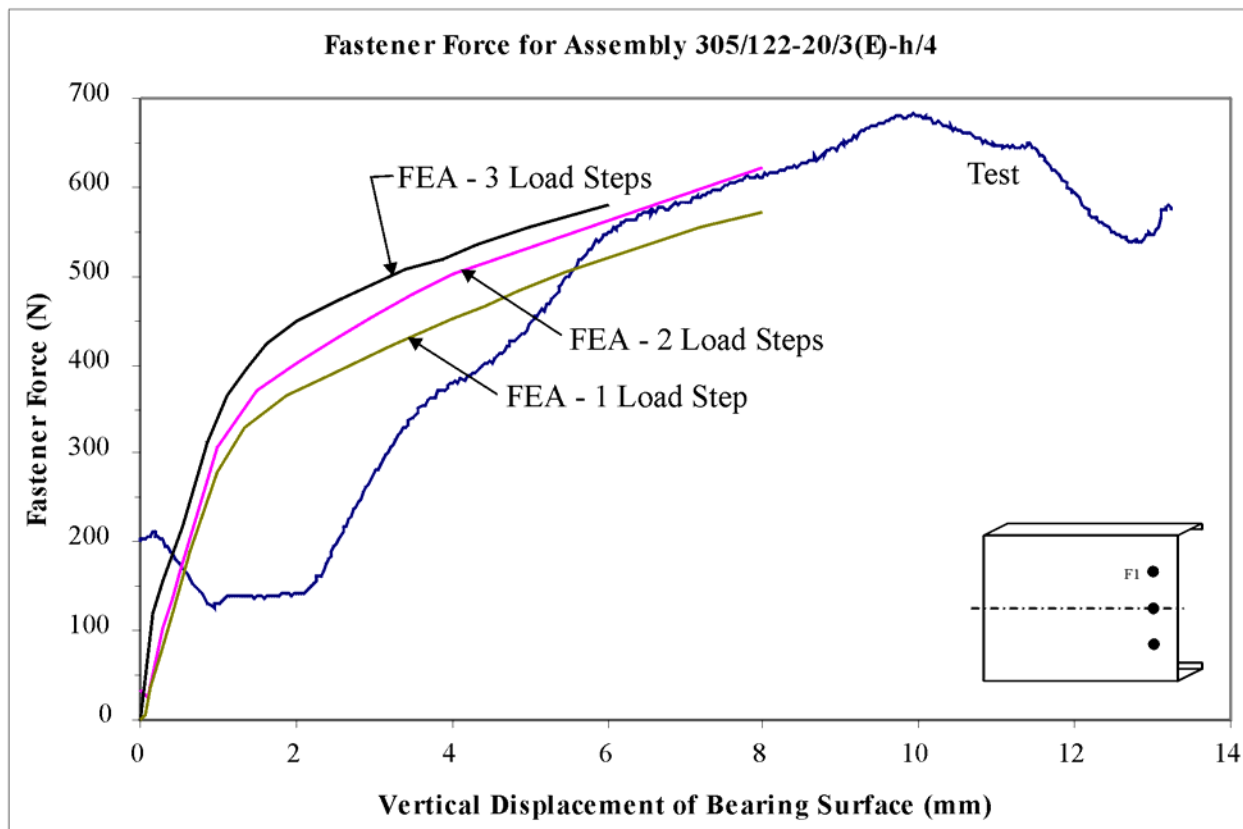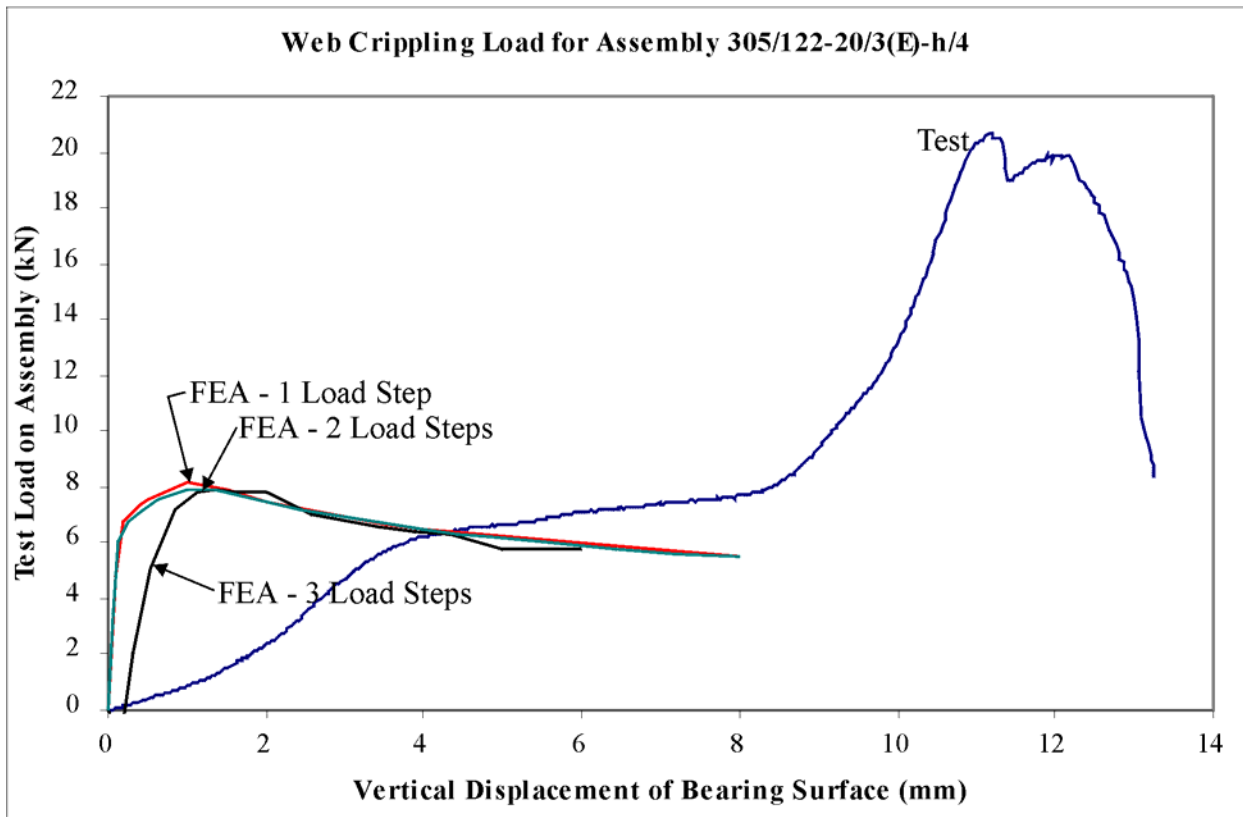
Figure 8.3.7: Comparison of Different Load Step Options on the FEA Results

8.4 COMPARISONS OF FEA MODEL WITH TEST DATA

8.4.1 Measuring the Web Crippling Loads and Fastener Forces by Test

One of the key objectives of the FE study is to develop a numerical model that can reasonably predict the web crippling capacity of a joist with a bearing stiffener. In order to verify that the FE model is providing acceptable results, a series of laboratory tests were carried out [19] that measured the load-deflection characteristics of various stiffened joist assemblies. The details of these tests were presented in Section 5.

8.4.2 Comparing the FEA and Tested Load-Deflection Curves

The results of the FE solution were compared to the load deflection curves measured in the laboratory tests. Figures 8.4.1, 8.4.2, 8.4.3 and 8.4.4 provide some representative comparisons.

The FE results for the web crippling capacity were generally higher that the tested values. This can be due to a number of causes.

1. The discretization of the assembly in the FE process will naturally yield a stiffer model than the actual specimen. If a finer FE mesh were used this difference could be reduced, but at the cost of added computational time.

2. The FE model does not take into account the many initial imperfections that are present in the physical model. Initial imperfections could be built into the FE model, but the imperfections present in a physical model could not be completely predicted.

3. The FE model does not accurately model the initial flange rotation of the joist prior to web crippling. This rotation will have the effect of applying an initial curvature to the joist web, which would reduce the buckling capacity.

4. The FEA also does not model the test specimen having two separate joist members loaded simultaneously. The test set-up endeavored to load the assembly symmetrically, but no measurement was made of the load carried by each individual joist. Consequently, it is likely that the load would not be perfected distributed and one joist would be carrying more of the load than the other. This would tend to precipitate a failure in the joist with the higher load, and lead to a lower average load for the pair than would be the case if the load was equally divided between the two specimens.

The plots of the FE and tested web crippling loads in Figures 8.4.1 through 8.4.4, are similar in shape to column buckling curves with different degrees of initial imperfections. As the imperfections increase, the load-deflection curve develops a more rounded shape. This phenomenon is consistent with the earlier discussion about the differences between the FE model and the physical model. Even though the FE

solution will normally yield higher ultimate loads, the results are still useful as long as they are consistent and calibrated to the test data.

The plots in Figures 8.4.1 through 8.4.4 show that the fastener forces predicted by the FE analysis generally agree with the test results both in the magnitude and general shape of the load-deflection curves. There are, however, a number of variables in the physical test that are not included in the FE analysis.

1. When the screws were installed they were given an initial pre-load that would correspond to the clamping force generated during the normal screw installation. The load-deflection curves for the tests shown in the figures all start from a load corresponding to this pre-load. The attached load cell will not begin to record any additional load until the force generated in the fastener, as a result of web buckling, has exceeded the pre-load amount. In the three-screw configurations illustrated in Figure 5.3.1, the screw at the centre of the joist does not carry any additional load since the deformation of the joist web is towards the stiffener, not away from it.

2. In order for the load cell under the screw head to measure any force, a pilot hole was drilled in the joist web that was larger than the diameter of the screw but smaller than the diameter of the load cell. This created a situation where the clamping action between the stiffener and the joist web was transferred through the load cell. While this allowed the measurement of the screw force, it also changed the buckling behavior of the joist web. The hole around the screw allowed the joist web to move slightly relative to the stiffener, which would have an effect of changing the stress distribution. This phenomenon was most apparent when the fasteners were located nearest the flange (i.e. h/12).

The comparisons of the FE and test load-deflection curves agree sufficiently to provide a degree of confidence in the numerical solution within the limitations to be discussed later in section 8.4.6.
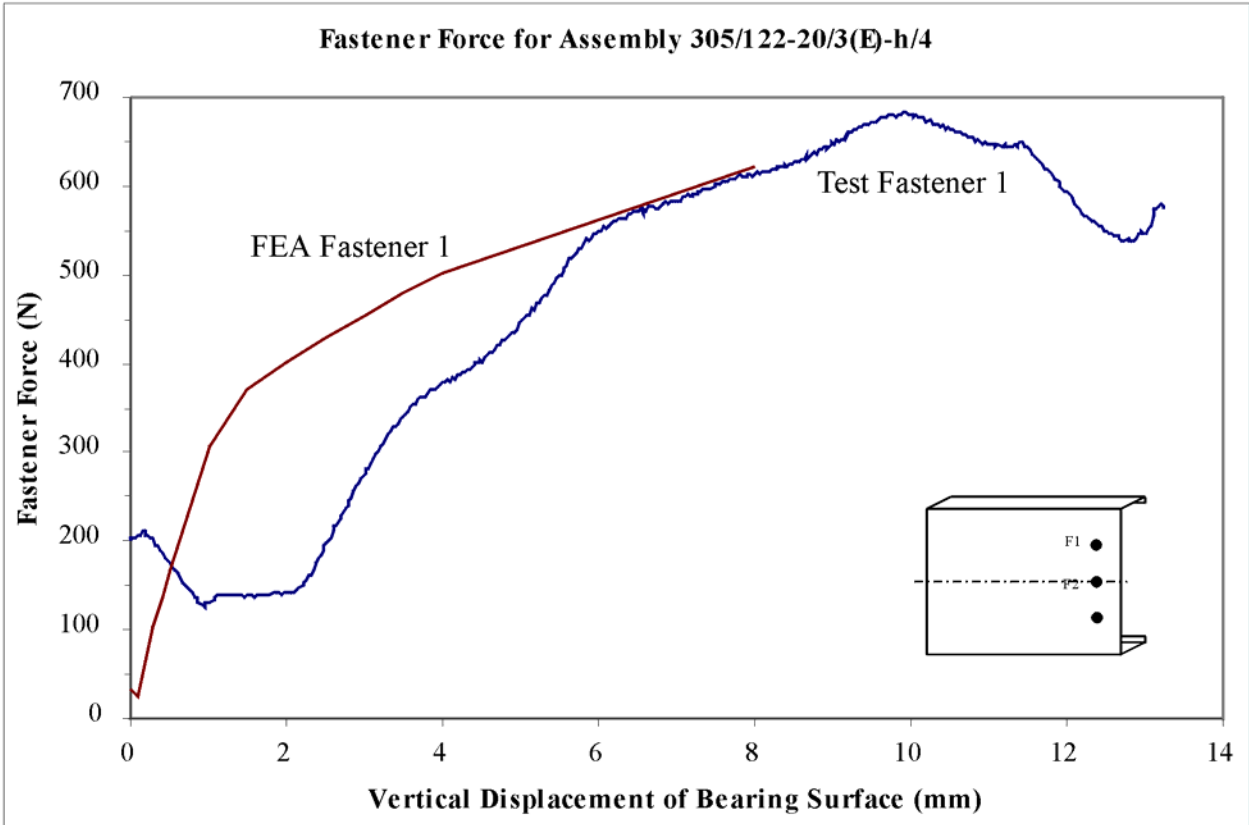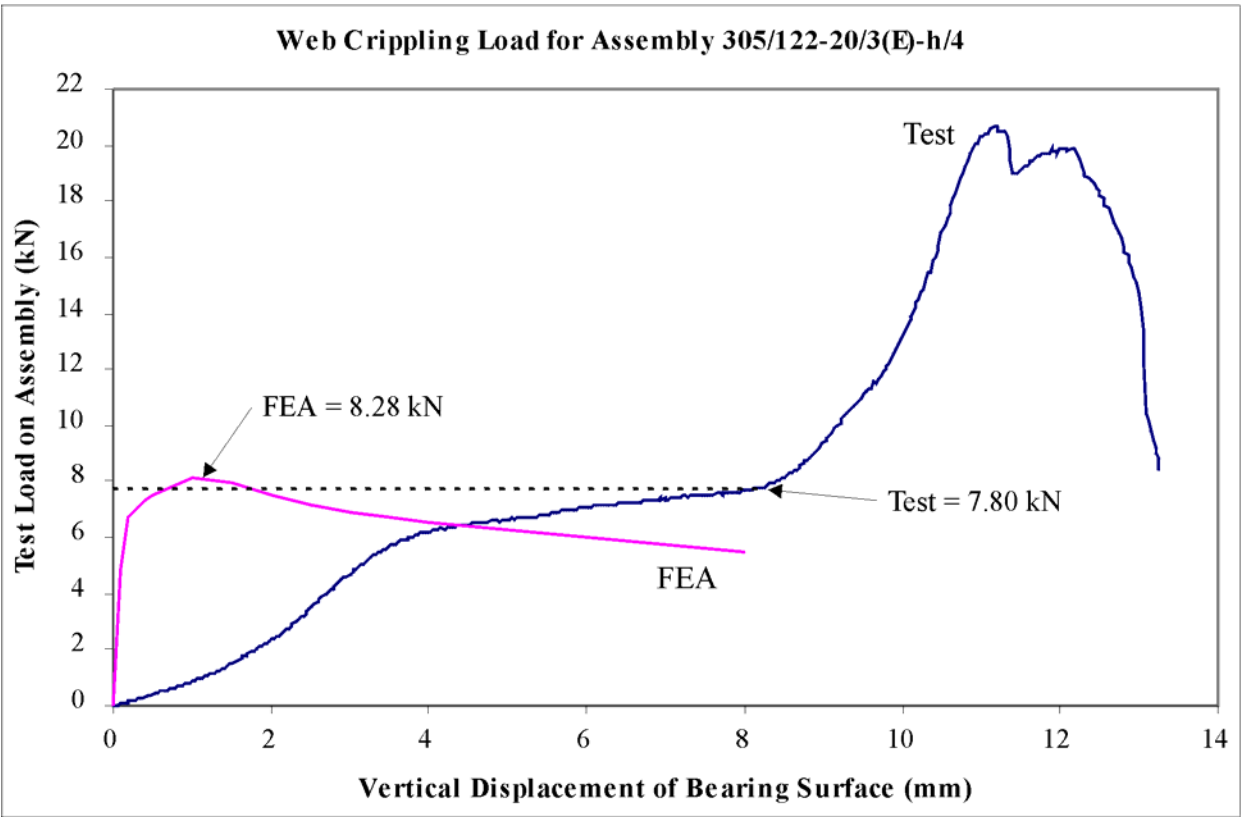
Figure 8.4.1: Comparison of FEA and Test Results for Assembly 305/122-20/3(E)-h/4
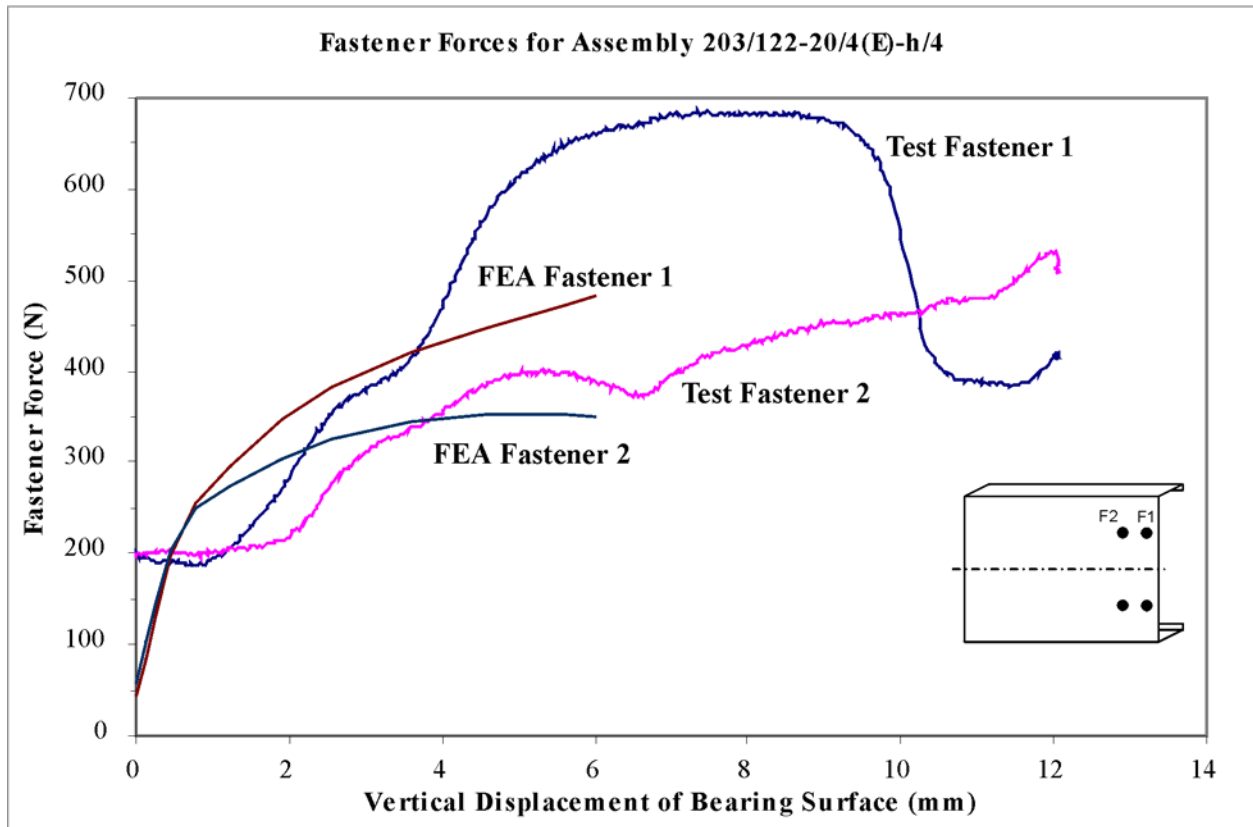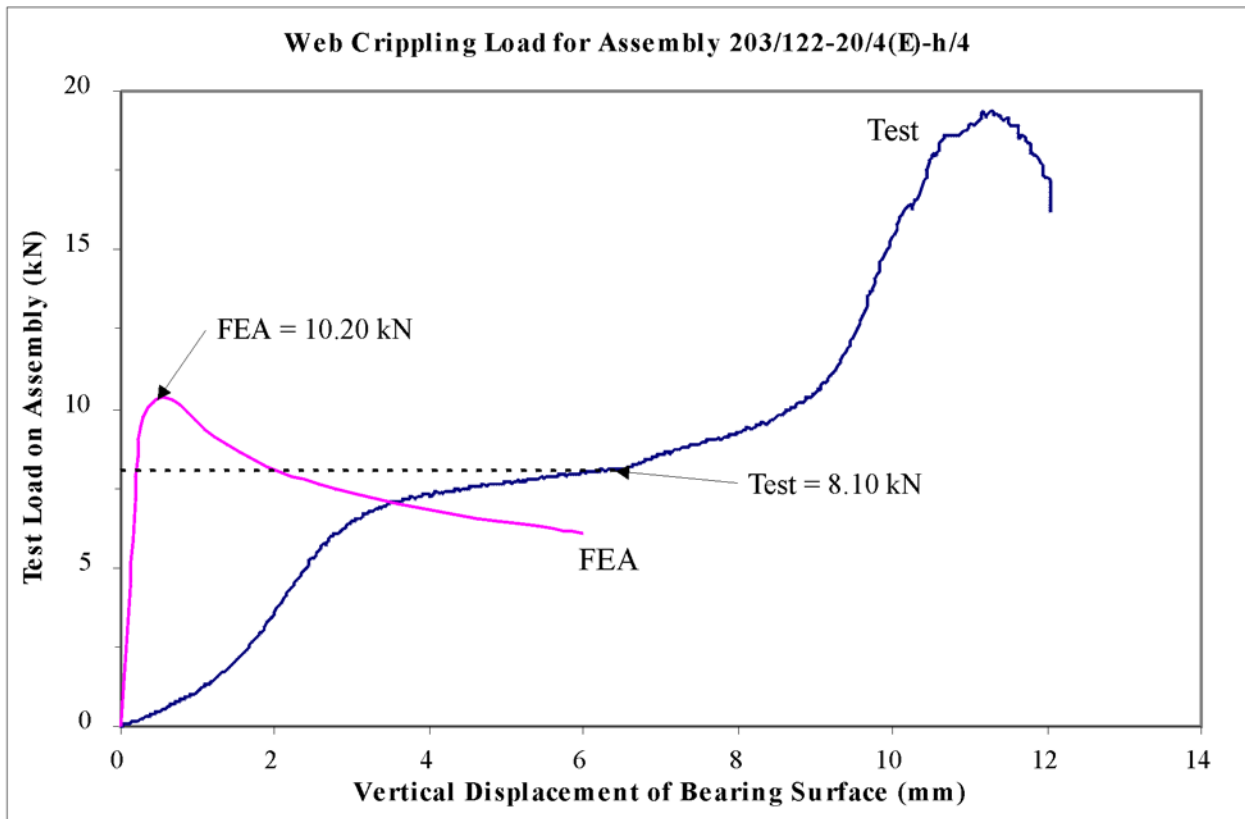
Figure 8.4.2: Comparison of FEA and Test Results for Assembly 203/122-20/4(E)-h/4
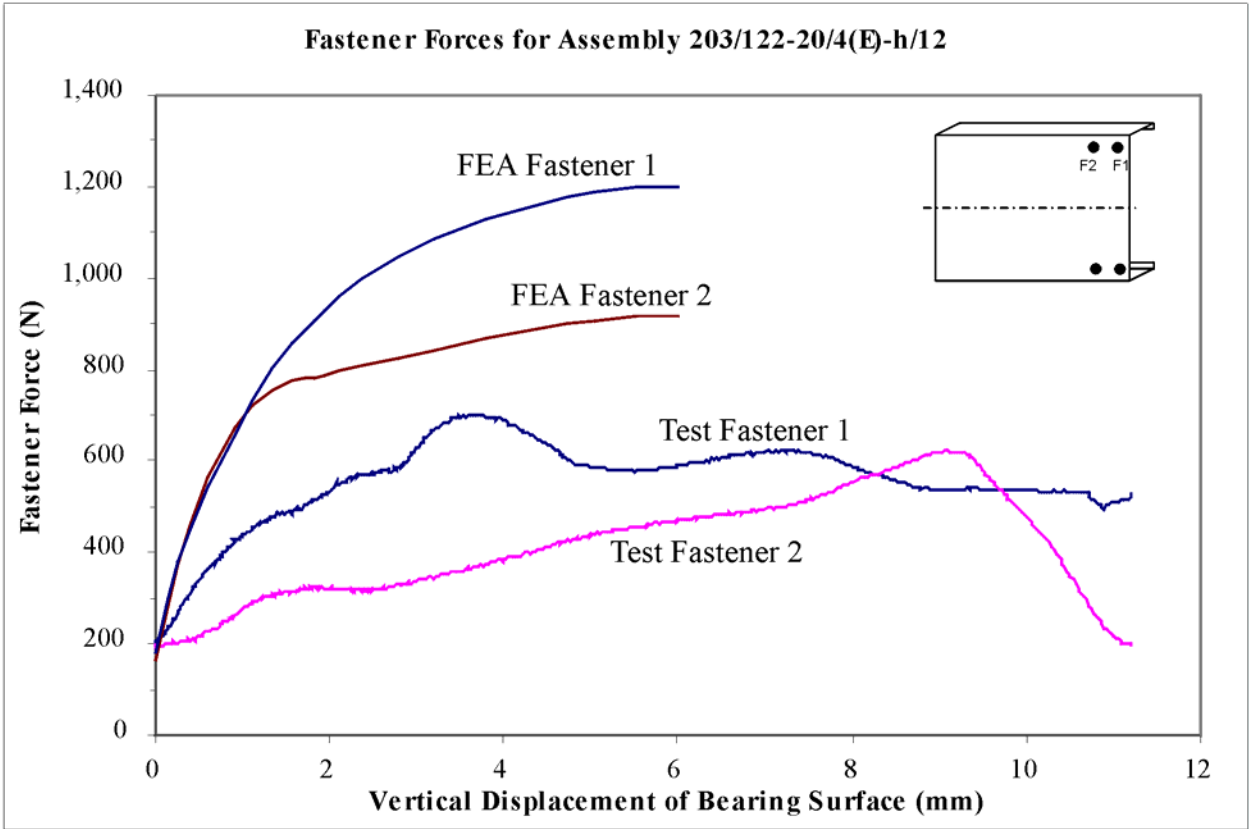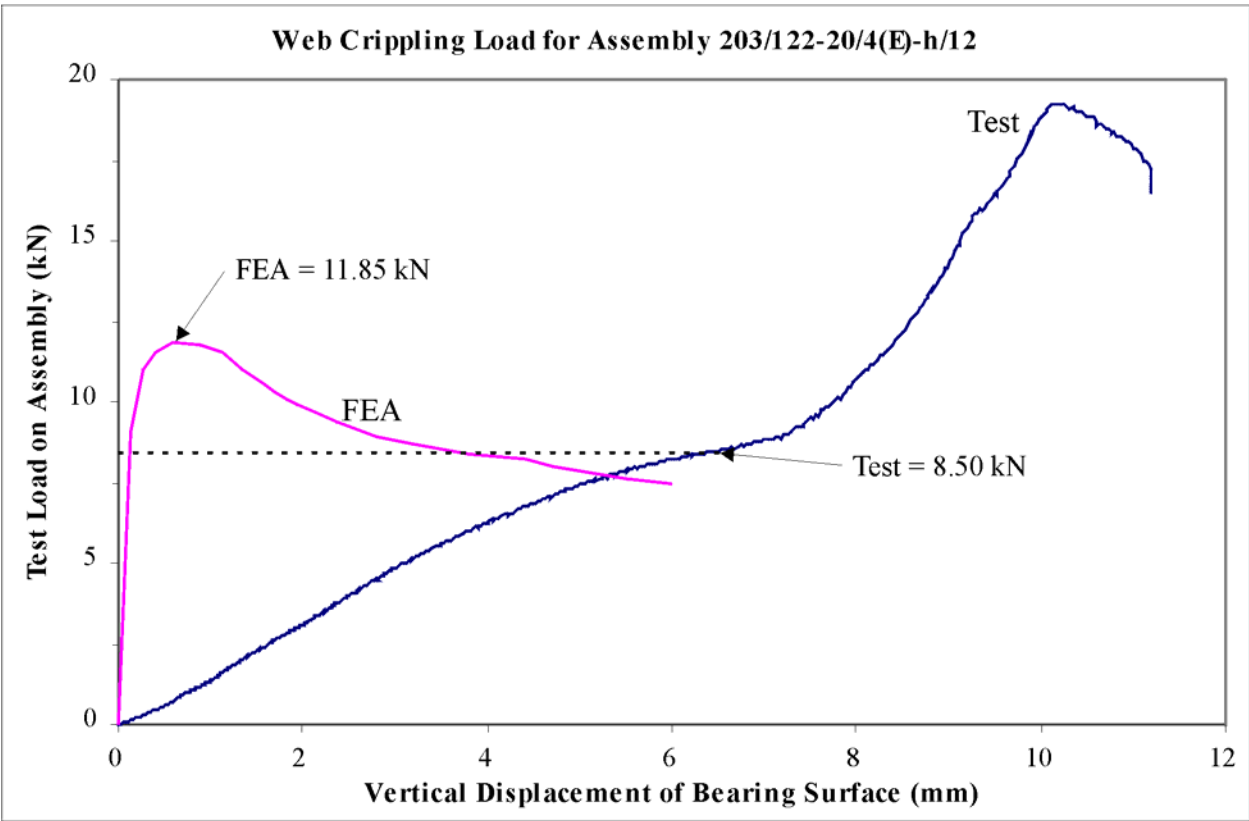
Figure 8.4.3: Comparison of FEA and Test Results for Assembly 203/122-20/4(E)-h/12
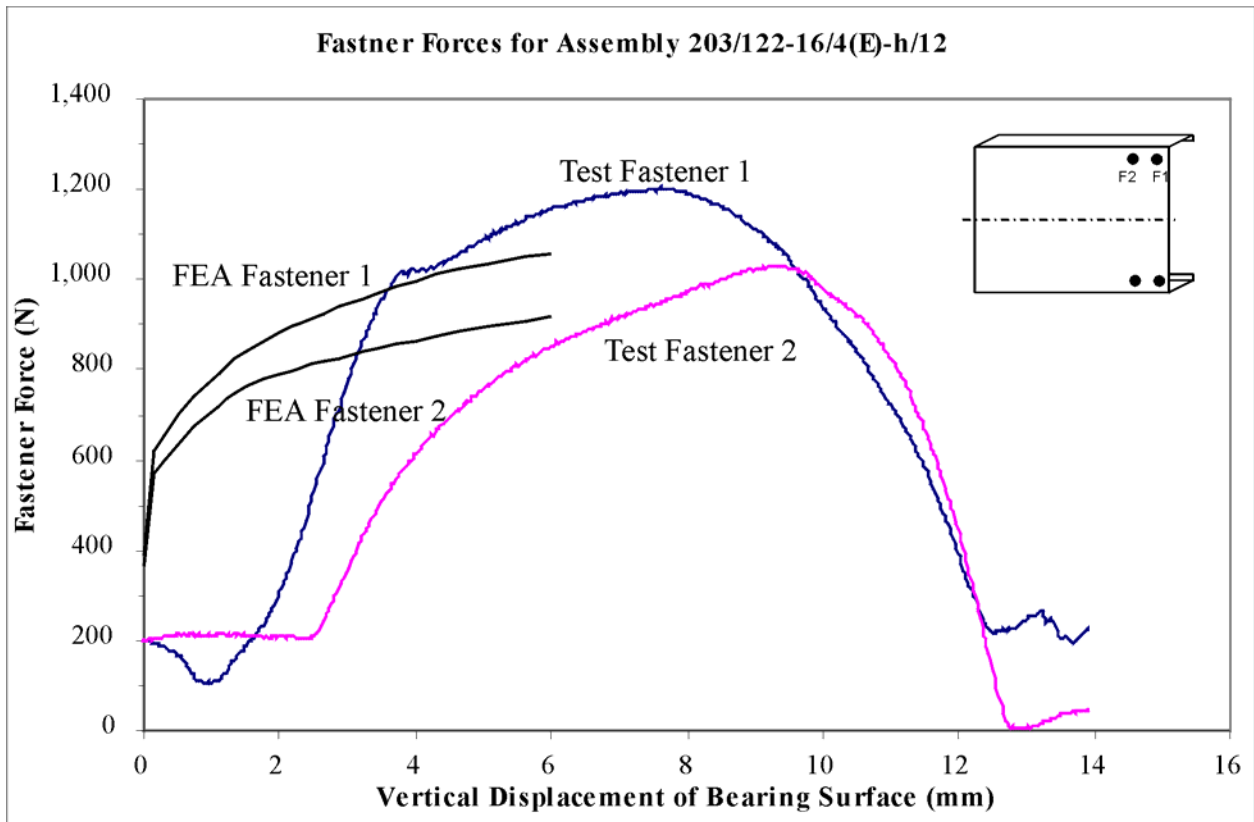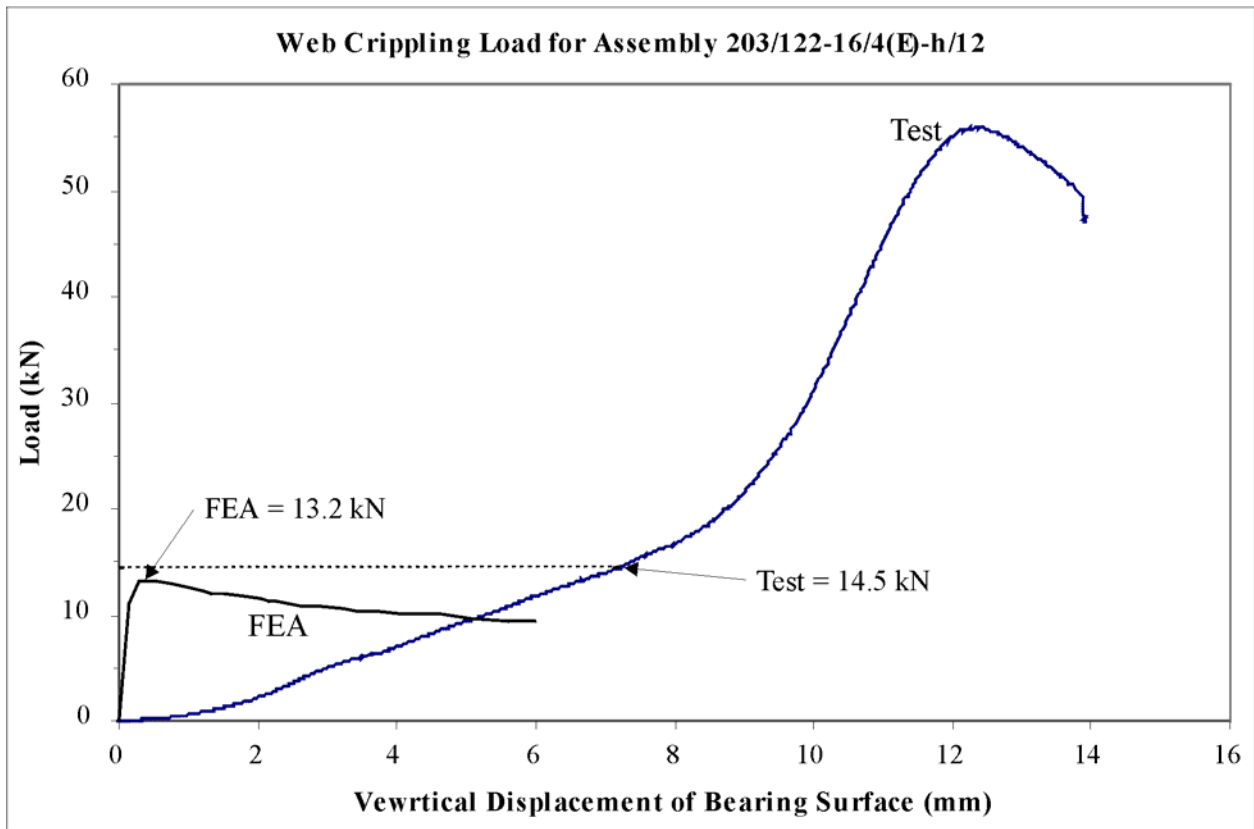
Figure 8.4.4: Comparison of FEA and Test Results for Assembly 203/122-20/4(E)-h/12

8.4.3 Comparing the FEA and Measured Deformed Shape

As discussed previously, one of the requirements of the FE model would be its ability to correctly predict the deformed shape. To check this ability, the results of a FEA were compared to a laboratory test that physically measured the deformed shape of the joist web. The details of this tests were discussed in Section 7. A test specimen was constructed as shown in the photograph in Figure 8.4.8. A rectangular grid was marked on the upper corner of the joist web under the bearing plate. As the specimen was subjected to increasing load, measurements of the out-of-place deflection were taken at each of the grid points. The resulting measurements were then used to plot the deformed shape. A FE analysis of a model corresponding to this assembly was also carried out.
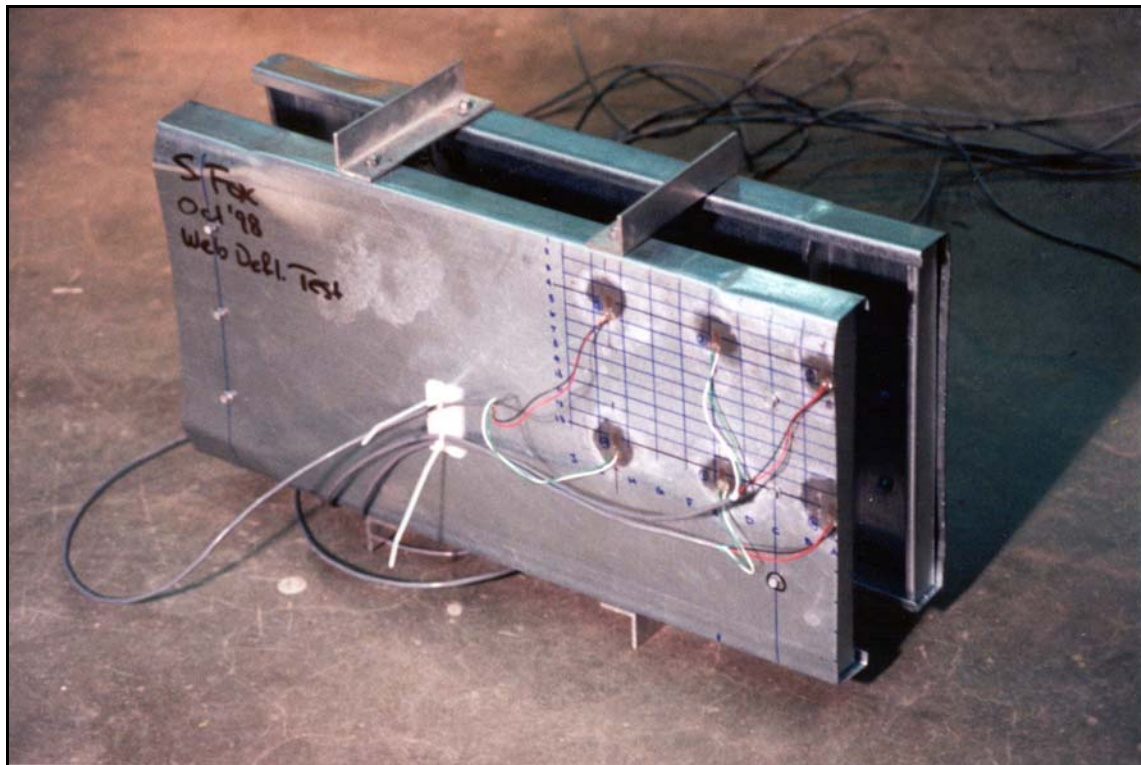
Figure 8.4.5: Test Specimen for Measuring the Deformed Shape

A comparison of the deformed shape measured in the test and that predicted by the FEA are shown in Figures 8.4.6 and 8.4.7. Figure 8.4.6 shows an end view of the test specimen under load along with the corresponding deformed shape predicted by the FEA. The surface plots provided in Figure 8.4.7 are the results of the measurements taken of the deformation of the test specimen and the deformations predicted by the FE model. For this assembly configuration, the FE model predicted larger deflections and higher curvatures than the tested values, but the basic shape was the same.

84

In addition to the detailed measurements of the deformed shape just described, a description of the deformed shapes were recorded for all of the laboratory tests carried during the study of the web crippling loads and fastener forces.
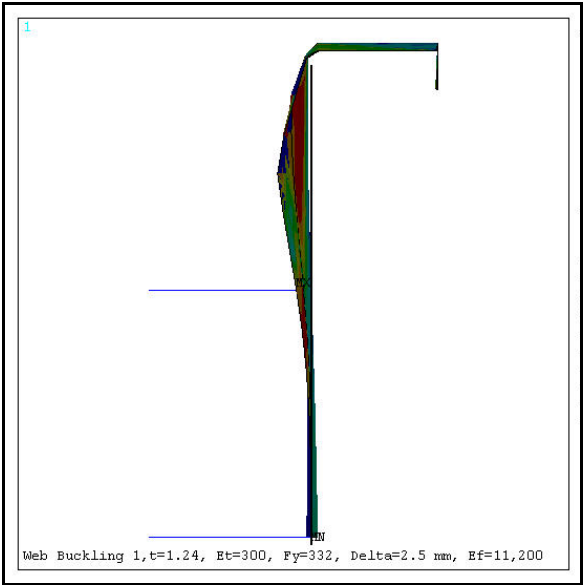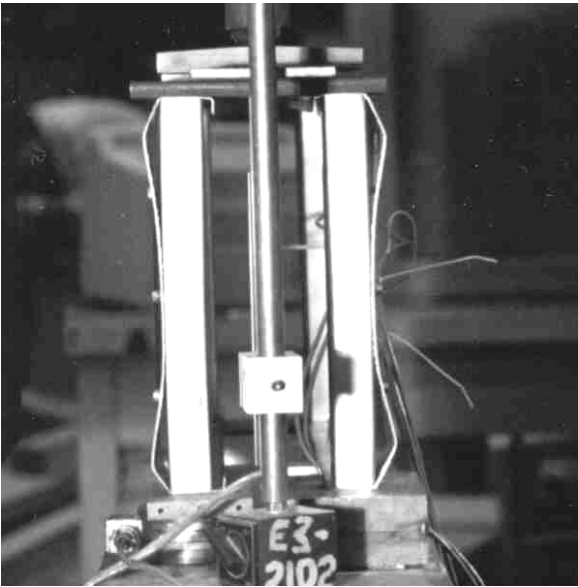
<table>
<tr><td>(a) FE Analysis</td><td>(b) Test Specimen</td></tr>
</table>

Figure 8.4.6: FEA and Tested Deflected Shapes for Web Buckling Measurements

Deflected Shape at 9170 N (Test)

Deflected Shape from FEA
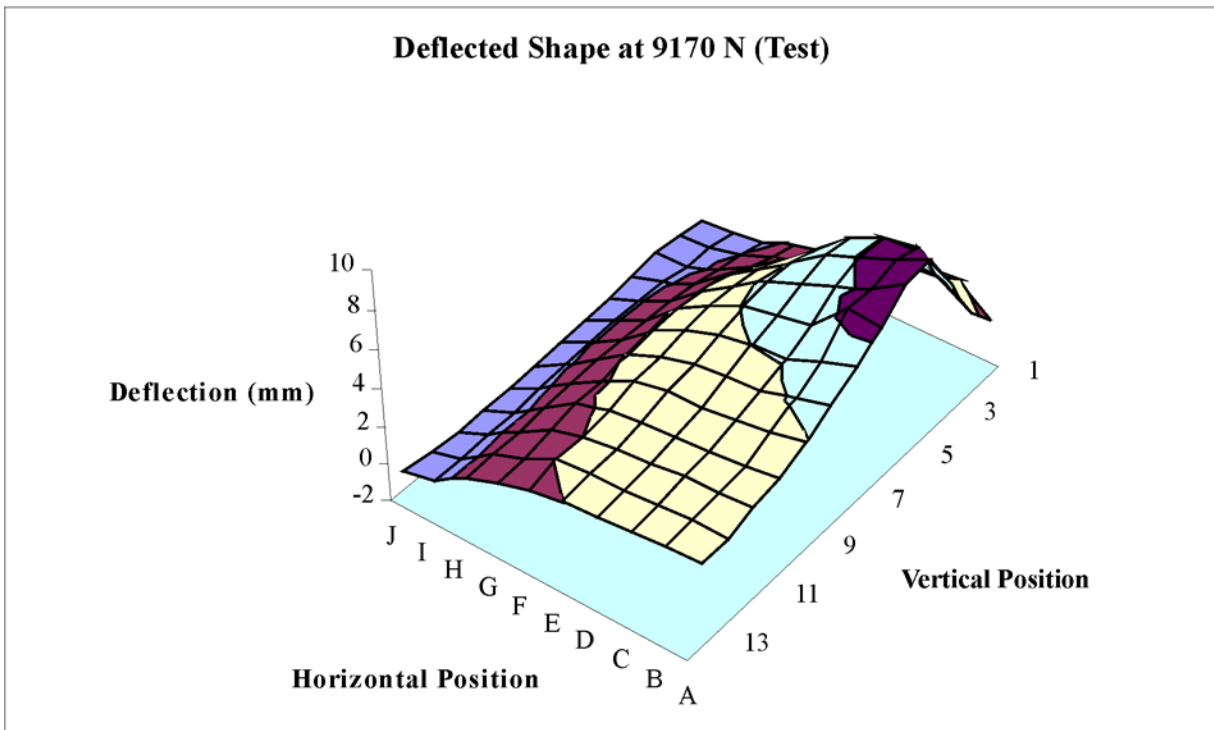
Figure 8.4.7: Comparison of the Measured and FEA Deformed Shape

8.4.4 Comparing the FEA and Measured Strains

The test described in the previous Section that measured the deformed shape, also included strain gauges. A total of six gauges were fixed to the joist web as illustrated in Figure 6.2.3 and measured the strain in the vertical direction only. Shown in Figure 8.4.8 are the strain gauge readings corresponding to the

86

applied deflection of the bearing surface as well as the strains at these same locations computed by the FE analysis of the same assembly. These are the total strains in the vertical (y-axis) direction.
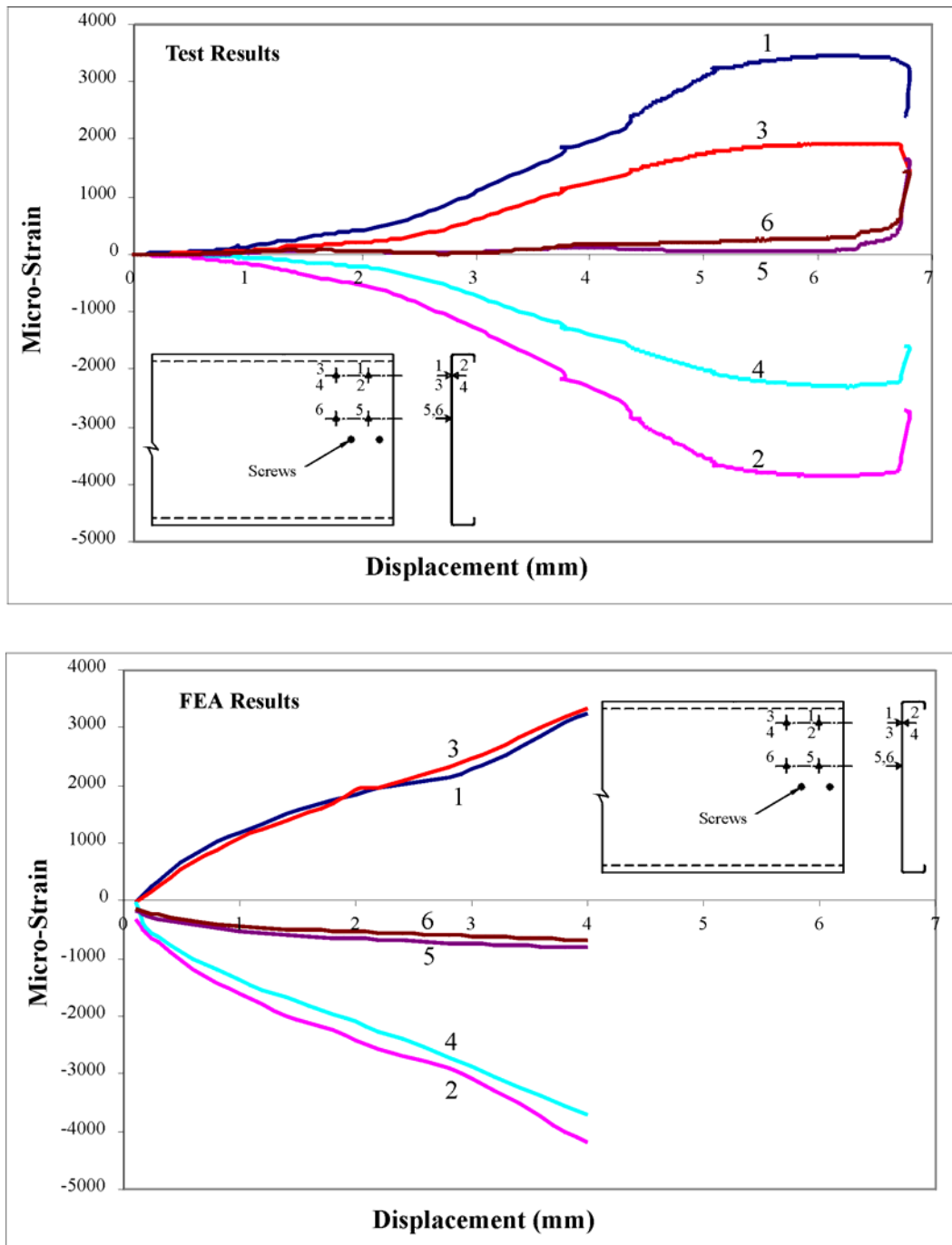
Figure 8.4.8: Comparison of the Measured and FEA Strains

8.4.5 Comparing the Fastener Forces and Web Crippling Loads Determined by FEA to Test Results

Listed in Table 8.4.1 are the results from all of the tests as well as the FE analyzes for each of the 48 different assemblies. The test designation describes the assembly as follows:

Example: 305/1.22-16/3(E)-h/12

Where,

305 = joist depth, mm (305 or 203)

1.22 = joist thickness, mm (1.22, 1.52, or 1.91)

16 = stiffener thickness, gauge (16 or 20)

(E) = stiffener at the end of the joist

h/12 = location of top screw relative to the joist depth, h (h/12, h/6 or h/4)

The fasteners were numbered according to their location. In the 3-screw tests the top screw was number 1 and the centre screw was number 2. In the 4-screw tests the screw closest to the end of the joist was number 1 and the other was number 2. The "contact area reaction" was the contact force generated between the FE contact area and the joist web due to buckling. This would correspond to the reaction of the joist web against the bearing stiffener, which would be useful for the design of the stiffener. The contact area reaction only occurs in the 3-screw assemblies.

Some of the FE models did not converge for various reasons, normally associated with the buckling mode. These are designated as DNC in the table. There are two tests were the fastener pulled out of the stiffener, which precipitated an early failure. In one test mechanical difficulties prevented the measurement of the web crippling load. A positive number for the fastener load indicates tension in the fastener. A negative number for the contact area force indicates that the joist web is pushing against the stiffener. The forces recorded in Table 8.4.1 for the contact area and the centre fastener in the 3-screw arrangement are double what was predicted by the FEA. This is necessary to recognize that the FEA only modeled one half of the assembly.

Table 8.4.1: Comparison of Tested and FEA Results

Test Designation	Measured Fastener Forces		FEA Fastener Forces		Contact Area Reaction (N)	Measured Web Crippling (kN)	FEA Web Crippling (kN)
	F1 (N)	F2 (N)	F1 (N)	F2 (N)			
305/1.22-16/3(E)-h/12	1100	1170	1398	10	-692	11.60	12.12
305/1.22-20/3(E)-h/12	1270	1240	1402	12	-722	7.65	11.96
305/1.22-16/3(E)-h/6	1090	<200	946	26	-960	8.70	10.41
305/1.22-20/3(E)-h/6	960	590	747	8	-676	8.65	9.70
305/1.22-16/3(E)-h/4	970	<700	680	-8	-920	7.75	8.75
305/1.22-20/3(E)-h/4	680	<200	565	0	-700	7.80	8.28

203/1.22-16/3(E)-h/12	1230	1050	1554	0	-344	10.90	11.38
203/1.22-20/3(E)-h/12	760	820	1353	208	0	N/R	9.96
203/1.22-16/3(E)-h/6	830	<600	1112	0	-518	9.25	11.76
203/1.22-20/3(E)-h/6	<1260	<1260	939	0	-552	9.50	10.44
203/1.22-16/3(E)-h/4	1020	<200	848	0	-922	8.50	9.85
203/1.22-20/3(E)-h/4	970	<200	679	-1	-602	8.20	9.57
203/1.22-16/4(E)-h/12	1200	1030	918	1056	-1046	14.50	13.22
203/1.22-20/4(E)-h/12	700	630	918	1200	-428	8.50	11.85
203/1.22-16/4(E)-h/6	1170	900	616	717	-1438	11.00	11.80
203/1.22-20/4(E)-h/6	610	590	573	546	-1160	9.75	11.52
203/1.22-16/4(E)-h/4	460	630	618	433	-1412	8.75	10.60
203/1.22-20/4(E)-h/4	680	450	482	351	-544	8.10	10.20
305/1.22-16/4(E)-h/12	650	600	DNC	DNC	DNC	11.00	DNC
305/1.22-20/4(E)-h/12	740	300	687	735	-868	7.00	12.55
305/1.22-16/4(E)-h/6	810	760	DNC	DNC	DNC	6.50	DNC
305/1.22-20/4(E)-h/6	850	540	488	387	-956	7.50	10.48
305/1.22-16/4(E)-h/4	960	760	515	338	-1298	7.25	9.19
305/1.22-20/4(E)-h/4	610	600	413	275	-962	7.25	8.80
305/1.52-16/4(E)-h/12	1030	1030	1224	1369	-2058	20.50	22.04
305/1.52-20/4(E)-h/12	590	490	909	1199	0	10.00	15.98
305/1.52-16/4(E)-h/6	1220	820	685	724	-1644	15.50	16.86
305/1.52-20/4(E)-h/6	1020	720	749	625	-1334	11.50	17.68
305/1.52-16/4(E)-h/4	1260	1190	765	543	-1896	12.50	15.46
305/1.52-20/4(E)-h/4	660	470	612	429	-1362	12.00	15.03
305/1.52-16/3(E)-h/12	1000	2050	2157	768	0	13.00	16.37
305/1.52-20/3(E)-h/12	550	1210	1439	394	0	11.75	14.00
305/1.52-16/3(E)-h/6	1480	<370	1421	32	-1476	13.75	17.59
305/1.52-20/3(E)-h/6	1540	<600	1137	0	-884	13.00	15.76
305/1.52-16/3(E)-h/4	1570	<630	1053	-6	-1358	12.75	14.89
305/1.52-20/3(E)-h/4	1000	<250	816	-4	-926	12.25	13.94
203/1.91-16/3(E)-h/12	1060	2010	3536	-802	0	24.00	29.62
203/1.91-20/3(E)-h/12	<830	1910	DNC	DNC	DNC	Screw pull-out	23.62
203/1.91-16/3(E)-h/6	2200	1130	2615	-12	-1436	20.50	29.68
203/1.91-20/3(E)-h/6	<750	1980	DNC	DNC	DNC	Screw pull-out	25.95
203/1.91-16/3(E)-h/4	1900	<900	1910	-12	-1588	21.00	27.58
203/1.91-20/3(E)-h/4	<1400	1760	1244	-10	-566	19.00	25.91
203/1.91-16/4(E)-h/12	1760	1930	DNC	DNC	DNC	16.75	DNC
203/1.91-20/4(E)-h/12	890	950	DNC	DNC	DNC	16.25	DNC
203/1.91-16/4(E)-h/6	1650	1860	1581	1573	-2782	21.50	32.66
203/1.91-20/4(E)-h/6	1080	1590	1548	1268	-1484	16.50	29.78
203/1.91-16/4(E)-h/4	1350	1350	517	410	-1242	21.25	21.54
203/1.91-20/4(E)-h/4	1610	1380	473	347	-818	17.00	20.14

Notes: DNC = FE solution did not converge

      N/R = data was not recorded

      1 kN = 224.8 lbs, 1 N = 0.2248 lbs, 1 mm = 0.0394 in.

Figure 8.4.9 shows the ratio of the web crippling loads predicted by the FEA to the loads measured by test. The overall average FEA-to-test ratio is 1.26 with a coefficient of variation of 0.157. It is apparent

from Figure 8.4.9 that the FEA consistently over-predicts that capacity of the assembly, and that there is a considerable amount of variance when the data is considered as a whole.
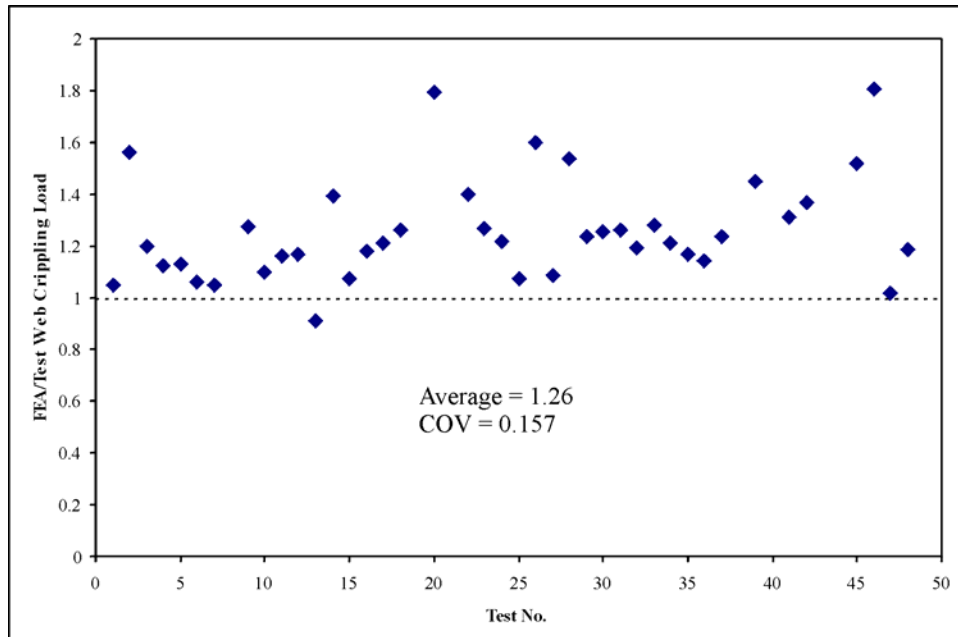
Figure 8.4.9: FEA/Test Web Crippling Load Ratios

One of the variables that was found to cause convergence problems during the FEA was the location of the top fastener. Assemblies with a ratio of h/12 were more apt not to converge, or to predict an incorrect deformed shape. Figures 8.4.10 and 8.4.11 show the data given in Table 8.4.1 separated according to the location of the top fastener. These plots confirm that the h/12 location for the fasteners was not well predicted by the FEA. If these data points are excluded from the comparison, then the average FEA-to-test ratio for the web crippling capacity becomes 1.25 with a coefficient of variation of 0.133. This is some improvement over the whole data set shown in Figure 8.4.9.

A more significant improvement in the results can be seen in the prediction of the fastener forces. The plot in Figure 8.4.11 clearly shows the variability in the forces predicted by the FEA for the h/12 location.
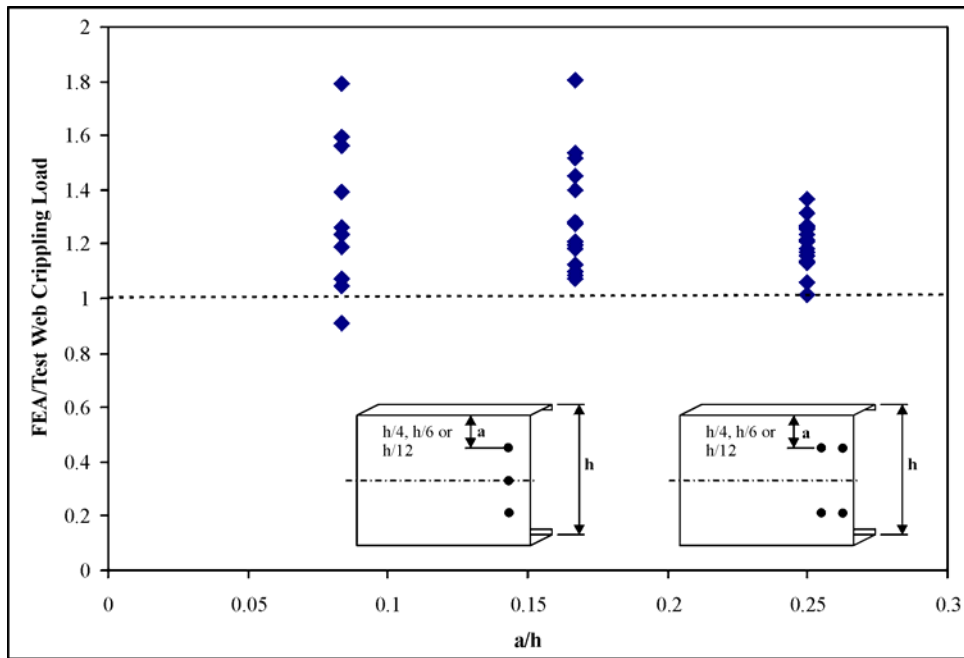
Figure 8.4.10: FEA/Test Results for Web Crippling Load Sorted by Fastener Location
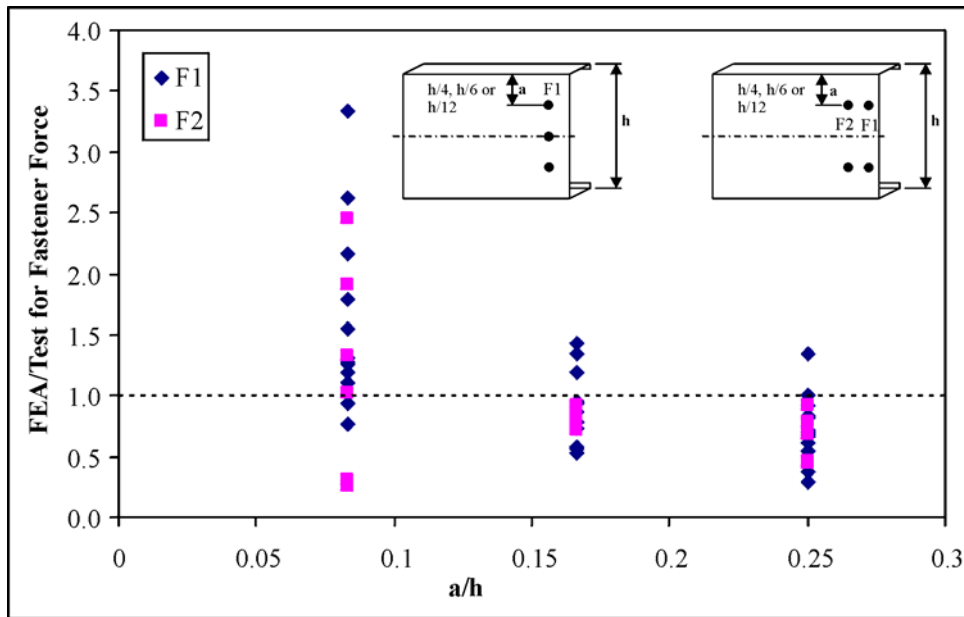
Figure 8.4.11: FEA/Test Results for Fastener Forces Sorted by Fastener Location

8.4.6   Limitations of the FEA Modeling

The discussion in the previous section about the comparisons between the FEA and the test results indicated that the FE model may not be an adequate predictor for certain assembly configurations. Within the range of assemblies investigated, the condition that caused the most convergence problems were those assemblies that failed with web buckling like those shown in the photographs in Figure 8.4.12.
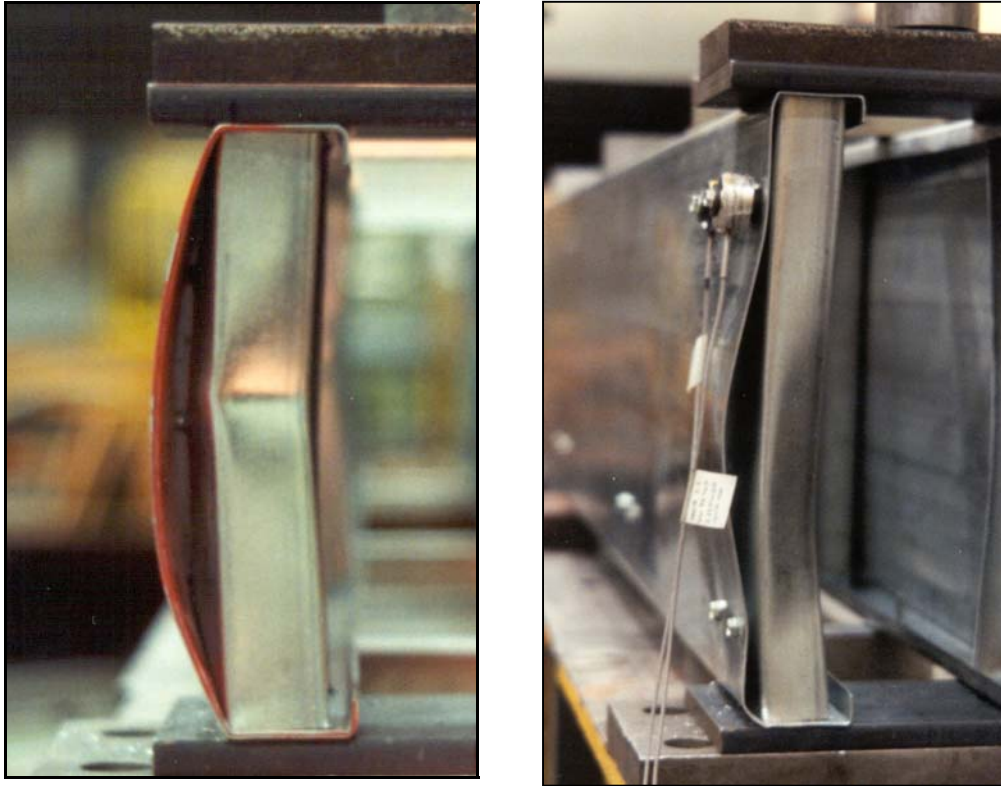
Figure 8.4.12: Buckled Shapes that Cause Convergence Problems in FEA

These photos show the web buckling occurring at the mid-height of the web, not between the bearing plate and the top fastener, which is the more common mode. The buckling mode illustrated in these photos can occur abruptly, and the FE model will have difficulty following the deformed shape. This type of buckling mode is a function of the web slenderness ratio (h/t) and the thickness of the bearing stiffener material, as well as the fastener stiffness.

The left hand photograph in Figure 8.4.12 is 203 mm (8 in.) deep joist with a thickness of 1.91 mm 0.075 in.), giving it a web slenderness of 106. Four of the assemblies listed in Table 8.4.1 that did not converge were for joists of this size. The force required to restrain these sections from web buckling requires a fastener with sufficient pull-out capacity, and located nearer to the middle of the web. The 3-screws in 20 gauge stiffeners, and the 4-screw assemblies at h/12 experienced convergence problems.

The right hand photo in Figure 8.4.12 is a 305 mm (12 in.) deep joist with the 4-screw fastener arrangement into 16 gauge stiffeners. In both the h/12 and h/6 configuration there were convergence problems.

In two of the tests the fastener pulled out of the stiffener before the ultimate load of the assembly was reached. The FE model does not predict fastener pull-out, although it could be checked after the FE analysis provided the fastener forces.

8.5 CONCLUSIONS AND RECOMMENDATIONS

This study has shown how a cold formed steel C-section joist with a bearing stiffener subjected to end-two-flange loading can be successfully modeled by finite element analysis. This FE model can provide a prediction of the web crippling capacity of the joist and the forces in the fasteners connecting the joist to the stiffener. The pull-out capacity of the fastener in the stiffener should be checked as a design limit state in 3-screw assemblies with web slenderness ratios (h/t) less than 110. There are limitations on the applicability of this FE model, and caution should be used in applying the FE solution outside of the range of tested assemblies.

The following recommendations for future work are proposed:

1. The FE model can be used to generate additional data to supplement test results, which can then be used to develop an empirical design expression for the web crippling capacity of the stiffened joist assembly. This web crippling capacity is the serviceability limit state for these cold formed steel C-section joists with bearing stiffeners.

2. The FE model can be used to develop additional data to supplement test results for the fastener forces in these stiffened joist assemblies. An empirical expression could then be developed to predict the fastener forces. Since the bearing stiffener acts as a beam column subjected to axial loads as well as the transverse loads from the fasteners, it is important for the design of these members to know the fastener forces.

3. A similar study and FE model should be developed for the cold formed steel C-section with bearing stiffeners at an intermediate location (i.e. within the span).

4. More complex FE models could be developed that would incorporate more of the features of the real assembly (i.e. initial flange rotation and contact with the top of the stiffener, variations in the corner radius).

5. Alternative FE solution methods should be investigated to overcome the convergence limitations.

9   ANALYSIS OF TEST RESULTS

9.1   COMPARISON OF VARIOUS PREDICTOR METHODS TO TEST RESULTS

Described in this section are comparisons of various predictor methods used to model the test results.

9.2   CURRENT AISI METHOD

The current AISI method was described in Section 2.2. This method assumes that the stiffener is fully effective and that a portion of the joist web acts together with the stiffener to carry the load. This method does not apply to the stud and track stiffeners since these members are not fully effective; however, the channel stiffeners do meet the requirements of the Specification and should be designed accordingly. Only a limited number of tests were carried out on the channel stiffeners since these types of sections were not the primary focus of this research effort. The channels were tested to provide a comparison to the capacities predicted by the current Specification. The summary of the test-to-predicted ratios are reported in Table 9.2.1 and illustrated in Figure 9.2.1. Only tests with the stiffener at the end location were carried out.

Table 9.2.1: Test-to-Predicted Results for the AISI Method with Channel Stiffeners

Configuration	No. of Tests	Mean Test-to-Predicted	C.O.V.
Track-End-Inside	16	0.59	0.236
Track-End-Outside	12	0.74	0.096
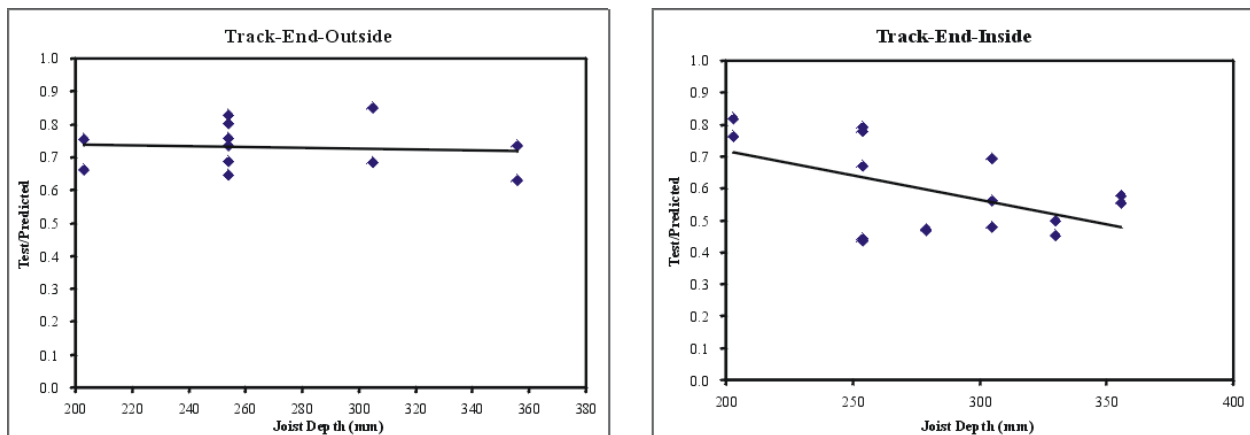
Figure 9.2.1: Plots of the Test-to-Predicted Ratios for the AISI Method with Channel Stiffeners

The results would indicated that the current design method over-estimates the capacity of these sections, particularly for the end-inside configuration. The differences between the tested capacities and those predicted by the Specification can be attributed to the following factors:

- The Specification provisions are based on the results of the test program carried out by Nguyen & Yu [7] described in Section 2.1. During their test set-up they applied the load to the assembly such that the measured strains in each stiffener were the same. This ensured equal load distribution between the stiffeners. In the current test series, the load was centred between the stiffeners, but no measurement of the strains in each stiffener were recorded to ensure equal load distribution. It is probable that the load was not equally distributed between the two stiffeners. This situation would result in lower tested loads since the stiffener with the higher load would fail prematurely. The average load for the two stiffeners would be less than if the load was equally balanced. Consequently, the test-to-predicted ratios would be less than one.

- The work by Nguyen & Yu tested only stiffeners on the outside of the joist web, none on the inside. This choice of this configuration was logical based on the historical precedent with other types of bearing stiffeners. The outside location also provides for full end bearing of the stiffener, another requirement of the Specification. When the stiffener is located on the inside of the joist, the forces on the stiffener will be different since the load transfer is through the joist flange. For these reasons it is reasonable to expect that the test-to-predicted ratios for the end-inside tests will be less than one.

- The specimens tested by Nguyen & Yu connected the stiffener to the joist web with closely spaced #12 screws or 19 mm (3/4 in.) bolts. In the current tests series typically only 4 #10 screws were used to connect the stiffener to the joist. The extra fasteners would certainly contribute to the combined behaviour of a portion of the joist web along with the stiffener section. With only four fasteners the shear transfer between the stiffener and joist web would be significantly reduced and less composite action would be developed.

- The end-inside stiffener configuration will behave much different than the end-outside configuration because of the nature of the buckling behaviour of the joist and stiffener elements. This difference is illustrated in Figure 9.2.2. The C-section stiffener will always buckle in the direction that puts the free ends of the flanges in compression. Similarly, the joist web will always buckle outwards. These two conditions are illustrated in Figure 9.2.2. The interaction between the buckling of the joist web and the buckling of the stiffener is going to influence the capacity of the assembly. When the stiffener is on the outside of the joist the buckling modes will opposed each other and the joist web will provide some support to the stiffener to increase its buckling capacity. Conversely, when the stiffener is between the joist flanges the buckling modes coincide and the joist web buckling will contribute to earlier buckling of the stiffener. This interactive behaviour is the reason the plots of the test-to-predicted ratios for the end-inside stiffeners in Figure 9.2.1 show a decreasing value as the stiffener length increases.

Buckled Shape of
Stiffener End-Inside

Buckled Shape of
Stiffener End-Outside
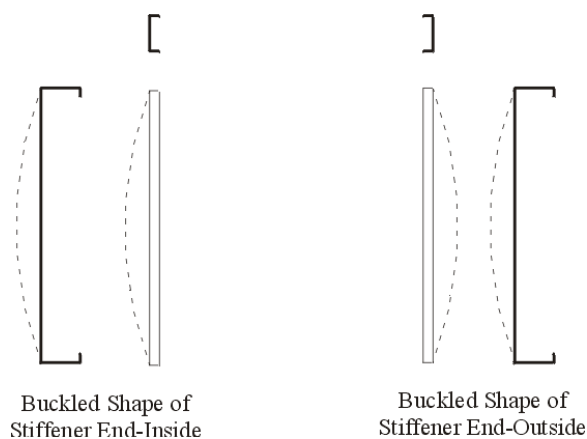
Figure 9.2.2: Buckled Shape of Channel Stiffener and Joist Combinations

9.3   REDUCTION FACTOR WITH GROSS AREA

One of the simplest design methods would be to assume that the stiffener acts as the only load-carrying element in the assembly (as a short compression member) and that the gross area of the stiffener is used to determine its capacity. The following design expression would be used:

$$P_n = RF_yA_g$$

Where,

P_n =   Nominal capacity of the bearing stiffener assembly

R   =   Reduction Factor depending on stiffener type and location (see Table 9.3.1)

F_y =   Yield strength of stiffener steel

A_g =   Gross area of stiffener under uniform compression

Normally the stud and track stiffeners are subject to effective width reductions, however, in this simplified design approach the added work of determining the effective area is ignored in favour of the gross section properties. The comparisons for all of the stud and track assemblies are provided in Table 9.3.1.

Table 9.3.1: Test-to-Predicted Results for the Simplified Gross Area Method

Configuration	No. of Tests	Mean Test-to-Predicted	C.O.V.	R-Factor
Stud Stiffeners				
Stud-End-Inside	109	1.00	0.181	0.494
Stud-End-Outside	21	1.00	0.158	0.557
Stud-Intermediate-Inside	68	1.00	0.162	0.604
Stud-Intermediate-Outside	14	1.00	0.137	0.621
Track Stiffeners				
Track-End-Inside	15	1.00	0.170	0.273
Track-End-Outside	20	1.00	0.307	0.413

Track-Intermediate-Inside	8	1.00	0.061	0.510
Track-Intermediate-Outside	8	1.00	0.085	0.539

9.4 REDUCTION FACTOR WITH EFFECTIVE AREA

Under an applied load, the stud and track stiffener members will be subject to local buckling and the effective section properties should be used. The next design method investigated includes the effective area of the stiffeners in the determination of the capacity of the assembly. The following design expression would be used:

$$P_n = RF_yA_e$$

Where,

P_n = Nominal capacity of the bearing stiffener assembly

R = Reduction Factor depending on stiffener type and location (see Table 9.4.1)

F_y = Yield strength of stiffener steel

A_e = Effective area of stiffener under uniform compression determined at $f = F_y$

In these calculations, any contribution from the joist is ignored and the load is assumed to be carried completely by the stiffener. In addition, it is assumed that the effective length of the stiffener is short enough that overall buckling of the stiffener as a compression member is not a factor. This assumption is valid for stud and track stiffeners in the sizes tested, and was borne out by the observations of the numerous tests where only the channel stiffeners failed in overall buckling.

To simplify the calculation procedure, the effective area of the stiffener is calculated at its yield stress as a concentrically loaded member. The influence of any end eccentricities on the stiffener are considered in a later section.

Table 9.4.1: Test-to-Predicted Results for the Effective Area Method

Configuration	No. of Tests	Mean Test-to-Predicted	C.O.V.	R-Factor
Stud Stiffeners				
Stud-End-Inside	109	1.00	0.115	0.791
Stud-End-Outside	21	1.00	0.144	0.846
Stud-Intermediate-Inside	68	1.00	0.163	0.927
Stud-Intermediate-Outside	14	1.00	0.135	0.938
Track Stiffeners				
Track-End-Inside	15	1.00	0.168	0.788
Track-End-Outside	20	1.00	0.131	0.891
Track-Intermediate-Inside	8	1.038	0.061	1.0
Track-Intermediate-Outside	8	1.081	0.109	1.0

9.5   MODIFIED AISI METHOD

It would be logical to assume that the capacity of the stiffened joist assembly would be influenced by the joist section, and would not only be a function of the stiffener. One method of incorporating the effects of the joist would be to assume that a portion of the joist web area acts with the stiffener. The next design method investigated includes the effective area of the stiffeners plus a portion of the joist web as determined by the AISI Specification [1] in the determination of the capacity of the assembly. The following design expression is used:

$$P_n = RF_{yw}A_{ce}$$

Where,

P_n =   Nominal capacity of the bearing stiffener assembly

R   =   Reduction Factor depending on stiffener type and location (see Table 9.5.1)

F_{yw} =   Lower value of the yield strength of stiffener section or joist web

A_{ce} = $10t^2 + A_e$ for a stiffener at an end support

= $18t^2 + A_e$ for a stiffener at an intermediate support

A_e =   Effective area of stiffener under uniform compression determined at $f = F_y$

Table 9.5.1: Test-to-Predicted Results for the Modified AISI Method

Configuration	No. of Tests	Mean Test-to-Predicted	C.O.V.	R-Factor
Stud Stiffeners				
Stud-End-Inside	109	1.00	0.152	0.705
Stud-End-Outside	21	1.00	0.125	0.758
Stud-Intermediate-Inside	68	1.00	0.108	0.731
Stud-Intermediate-Outside	14	1.00	0.206	0.700
Track Stiffeners				
Track-End-Inside	15	1.14	0.146	1.0
Track-End-Outside	20	1.00	0.208	0.954
Track-Intermediate-Inside	8	1.00	0.062	0.603
Track-Intermediate-Outside	8	1.00	0.079	0.670

9.6   WEB CRIPPLING PLUS STIFFENER CAPACITY

The previous method assumed that the contribution from the joist web came in the form of an effective area added to the area of the stiffener acting as a short concentrically loaded compression member. Another possible mechanism whereby the joist contributes to the capacity of the assembly is through its web crippling strength.

The calculation of the web crippling capacity was determined according to the provisions proposed by Beshara [9], which will appear in the next editon of the AISI Specification. A simplification was needed in the selection of the appropriate web crippling expression. Ordinarily, the web crippling capacity of a C-section would be determined using the provisions for a single web member. This method assumes, however, that the joist web is not restrained in any way. The web of a joist with a bearing stiffener will be restrained from buckling by the connection between the stiffener and the joist. Consequently, the web crippling expressions are not directly applicable. A more complete model would need to account for the restraint imposed by the stiffener on the joist buckling, as well as the position of the fasteners and the physical properties of the stiffener. The current method has calculated the two limits of the web crippling capacity: assuming the stiffener-joist assembly acts like a pair of C-section members back-to-back (upper bound), assuming the joist behaves like a single web member (lower bound). The following design expression is used:

$$P_n = P_{wc} + RF_yA_e$$

Where,

P_n = Nominal capacity of the bearing stiffener assembly

P_{wc} = Nominal web crippling capacity of the joist

R = Reduction factor depending on stiffener type and location (see Table 9.6.1 or 9.6.2)

F_y = Yield strength of stiffener steel

A_e = Effective area of stiffener under uniform compression determined at $f = F_y$

Table 9.6.1: Test-to-Predicted Results for the Web Crippling plus Stiffener Capacity Method
(Single Web Sections)

Configuration	No. of Tests	Mean Test-to-Predicted	C.O.V.	R-Factor
Stud Stiffeners				
Stud-End-Inside	109	1.00	0.109	0.719
Stud-End-Outside	21	1.00	0.103	0.766
Stud-Intermediate-Inside	68	1.00	0.086	0.723
Stud-Intermediate-Outside	14	1.00	0.248	0.817
Track Stiffeners				
Track-End-Inside	15	1.00	0.166	0.744
Track-End-Outside	20	1.00	0.082	0.803
Track-Intermediate-Inside	8	1.00	0.061	0.673
Track-Intermediate-Outside	8	1.00	0.073	0.735

Table 9.6.2: Test-to-Predicted Results for the Web Crippling plus Stiffener Capacity Method
(Built-Up Sections)

Configuration	No. of Tests	Mean Test-to-	C.O.V.	R-Factor

		Predicted		
Stud Stiffeners				
Stud-End-Inside	109	1.00	0.126	0.651
Stud-End-Outside	21	1.00	0.135	0.765
Stud-Intermediate-Inside	68	1.00	0.123	0.646
Stud-Intermediate-Outside	14	1.00	0.165	0.584
Track Stiffeners				
Track-End-Inside	15	1.00	0.166	0.694
Track-End-Outside	20	1.00	0.080	0.722
Track-Intermediate-Inside	8	1.00	0.063	0.526
Track-Intermediate-Outside	8	1.00	0.129	0.596

9.7   END ECCENTRICITY METHOD

In the analysis described in Section 9.4, the stiffener was assumed to be a short concentrically loaded column (stub-column) spanning between the joist flanges. It is also assumed that at the ultimate limit state the stiffener column was carrying the entire load. The average of the test-to-predicted ratios in Table 9.4.1 show that the stub-column capacity generally over-predicts the tested capacity. One explanation for this over-prediction would be an eccentricity of the load application on the end of the stiffener. The deformation of the joist during the loading cycle was discussed in Section 4.2, where it was shown that the joist flange rotation initially contacts one side of the stiffener. It is logical to assume that at the ultimate capacity the load will not be perfectly concentric.

To account for the influence of this end eccentricity, the following strength interaction equation is used:

$$\frac{C_f}{C_r} + \frac{M_{fy}}{M_{rye}} \leq 1.0 \quad \text{which is rewritten as} \quad \frac{C_{test}}{C_r} + \frac{e(C_{test})}{M_{rye}} = 1$$

Where,

C_{test} =   tested load, kN

C_r =   resistance of a concentrically loaded stiffener column, kN

e   =   eccentricity, mm

M_{rye} =   effective moment resistance of the stiffener about the weak axis, kN.mm

The magnitude of the eccentricity is determined by re-arranging the interaction equation as follows:

$$e = \left[1 - \frac{C_{test}}{C_r}\right]\left(\frac{M_{rye}}{C_{test}}\right)$$

An end eccentricity is calculated for each test by assuming the stiffener carries all of the load, and that the difference between the tested capacity and the local buckling capacity (A_eF_y) is caused by this eccentricity. The average end eccentricity is determined based on all of the tests. This end eccentricity is

then used in the interaction equation shown above to in turn predict the capacity of the stiffener. A comparison of the test-to-predicted capacities calculated in this way are presented in Table 9.7.1

Table 9.7.1: Test-to-Predicted Results for the End Eccentricity Method

Configuration	No. of Tests	Eccentricity (mm)	Mean Test-to-Predicted	C.O.V.
Stud Stiffeners				
Stud-End-Inside	109	0.57	1.00	0.142
Stud-End-Outside	21	1.12	1.00	0.167
Stud-Intermediate-Inside	68	0.41	1.00	0.163
Stud-Intermediate-Outside	14	0.34	1.00	0.145
Track Stiffener				
Track-End-Inside	15	9.19-h/39.4	1.03	0.179
Track-End-Outside	20	4.5	1.00	0.124
Track-Intermediate-Inside	8	0	1.09	0.062
Track-Intermediate-Outside	8	0	1.13	0.102

9.8   WEB CRIPPLING

The deformation of C-sections joists with bearing stiffeners between the joist flanges subjected to two-flange loading has been described in section 4.2. As the assembly is loaded, the web of the C-section will collapse (web crippling) until the joist flange is bearing on the end of the stiffener. Depending on the size of the gap between the end of the stiffener and the joist flange, this shortening of the member may have consequences for other components in the structure. In multi-storey platform construction, typical of current cold formed steel residential construction, it is possible that the shortening could accumulate to a significant degree. It is proposed, therefore, that the web crippling capacity of the C-section be used as a serviceability limit state for assemblies with the stiffener between the joist flanges. When the stiffener is attached to the back of the joist the stiffener is the same depth as the joist and will immediately carry load without web crippling of the joist.

There are design equations available [9] for the calculation of the web crippling capacity of various member configurations. These expressions are based on tests of individual members, and do not apply to members such as a C-section with an attached bearing stiffener. The bearing stiffener will restrain the joist web buckling and increase the web crippling capacity of the member. During the study described in Section 5, test data was collected on the web crippling capacity of various end-two-flange and interior-two-flange loaded assemblies. This data was compared to the capacities predicted using the following web crippling equation:

$$P_n = Ct^2F_y\left(1 - C_R\sqrt{R}\right)\left(1 + C_N\sqrt{N}\right)\left(1 - C_H\sqrt{H}\right)$$

Where,

C	=	web crippling coefficient
C_R	=	inside bend radius coefficient
C_N	=	bearing length coefficient
C_H	=	web slenderness coefficient
F_y	=	yield strength of stud material
H	=	h/t
h	=	flat dimension of stud web measured in plane of web
N	=	n/t
n	=	stud bearing length
R	=	r/t
r	=	stud inside bend radius
t	=	thickness of web

The following coefficients are used:

		C	C_R	C_N	C_H
End-two-flange (Unfastened)	Single web member	13	0.32	0.05	0.04
	Built-up section	15.5	0.09	0.08	0.04
Interior-two-flange (Unfastened)	Single web member	24	0.52	0.15	0.001
	Built-up section	36	0.14	0.08	0.04

The test-to-predicted ratios are plotted in Figures 9.8.1 and 9.8.1 for the tests in each series. As expected, these plots show that the test-to-predicted ratios based on the single web member predictor equation are greater than one, especially for the end location. The equation for built-up sections is a better predictor in both the end and interior two-flange loadings, although there is over 20% variance in the results. Since this is a serviceability limit state check, it may be acceptable to use the equation for built-up members even though some data points are unconservative.

It should be pointed out that the preceding analysis assumes that the measurement of the web crippling capacity is accurate. The discussion presented in section 5.4 illustrated how the load deflection curves were used to determine the web crippling capacity. In many cases the inflection point on the curve was not clearly defined and judgment had to be used. It is possible that some of the scatter in the data plotted in Figures 9.8.1 and 9.8.2 are from this source, and not a reflection of the accuracy of the predictor equation.
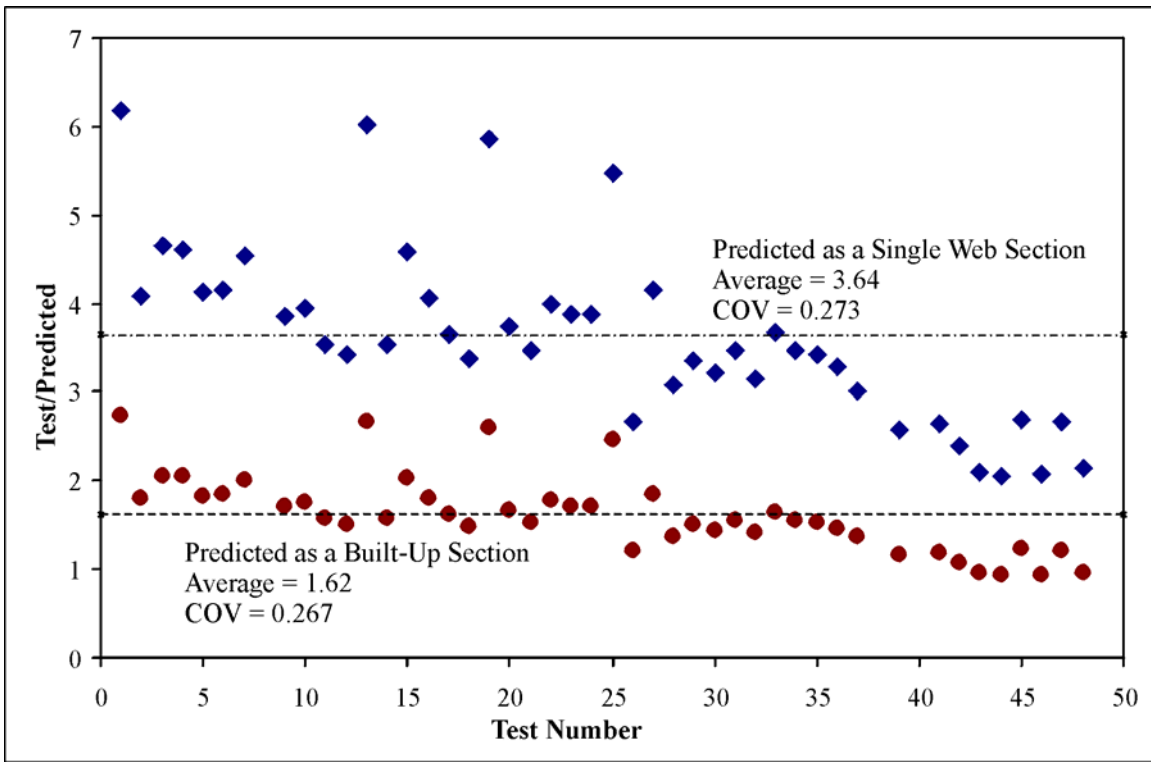
Figure 9.8.1: Web Crippling Test-to-Predicted Ratios for End-Two-Flange Loading
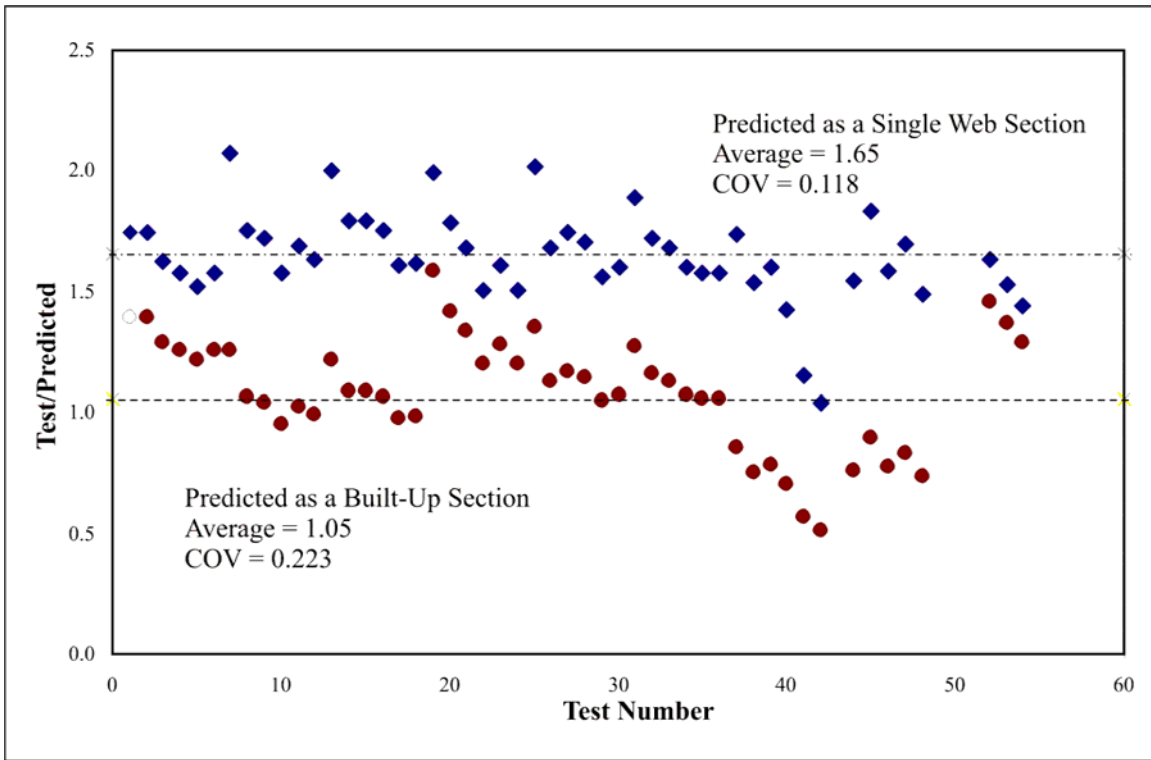
Figure 9.8.2: Web Crippling Test-to-Predicted Ratios for Interior-Two-Flange Loading

103

9.9   COMBINED RESULTS AND CONCLUSIONS

The comparisons of the various prediction methods discussed in the previous sections considered each type of stiffener and configuration separately. The reduction factors were selected to provide the best fit to the data. In practice, it would be more convenient if only one reduction factor or prediction method were used. Table 9.9.1 shows the results if the prediction methods are applied to all of the data for a particular stiffener type. The results in Table 9.9.1 indicate that the best predictor, from those methods investigated, is a reduction of the strength based on the addition of the web crippling capacity of the joist plus the stub column capacity of the stiffener.

Table 9.9.1: Test-to-Predicted Results for All Tests Combined

Configuration	Reduction Factor	No. of Tests	Mean Test-to-Predicted	C.O.V.
Stud Stiffeners				
Gross Area - Reduced Stress	0.50	212	1.09	0.194
Effective Area - Reduced Stress	0.85	212	1.00	0.158
Modified AISI	0.70	212	1.03	0.143
Single Web WC + Stiffener A_eF_y	0.70	212	1.03	0.103
Built-up Section WC + Stiffener A_eF_y	0.65	212	1.00	0.128
Beam-Column Eccentricity of 1.2 mm	N/A	212	1.00	0.179
Track Stiffeners				
Gross Area - Reduced Stress	0.40	51	1.02	0.322
Effective Area - Reduced Stress	0.91	51	1.00	0.171
Modified AISI	0.90	51	1.01	0.278
Single Web WC + Stiffener A_eF_y	0.75	51	1.01	0.123
Built-up Section WC + Stiffener A_eF_y	0.66	51	1.00	0.161
Beam-Column Eccentricity of 2.3 mm	N/A	51	1.00	0.167

It would also be advantageous if a predictor equation could be developed that would apply to both track and stud stiffeners, for all configurations. All of the test data for the stud and track stiffeners were combined and analyzed to determine an appropriate reduction factor. The results are summarized in Table 9.9.2. The results indicate that a 0.70 reduction factor applied to the web crippling plus stub column capacity predictor equation could be applied to both stud and track stiffeners within the limits of the test program.

Table 9.9.2: Test-to-Predicted Results for the Tests Combined

Configuration	Reduction Factor	No. of Tests	Mean Test-to-Predicted	C.O.V.
Stud and Track Stiffeners				
Single Web WC + Stiffener A_eF_y	0.70	263	1.04	0.108

10 SUMMARY AND CONCLUSIONS

The following is a brief summary of the work carried out and the resulting conclusions:

- The behavior of the stiffened joist assembly is a complex interaction of the web crippling of the joist and the action of the bearing stiffener as a beam-column. The parameters that affect the strength of the assembly include the following:
    - Joist size and physical properties.
    - Stiffener type (stud, track, channel) and physical properties (size, thickness, yield strength).
    - Stiffener location (end, intermediate, inside, outside).
    - Bearing width.
    - Number of fasteners and the fastening pattern.
    - Gap between the end of the stiffener and the joist flange.
- The following predictor equations were investigated as possible simplified design methods:
    - A reduced stress on the gross stiffener area.
    - A reduction factor applied to the stub column capacity of the stiffener (i.e. effective stiffener area times the yield stress).
    - A reduction factor applied to the current AISI design approach, but incorporating the effective area of the stiffener.
    - A reduction factor applied to the addition of the web crippling capacity of the joist calculated as a single web member plus the stub column capacity of the stiffener.
    - A reduction factor applied to the addition of the web crippling capacity of the joist calculated as a built-up section plus the stub column capacity of the stiffener.
    - The stiffener designed as a beam-column with a minimum eccentricity.
- The predictor equation that gave the best fit with the combined test data (i.e. all stiffener types and configurations) was the reduction factor applied to the addition of the web crippling capacity of the joist calculated as a single web member plus the stub column capacity of the stiffener. A reduction factor of 0.70 should be applied in this expression. The coefficient of variation for the test-to-predicted values is 0.108.
- The average test-to-predicted ratio for channel stiffeners meeting the requirements of the current AISI specification was approximately 0.75. There were only 12 of tests carried out of this type, but it could indicate that the current design provisions may need to be re-evaluated based on current construction practices.
- The capacity of the assembly is reduced if there is not full bearing under the stiffener. For those stiffeners on the back of the joist where there is not complete end bearing, the strength should be reduced by 50%.

- Fastening the joist flanges to the support does not have a significant effect on the strength of the assembly.

- The gap between the stiffener and the joist flange (inside locations) does not have a significant effect on the ultimate strength of the assembly, however, this gap could lead to serviceability problems. It is recommended that the length of the stiffener should be not less than the depth of the joist minus 10 mm (3/8 in.). This will provide sufficient clearance for installation and limit the deformations.

- The fasteners should be spaced at least a distance of $h/6$ (where h = depth of the joist) away from the joist flanges.

- The web crippling capacity of the joist should be considered as the serviceability limit state for the assembly. From the data collected, the web crippling capacity of the stiffened joist can be predicted using the new AISI design expression for built-up members. This expression will over-estimate the capacity, however, this conservatism may be justified given the scatter in the test data.

- A finite element model of the joist has been developed and calibrated to test results. This model can predict the web crippling capacity of the joist as well as the forces developed in the fasteners connecting the joist to the stiffener. This model will be used in future work to run parametric studies on the influence of varying factors such as fastener location and material properties, and eventually to develop a design expression to calculate the web crippling capacity of joists with bearing stiffeners.

- If a more comprehensive model of the stiffener were to be developed, it would need to recognize that the stiffener behaves as a beam-column acted upon forces in the fasteners connecting the stiffener to the joist as well as an eccentric axial load. The finite element model could be used to provide data to support the development of a design method.

11 PROPOSED DESIGN EXPRESSIONS AND AISI SPECIFICATION CHANGE

11.1 SIMPLIFIED DESIGN EXPRESSION (STRENGTH LIMIT STATE)

Based on the summary and conclusions discussed in Section 9.9, the following simplified design expression for the two-flange loading of C-section members with bearing stiffeners is proposed:

$$P_n = 0.7(P_{wc} + A_e F_y)$$

United States and Mexico		Canada
ASD, S	LRFD, N	LSD, N
1.685	0.910	0.783

Note: Calculated according to the AISI Specification Commentary
using the statistical data from Table F1 for transverse stiffeners.

Where,

P_{wc} = web crippling strength for the C-section joist calculated in accordance with the new AISI Specification provisions for single web members, end or interior locations.

A_e = effective area of the bearing stiffener subjected to uniform compressive stress, calculated at the yield stress

F_y = yield strength of the stiffener steel

This expression applies within the following limits:

1. Stiffeners can be stud or track members (nominal 3-5/8" wide)
2. The stiffener is attached to the joist web with at least three fasteners
3. The length of the stiffener shall not be less then the depth of the joist minus 3/8"
4. The end of the stiffener must have complete end bearing

If the width of bearing is less than the width of the stiffener, the capacity must be reduced by 50%.

11.2 WEB CRIPPLING (SERVICEABILITY LIMIT STATE)

The serviceability limit state is based on the web crippling of the joist member for those assemblies with the bearing stiffener installed between the joist flanges. Those assemblies with the stiffener on the back of the joist web should specify that the stiffener must be the same length as the joist depth, which will preclude web crippling. The web crippling capacity should be calculated based on the new AISI design equations for two-flange loading of built-up sections.

11.3 PROPOSED AISI SPECIFICATION

Add a new Section B6.2 to the Specification as follows and re-number the following sections accordingly:

6.2 Bearing Stiffeners in C-Section Joists

For the two-flange loading of C-section flexural members with bearing stiffeners, the nominal strength P_n is determined as follows:

$$P_n = 0.7(P_{wc} + A_e F_y) \qquad\qquad (Eq. \text{ B6.2-1})$$

United States and Mexico		Canada
ASD	LRFD	LSD
1.69	0.91	0.78

Where,

P_{wc} = web crippling strength for the C-section flexural member calculated in accordance with Equation X-X for single web members, end or interior locations

A_e = effective area of the bearing stiffener subjected to uniform compressive stress, calculated at the yield stress

F_y = yield strength of the stiffener steel

This expression applies within the following limits:

1. Stiffeners can be stud or track members (nominal 3-5/8" wide)
2. The stiffener is attached to the joist web with at least three fasteners
3. The length of the stiffener shall not be less then the depth of the joist minus 3/8"
4. The end of the stiffener must have complete end bearing

If the width of bearing is less than the width of the stiffener, the capacity must be reduced by 50%.

12 FUTURE WORK

12.1 STIFFENER BEAM-COLUMN MODEL

The work described in this report was a compilation of tests aimed at determining the behaviour of joist assemblies with bearing stiffeners. Some general conclusions were derived from the analysis of the results; however, the proposed predictor equation is essentially empirical. To develop a more generic predictor equation it is first necessary to develop a model representing the stiffener that incorporates its interaction with the deformation of the joist web. Such a model is shown in Figure 12.1.1 for a stiffener inside the joist flanges with two different fastener patterns. Similar models can be developed for the other assembly combinations.
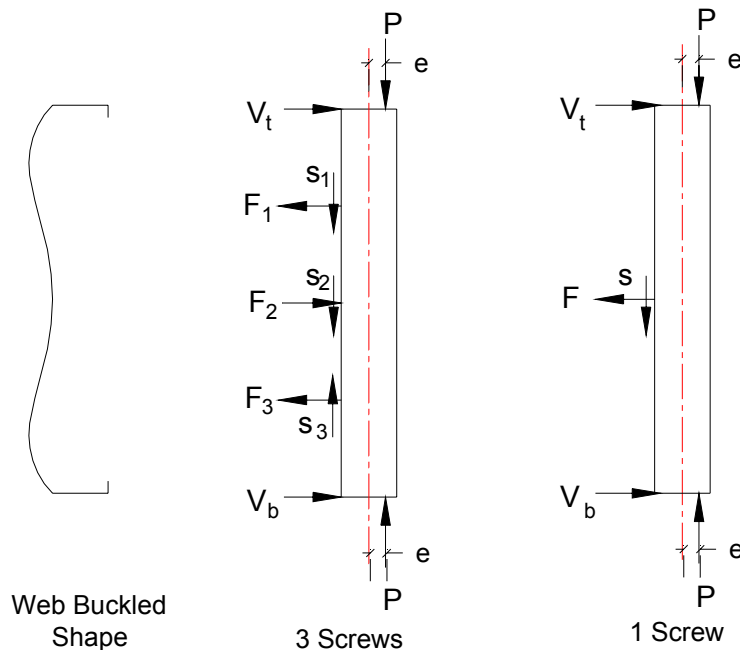
Figure 12.1.1: Stiffener Beam-Column Model

The forces, F_1, F_2 and F_3, are the forces exerted on the stiffener by the fasteners and are caused by the joist web buckling. The web buckling study discussed in Section 7 and the measurements of the fastener forces discussed in Section 5.6 corroborate this model. The shear forces at the fasteners, s_1, s_2 and s_3, have not been measured in any of the work so far, but are expected to be present as a result of the deflection of the web. The force, P, is the applied load and the eccentricity of this load is defined as, e. The end shear forces, V_t and V_b, are needed to balance the fastener forces. The other stiffener beam-column model shown in Figure 12.1.1 is for a single fastener (or pair of fasteners) at mid-height. In general, the forces are the same except for the direction of the fastener force, F.

The design of this stiffener could be carried out according to the current provisions of the AISI Specification for beam-columns if the eccentricity of the applied load and the fastener forces were known. This information could be obtained through the following process:

Step 1: Use the finite element model described in Section 8 to run a parametric study on the influence of fastener location and fastener stiffness on the fastener forces.
Step 2: Statistically analyze the results of the FE parametric study to develop a multiple regression equation that can be used to predict the fastener forces in a stiffener assembly.
Step 3: Use the regression equation from Step 2 to determine the forces in the fasteners for each of the assemblies tested. Once the fastener forces are known the equivalent eccentricity of the load can be calculated based on the beam-column interaction equation. A relationship can be developed relating relevant parameters of the assembly to the resulting eccentricity.
Step 4: The predictor equation for the fastener forces along with the predictor equation for the end eccentricity can be incorporated into a beam-column design expression that could be included in the AISI Specification as an alternative to the simplified design expressions.

The overall column buckling capacity of the stiffener will also be a consideration. The discussions so far have focused on stiffeners that fail through local buckling, but there are other stiffeners (i.e. channel members) that will fail by overall column buckling. A stability check on the stiffener will need to be included for these smaller stiffeners. One task will be to find the limiting slenderness where overall buckling takes over from local buckling.

12.2 STIFFENED PLATE MODEL

The tests of the channel stiffeners have shown that one of the failure modes is overall buckling of the stiffener and joist web. This type of failure mechanism is quite different from the local buckling type of failure observed for the stud and track stiffeners. The buckling mode of failure lends itself to an alternative model of the assembly, specifically a stiffened plate model.

The bucking of plates subject to edge loading has been investigated by many researchers over the years. The exact solution for the critical elastic buckling stress is possible for very simple plates and loading configuration, but for more complicated assemblies, approximate solutions must be used or the assembly must be tested. There have been a large number of research projects carried out investigating the web crippling capacity of cold formed steel structural members. There have also been many studies of the behavior of stiffened plates, originating with the ship building industry and then expanded upon considerably by the aircraft designers.

The development of the stiffened plate model for the stiffened C-section could consider the interactive buckling of a stiffener connected to a plate by discrete fasteners. The reason for pursuing this type of study would be to determine the limit when an assembly stops behaving like a stiffener plate subjected to patch loading, and starts to behave like a stiffener subjected to eccentric loads and fastener forces.

12.3 SERVICABILITY LIMIT STATE

The discussion in Section 9.8 indicated that web crippling of the joist could be considered as a serviceability limit state. A design expression to calculate this capacity could be determine using the following methodology:

Step 1: The finite element model described in Section 8 can be used to run a parametric study on the influence of fastener location and stiffness on the web crippling capacity of the joist.

Step 2: The results of the FE parametric study can be statistically analyzed to develop a multiple regression equation that can be used to predict the web crippling capacity of the joist in a stiffened assembly. This predictor equation would be of the same form as the AISI Specification (see section 9.8) and would incorporate parameters such as the fastener pattern and location, joist properties, stiffener properties.

12.4 OTHER ASSEMBLIES AND STIFFENER TYPES

The following are suggestions for future research topics:

- A cold formed steel C-section with a bearing stiffener is normally part of an assembly that can include a rim track and a plywood sub-floor. Additional testing needs to be carried out on these assemblies to determine what additional capacity is developed.

- The use of other types of bearing stiffeners such as clip angles should be investigated.

- All of the tests carried out as part of this research have been two-flange loading. This was selected since it is the most severe loading condition that a stiffener will experience. In practice there are situations where the member is subjected to one flange loading, or a combination of one and two flange loading. These conditions also need to be investigated.

- Additional data would be useful for the track stiffeners.

13 ACKNOWLEDGMENTS

14 REFERENCES

1. American Iron and Steel Institute, *Specification for the Design of Cold-Formed Steel Structural Members* with the 1999 Supplement, Washington, D.C. , June, 1997

2. Canadian Standards Association, CSA-S136-94 *Cold Formed Steel Structural Members*, Rexdale (Toronto), Ontario, Canada 1994

3. LaBoube, R.A., and Yu, W.W., *Structural Behavior of Beam Webs Subjected toBending Stress*, final report, civil engineering study 78-1, University of Missouri-Rolla, June 1978

4. LaBoube, R.A., and Yu, W.W., *Structural Behavior of Beam Webs Subjected Primarily to Shear*, final report, civil engineering study 78-2, University of Missouri-Rolla, June 1978

5. LaBoube, R.A., and Yu, W.W., *Structural Behavior of Beam Webs Subjected to a Combination of Bending and Shear*, final report, civil engineering study 78-3, University of Missouri-Rolla, June 1978.

6. Hetrakul, N., and Yu, W.W., *Structural Behavior of Beam Webs Subjected to Web Crippling and a Combination of Web Crippling and Bending,* final report, civil engineering study 78-4, University of Missouri-Rolla, June 1978

7. Nguyen, P., and Yu, W.W., *Structural Behavior of Transversely Reinforced Beam Webs,* final report, Civil Engineering Study 78-5, University of Missouri-Rolla, USA, June 1978

8. Nguyen, P., and Yu, W.W., *Structural Behavior of Longitudinally Reinforced Beam Webs,* final report, Civil Engineering Study 78-6, University of Missouri-Rolla, USA, June 1978

9. Beshara, B., *Web Crippling of Cold Formed Steel Members*, M.A.Sc. Thesis, University of Waterloo, Canada, 1999

10. American Iron and Steel Institute, *Specification for the Design of Cold-Formed Steel Structural Members*, Washington, D.C., June, 1997, Including Supplement No.1, July 30, 1999

11. Canadian Standards Association, CSA-S136-94 *Cold Formed Steel Structural Members*, Rexdale (Toronto), 1994

12. Nguyen, P., and Yu, W.W., *Structural Behavior of Transversely Reinforced Beam Webs,* final report, Civil Engineering Study 78-5, University of Missouri-Rolla, USA, June 1978

13. Fox, S.R and Schuster, R.M., "Tests of Cold Formed Steel Floor Joists With Bearing Stiffeners", Proceedings of the 14th International Specialty Conference on Cold Formed Steel Structures, University of Missouri-Rolla, October 1998

14. Fox, S.R. and Schuster, R.M. "First Summary Report: Bearing Stiffeners in Cold Formed Steel C-Sections", American Iron and Steel Institute, Washington, D.C., February, 2000

15. Fox, S.R and Schuster, R.M., "Strength of Bearing Stiffeners in Cold Formed Steel C-Sections", Proceedings of the 15th International Specialty Conference on Cold Formed Steel Structures, University of Missouri-Rolla, October 2000

16. Fox, S.R., "Effect of End Gap and Screw Pattern on the Bearing Capacity of Stiffened Cold Formed Steel C-sections", Canadian Cold Formed Steel Research Group report, University of Waterloo, Waterloo, Ontario, Canada, October 1999

17. Fox, S.R., "Effect of Bearing Width on the Bearing Capacity of Stiffened Cold Formed Steel C-sections", Canadian Cold Formed Steel Research Group report, University of Waterloo, Waterloo, Ontario, Canada, October 1999

18. Fox, S.R., "Effects of Material Thickness and Fastening the Joist Flanges on the Capacity of Bearing Stiffeners in Cold Formed Steel C-sections", Canadian Cold Formed Steel Research Group report, University of Waterloo, Waterloo, Ontario, Canada, May 2000

19. Fox, S.R., "Measurement of the Fastener Forces and Web Crippling Capacity of Bearing Stiffeners in Cold Formed Steel C-Sections", Canadian Cold Formed Steel Research Group report, University of Waterloo, Waterloo, Ontario, Canada, February 2001

20. American Iron and Steel Institute, AISI/COFS/GP 2001, *Standard for Cold-Formed Steel Framing – General Provisions*, Washington, D.C., 2001

21. Canadian Sheet Steel Building Institute, *Residential Steel Framing – Installation Manual*, CSSBI 55-99, Cambridge, Ontario, August 1999.

22. Frisch-Fay, R., *Flexible Bars*, Butterworths Scientific Publications, London, 1962

APPENDIX A:

TEST SPECIMEN MATERIAL PROPERTIES AND STIFFENER DIMENSIONS

Table A1: Material Properties

Material Designation	Specimen Type	Thickness (mm)	Yield Stress F_y (MPa)	Tensile Stress F_u (MPa)	% Elong.
S1	92 mm (3-5/8 in.) Stud	0.81	341	387	32.0
S2	92 mm (3-5/8 in.) Stud	0.81	349	373	31.4
S3	92 mm (3-5/8 in.) Stud	0.82	357	390	33.3
S4	92 mm (3-5/8 in.) Stud	0.85	337	370	35.6
S5	92 mm (3-5/8 in.) Stud	0.86	336	376	34.7
S6	92 mm (3-5/8 in.) Stud	0.88	345	351	36.9
S7	92 mm (3-5/8 in.) Stud	1.09	354	380	35.1
S8	92 mm (3-5/8 in.) Stud	1.19	300	387	28.9
S9	92 mm (3-5/8 in.) Stud	1.46	409	495	28.1
S10	92 mm (3-5/8 in.) Stud	1.50	399	555	27.3
T1	92 mm (3-5/8 in.) Track	0.79	358	390	33.4
T2	92 mm (3-5/8 in.) Track	0.85	575	591	12.9
T3	92 mm (3-5/8 in.) Track	0.89	663	668	14.0
T4	92 mm (3-5/8 in.) Track	1.08	321	354	35.7
T5	92 mm (3-5/8 in.) Track	1.09	399	459	29.3
T6	92 mm (3-5/8 in.) Track	1.45	408	432	32.1
T7	92 mm (3-5/8 in.) Track	1.81	388	437	33.1
J1	203 mm (8 in.) Joist	0.87	352	372	37.2
J2	203 mm (8 in.) Joist	1.18	336	431	29.6
J3	203 mm (8 in.) Joist	1.21	323	376	32.7
J4	203 mm (8 in.) Joist	1.83	413	536	28.8
J5	203 mm (8 in.) Joist	1.85	390	489	29.7
J6	254 mm (10 in.) Joist	1.26	306	383	34.4
J7	254 mm (10 in.) Joist	1.33	293	367	36.0
J8	254 mm (10 in.) Joist	1.81	415	555	27.3
J9	279 mm (11 in.) Joist	1.28	297	356	35.3
J10	305 mm (12 in.) Joist	1.21	332	374	33.7
J11	305 mm (12 in.) Joist	1.24	308	360	34.1
J12	305 mm (12 in.) Joist	1.24	307	360	35.3
J13	305 mm (12 in.) Joist	1.49	385	511	27.3
J14	305 mm (12 in.) Joist	1.87	398	507	27.5
J15	330 mm (13 in.) Joist	1.28	329	358	35.3
J16	356 mm (14 in.) Joist	1.24	298	369	36.6

Note: Reported values are the average of three tests.
  1 kN = 224.8 lbs, 1 N = 0.2248 lbs, 1 mm = 0.0394 in., 1 MPa = 0.145 ksi

Table A2: Stiffener Dimensions (Stud-End-Inside)

Test Designation	Left Hand Stiffener					Right Hand Stiffener				
	lip1 (mm)	lip2 (mm)	flange1 (mm)	flange2 (mm)	web (mm)	lip1 (mm)	lip2 (mm)	flange1 (mm)	flange2 (mm)	web (mm)
Stud-E/I-1	7.0	8.5	31	31	92	8.8	7.3	30	32	92
Stud-E/I-2	9.0	7.0	32	32	91	8.5	8.5	32	32	92
Stud-E/I-3	7.5	8.6	31	31	92	8.7	7.2	31	31	92.3
Stud-E/I-4	7.3	8.3	31	31	92	7.3	8.2	31	31	92
Stud-E/I-5	8.5	7.5	31	32	93	8.6	7.6	32	32	92
Stud-E/I-6	8.0	8.0	31	31	92	8	7	33	31	93
Stud-E/I-7	7.0	8.6	31	32	91	8	7	31	32	91
Stud-E/I-8	7.0	8.5	31	32	91	8	7	31	31	91
Stud-E/I-9	7.5	7.0	31	32	92	7.5	7	31	32	92
Stud-E/I-10	7.5	7.0	31	32	92	7.5	7	31	33	92
Stud-E/I-11	7.0	8.5	31	32	91	7.3	8.8	31	31	92
Stud-E/I-12	7.5	8.0	30	31	91	8	8	31	31	91
Stud-E/I-13	7.5	8.0	30	31	91	8	8	31	31	91
Stud-E/I-14	7.0	7.5	31	31	91	7.5	7	31	31	91
Stud-E/I-15	7.5	7.5	31	32	91	7	7.5	31	32	91
Stud-E/I-16	8.0	7.0	31	31	91	7	8.5	31	31	91
Stud-E/I-17	8.0	7.0	31	31	91	7	8	31	31	91
Stud-E/I-18	7.5	8.0	30	31	91	8	8	31	31	91
Stud-E/I-19	5.0	7.0	32	32	91	5.0	7.0	32	32	91
Stud-E/I-20	5.0	7.0	32	32	91	5.0	7.0	32	32	91
Stud-E/I-21	5.0	7.0	32	32	91	5.0	7.0	32	32	91
Stud-E/I-22	6.0	7.0	31	32	90	6.0	7.0	31	32	90
Stud-E/I-23	5.0	7.0	32	32	91	6.0	7.0	31	32	90
Stud-E/I-24	6.0	7.0	31	32	90	6.0	7.0	31	32	90
Stud-E/I-25	5.0	7.0	32	32	91	5.0	7.0	32	32	91
Stud-E/I-26	5.0	7.0	32	32	91	5.0	7.0	32	32	91
Stud-E/I-27	5.0	7.0	32	32	91	5.0	7.0	32	32	91
Stud-E/I-28	6.0	7.0	31	32	90	6.0	7.0	31	32	90
Stud-E/I-29	5.0	7.0	32	32	91	5.0	7.0	32	32	91
Stud-E/I-30	6.0	7.0	31	32	90	6.0	7.0	31	32	90
Stud-E/I-31	7.0	6.0	32	32	91	7.0	6.0	32	32	91
Stud-E/I-32	7.0	6.0	32	32	91	7.0	6.0	32	32	91
Stud-E/I-33	7.0	6.0	32	32	91	7.0	6.0	32	32	91
Stud-E/I-34	7.0	6.0	32	32	91	7.0	6.0	32	32	91
Stud-E/I-35	7.0	6.0	32	32	91	7.0	6.0	32	32	91
Stud-E/I-36	7.0	6.0	32	32	91	7.0	6.0	32	32	91
Stud-E/I-37	7.0	6.0	32	32	91	7.0	6.0	32	32	91
Stud-E/I-38	7.0	6.0	32	32	91	7.0	6.0	32	32	91
Stud-E/I-39	7.0	6.0	32	32	91	7.0	6.0	32	32	91
Stud-E/I-40	7.0	6.0	32	32	91	7.0	6.0	32	32	91

Stud-E/I-41	7.0	6.0	32	32	91	7.0	6.0	32	32	91
Stud-E/I-42	7.0	6.0	32	32	91	7.0	6.0	32	32	91
Stud-E/I-43	7.0	6.0	32	32	91	7.0	6.0	32	32	91
Stud-E/I-44	7.0	6.0	32	32	91	7.0	6.0	32	32	91
Stud-E/I-45	7.0	6.0	32	32	90	7.0	7.0	32	32	91
Stud-E/I-46	7.0	6.0	32	32	90	7.0	7.0	32	32	91
Stud-E/I-47	7.0	6.0	32	32	90	7.0	6.0	32	32	91
Stud-E/I-48	7.0	6.0	32	32	90	7.0	7.0	32	32	91
Stud-E/I-49	7.0	6.0	32	32	90	7.0	7.0	32	32	91
Stud-E/I-50	7	7.5	33	33	93	7	7.5	33	33	91
Stud-E/I-51	7	7.5	33	33	93	7	7.5	33	33	91
Stud-E/I-52	7	7.5	33	33	93	7	7.5	33	33	91
Stud-E/I-53	7	7.5	33	33	93	7	7.5	33	33	91
Stud-E/I-54	7	7.5	33	33	93	7	7.5	33	33	91
Stud-E/I-55	7	7.5	33	33	93	7	7.5	33	33	91
Stud-E/I-56	7	7.5	33	33	93	7.5	7.5	33	33	91
Stud-E/I-57	7	7.5	33	33	93	7	7.5	33	33	91
Stud-E/I-58	7	7.5	33	33	93	7	7.5	33	33	91
Stud-E/I-59	7.5	7.5	33	33	93	7.5	7.5	33	33	91
Stud-E/I-60	7	7.5	33	33	93	7.5	7.5	33	33	91
Stud-E/I-61	7.5	7.5	33	33	93	7.5	7.5	33	33	91
Stud-E/I-62	8.0	7.5	32	32	93	7.5	7	32	32	91
Stud-E/I-63	7.0	8.0	32	32	93	7	8	32	32	91
Stud-E/I-64	7.0	8.0	32	32	93	7	8	32	32	91
Stud-E/I-65	7.5	7.5	32	32	93	7	8	32	32	91
Stud-E/I-66	7.0	8.0	32	32	93	7	8	32	32	91
Stud-E/I-67	7.0	8.0	32	32	93	7	8	32	32	91
Stud-E/I-68	7.0	7.5	32	32	93	7	7.5	32	32	91
Stud-E/I-69	7.5	7.5	32	32	93	7.5	7.5	32	32	91
Stud-E/I-70	7.0	7.5	32	32	93	7	7.5	32	32	91
Stud-E/I-71	7.0	8.0	32	32	93	7	7.5	32	32	91
Stud-E/I-72	7.0	8.0	32	32	93	7	8	32	32	91
Stud-E/I-73	7.0	8.0	32	32	93	7	8	32	32	91
Stud-E/I-74	7.5	7.5	32	32	93	7.5	7.5	32	32	91
Stud-E/I-75	7.0	8.0	32	32	93	7	8	32	32	91
Stud-E/I-76	6.5	8.0	32	32	93	7	8	32	32	91
Stud-E/I-77	7.0	8.0	32	32	93	7	8	32	32	91
Stud-E/I-78	7.0	7.0	32	32	93	7	7	32	32	91
Stud-E/I-79	7.0	8.0	32	32	93	7	8	32	32	91
Stud-E/I-80	7.0	8.0	32	32	93	7.5	8	32	32	91
Stud-E/I-81	7.0	8.0	32	32	93	7	8	32	32	91
Stud-E/I-82	7.5	7.5	32	32	93	7.5	7.5	32	32	91
Stud-E/I-83	7.0	8.0	32	32	93	7	8	32	32	91
Stud-E/I-84	8.0	7.5	32	32	93	7	8	32	32	91

Stud-E/I-85	7.0	8.0	32	32	93	7	8	32	32	91
Stud-E/I-86	7.5	7.0	32	32	93	7.5	7.5	32	32	91
Stud-E/I-87	7.0	8.0	32	32	93	7	8	32	32	91
Stud-E/I-88	7.0	8.0	32	32	93	7	8	32	32	91
Stud-E/I-89	7.0	8.0	32	32	93	7	8	32	32	91
Stud-E/I-90	7.5	7.5	32	32	93	7.5	7.5	32	32	91
Stud-E/I-91	7.0	8.0	32	32	93	7	8	32	32	91
Stud-E/I-92	7.5	7.5	32	32	93	7	8	32	32	91
Stud-E/I-93	7.0	7.5	32	32	93	7	7.5	32	32	91
Stud-E/I-94	7.5	7.5	32	32	93	7.5	8	32	32	91
Stud-E/I-95	7.0	8.0	32	32	93	7	8	32	32	91
Stud-E/I-96	7.5	7.0	32	32	93	7.5	7.5	32	32	91
Stud-E/I-97	7.0	8.0	32	32	93	7	8	32	32	91
Stud-E/I-98	7.0	7.5	32	32	93	7	7	32	32	91
Stud-E/I-99	7.0	8.0	32	32	93	7	8	32	32	91
Stud-E/I-100	7.0	8.0	32	32	93	7.5	8	32	32	91
Stud-E/I-101	7.0	7.5	32	32	93	7.5	7.5	32	32	91
Stud-E/I-102	7.0	7.0	32	32	93	7	7	32	32	91
Stud-E/I-103	7.0	8.0	32	32	93	7	8	32	32	91
Stud-E/I-104	7.0	8.0	32	32	93	7.5	8	32	32	91
Stud-E/I-105	7.0	8.0	32	32	93	7	8	32	32	91
Stud-E/I-106	7.0	8.0	32	32	93	7	8	32	32	91
Stud-E/I-107	7.0	7.5	32	32	93	7	7.5	32	32	91
Stud-E/I-108	7.0	8.0	32	32	93	7	8	32	32	91
Stud-E/I-109	7.0	8.0	32	32	93	7	8	32	32	91

1 kN = 224.8 lbs, 1 N = 0.2248 lbs, 1 mm = 0.0394 in., 1 MPa = 0.145 ksi

Table A3: Stiffener Dimensions (Stud-End-Outside)

Test Designation	Left Hand Stiffener					Right Hand Stiffener				
	lip1 (mm)	lip2 (mm)	flange1 (mm)	flange2 (mm)	web (mm)	lip1 (mm)	lip2 (mm)	flange1 (mm)	flange2 (mm)	web (mm)
Stud-E/O-1	7	8	32	32	93	8	7	32	33	93
Stud-E/O-2	7	8	32	32	93	7	8	33	32	93
Stud-E/O-3	7	6	32	32	90	7	6	32	32	90
Stud-E/O-4	7	6	32	32	90	7	6	32	32	90
Stud-E/O-5	12	12	42	42	92	12	12	42	42	92
Stud-E/O-6	12	12	42	42	92	12	13	42	42	92
Stud-E/O-7	13	12	42	42	92	12	13	42	42	92
Stud-E/O-8	13	12	42	42	92	12	13	42	42	92
Stud-E/O-9	11	12	42	42	93	12	12	42	42	93
Stud-E/O-10	12	12	42	42	93	12	12	42	42	93
Stud-E/O-11	12	12	42	42	94	12	12	42	42	94
Stud-E/O-12	12	12	42	42	94	12	12	42	42	94
Stud-E/O-13	7	7.5	33	33	93	7	7.5	33	33	93
Stud-E/O-14	7	7.5	33	33	93	7	7.5	33	33	93

Stud-E/O-15	7	8	33	33	93	7	8	33	33	93
Stud-E/O-16	7	8	33	33	93	7	8	33	33	93
Stud-E/O-17	7	7.5	33	33	93	7	7.5	33	33	93
Stud-E/O-18	7	7.5	33	33	93	7	7.5	33	33	93
Stud-E/O-19	7.5	7.5	33	33	93	7.5	7.5	33	33	93
Stud-E/O-20	7	7.5	33	33	93	7	7.5	33	33	93
Stud-E/O-21	7.5	7.5	33	33	93	7.5	7.5	33	33	93

1 kN = 224.8 lbs, 1 N = 0.2248 lbs, 1 mm = 0.0394 in., 1 MPa = 0.145 ksi

Table A4: Stiffener Dimensions (Stud-Intermediate-Inside)

Test Designation	Left Hand Stiffener					Right Hand Stiffener				
	lip1 (mm)	lip2 (mm)	flange1 (mm)	flange2 (mm)	web (mm)	lip1 (mm)	lip2 (mm)	flange1 (mm)	flange2 (mm)	web (mm)
Stud-I/I-1	8	7	33	32	93	8	7	32	33	92
Stud-I/I-2	7	8	32	32	93	7	8	33	32	93
Stud-I/I-3	8	7	32	32	92	7	8	32	31	92
Stud-I/I-4	8	7	31	32	91	8	7	32	32	92
Stud-I/I-5	8.3	7	31	31	91	8.3	7	31	31	91
Stud-I/I-6	7	8	32	32	91	7	8.3	31.5	31.5	91
Stud-I/I-7	7	8	32	32	92	7	8	32	32	92
Stud-I/I-8	7	8.3	31	31	92	7	8.3	31	32	92
Stud-I/I-9	7	6	32	32	90	7	6	32	32	90
Stud-I/I-10	7	7	32	32	90	7	6	32	32	90
Stud-I/I-11	7	7.5	33	33	93	7	7.5	33	33	93
Stud-I/I-12	7	7.5	33	33	93	7	7.5	33	33	93
Stud-I/I-13	7	7.5	33	33	93	7	7.5	33	33	93
Stud-I/I-14	7	7.5	33	33	93	7	7.5	33	33	93
Stud-I/I-15	7.0	8.0	32	32	93	7.5	7	32	32	93
Stud-I/I-16	7.0	8.0	32	32	93	7	8	32	32	93
Stud-I/I-17	7.0	8.0	32	32	93	7	8	32	32	93
Stud-I/I-18	7.0	8.0	32	32	93	7	7.5	32	32	93
Stud-I/I-19	7.5	7.5	32	32	93	7.5	7.5	32	32	93
Stud-I/I-20	7.5	7.5	32	32	93	7	7.5	32	32	93
Stud-I/I-21	7.5	8.0	32	32	93	7.5	8	32	32	93
Stud-I/I-22	7.0	8.0	32	32	93	7	8	32	32	93
Stud-I/I-23	7.0	7.5	32	32	93	7.5	7.5	32	32	93
Stud-I/I-24	7.0	7.5	32	32	93	7	7.5	32	32	93
Stud-I/I-25	7.0	7.5	32	32	93	7	7.5	32	32	93
Stud-I/I-26	7.0	8.0	32	32	93	7	7.5	32	32	93
Stud-I/I-27	7.5	7.5	32	32	93	7.5	7.5	32	32	93
Stud-I/I-28	7.0	8.0	32	32	93	7	8	32	32	93
Stud-I/I-29	7.0	8.0	32	32	93	7	8	32	32	93
Stud-I/I-30	7.0	8.0	32	32	93	7	8	32	32	93
Stud-I/I-31	7.0	7.5	32	32	93	7	7.5	32	32	93
Stud-I/I-32	7.0	8.0	32	32	93	7	8	32	32	93

Stud-I/I-33	7.0	8.0	32	32	93	7	8	32	32	93
Stud-I/I-34	7.0	7.5	32	32	93	7	7.5	32	32	93
Stud-I/I-35	7.5	8.0	32	32	93	7.5	7.5	32	32	93
Stud-I/I-36	7.0	8.0	32	32	93	7	8	32	32	93
Stud-I/I-37	7.0	8.0	32	32	93	7	8	32	32	93
Stud-I/I-38	7.0	8.0	32	32	93	7	8	32	32	93
Stud-I/I-39	7.5	7.5	32	32	93	7	7.5	32	32	93
Stud-I/I-40	7.0	8.0	32	32	93	7	8	32	32	93
Stud-I/I-41	7.0	8.0	32	32	93	7	8	32	32	93
Stud-I/I-42	7.0	7.5	32	32	93	7	8	32	32	93
Stud-I/I-43	8.0	7.5	32	32	93	7.5	7.5	32	32	93
Stud-I/I-44	7.5	7.0	32	32	93	7	8	32	32	93
Stud-I/I-45	7.5	7.5	32	32	93	7.5	8	32	32	93
Stud-I/I-46	7.0	8.0	32	32	93	7	8	32	32	93
Stud-I/I-47	7.5	7.5	32	32	93	7.5	7.5	32	32	93
Stud-I/I-48	7.0	8.0	32	32	93	7	7.5	32	32	93
Stud-I/I-49	7.5	7.5	32	32	93	7.5	7.5	32	32	93
Stud-I/I-50	7.5	7.0	32	32	93	7.5	7	32	32	93
Stud-I/I-51	7.0	7.5	32	32	93	7	8	32	32	93
Stud-I/I-52	7.0	8.0	32	32	93	7	8	32	32	93
Stud-I/I-53	7.0	8.0	32	32	93	7	8	32	32	93
Stud-I/I-54	7.0	8.0	32	32	93	7	8	32	32	93
Stud-I/I-55	7.0	7.0	32	32	93	7	7	32	32	93
Stud-I/I-56	7.0	8.0	32	32	93	7	8	32	32	93
Stud-I/I-57	6.5	8.0	32	32	93	7.5	8	32	32	93
Stud-I/I-58	7.0	8.0	32	32	93	7	7.5	32	32	93
Stud-I/I-59	7.0	7.5	32	32	93	7	7	32	32	93
Stud-I/I-60	7.0	7.5	32	32	93	7	7.5	32	32	93
Stud-I/I-61	7.5	8.0	32	32	93	7.5	8	32	32	93
Stud-I/I-62	7.0	8.0	32	32	93	7	8	32	32	93
Stud-I/I-63	7.0	6.0	32	32	91	7	6	32	32	91
Stud-I/I-64	7.0	6.0	32	32	91	7	6	32	32	91
Stud-I/I-65	7.0	6.0	32	32	91	7	6	32	32	91
Stud-I/I-66	7.0	6.0	32	32	91	7	6	32	32	91
Stud-I/I-67	7.0	6.0	32	32	91	7	6	32	32	91
Stud-I/I-68	7.0	6.0	32	32	91	7	6	32	32	91

1 kN = 224.8 lbs, 1 N = 0.2248 lbs, 1 mm = 0.0394 in., 1 MPa = 0.145 ksi

Table A5: Stiffener Dimensions (Stud-Intermediate-Outside)

Test Designation	Left Hand Stiffener					Right Hand Stiffener				
	lip1 (mm)	lip2 (mm)	flange1 (mm)	flange2 (mm)	web (mm)	lip1 (mm)	lip2 (mm)	flange1 (mm)	flange2 (mm)	web (mm)
Stud-I/O-1	12	12	42	42	91	12	12	42	42	91
Stud-I/O-2	12	12	42	42	91	12	13	42	42	91
Stud-I/O-3	11	12	42	42	94	12	12	42	42	94
Stud-I/O-4	11	12	42	42	93	11	12	42	42	94
Stud-I/O-5	7	7.5	33	33	93	7	7.5	33	33	93
Stud-I/O-6	7	7.5	33	33	93	7	7.5	33	33	93
Stud-I/O-7	7	8	33	33	93	7	8	33	33	93
Stud-I/O-8	7	8	33	33	93	7	8	33	33	93
Stud-I/O-9	7	7.5	33	33	93	7	7.5	33	33	93
Stud-I/O-10	7	7.5	33	33	93	7	7.5	33	33	93
Stud-I/O-11	7.5	7.5	33	33	93	7.5	7.5	33	33	93
Stud-I/O-12	7.5	7.5	33	33	93	7.5	7.5	33	33	93
Stud-I/O-13	7.5	7.5	33	33	93	7.5	7.5	33	33	93
Stud-I/O-14	7.5	7.5	33	33	93	7.5	7.5	33	33	93

1 kN = 224.8 lbs, 1 N = 0.2248 lbs, 1 mm = 0.0394 in., 1 MPa = 0.145 ksi

Table A6: Stiffener Dimensions (Track-End-Inside)

Test Designation	Left Hand Stiffener			Right Hand Stiffener		
	flange1 (mm)	flange2 (mm)	web (mm)	flange1 (mm)	flange2 (mm)	web (mm)
Track-E/I-1	32	32	93	32	32	93
Track-E/I-2	33	33	93	32	32	93
Track-E/I-3	32	32	94	32	32	94
Track-E/I-4	33	32	93	32	32	93
Track-E/I-5	32	32	93	32	32	92
Track-E/I-6	32	31.5	93	32	32	93
Track-E/I-7	33	32	93	32	32	93
Track-E/I-8	32	32	93	32	32	93
Track-E/I-9	32	32	93	32	32	93
Track-E/I-10	32	32	93	33	32	93
Track-E/I-11	32	32	92	32	32	93
Track-E/I-12	32	32	92	32	32	92
Track-E/I-13	32	32.5	92	32	32.5	92
Track-E/I-14	32	32	93	31	32	93
Track-E/I-15	32	32	92	32	32	92

1 kN = 224.8 lbs, 1 N = 0.2248 lbs, 1 mm = 0.0394 in., 1 MPa = 0.145 ksi

Table A7: Stiffener Dimensions (Track-End-Outside)

Test Designation	Left Hand Stiffener			Right Hand Stiffener		
	flange1 (mm)	flange2 (mm)	web (mm)	flange1 (mm)	flange2 (mm)	web (mm)
Track-E/O-1	32	32	93	32	32	92
Track-E/O-2	32	32	93	32	32	93
Track-E/O-3	33	32	94	32	32	94
Track-E/O-4	32	31.5	93	31.5	32	93
Track-E/O-5	32	31.5	92	32	32	93
Track-E/O-6	32	32	93	32	32	93
Track-E/O-7	32	32	92.5	32	32	93
Track-E/O-8	32	32	93	32	32	93
Track-E/O-9	32	33	95	33	33	95
Track-E/O-10	32	33	95	32	33	95
Track-E/O-11	32	34	95	33	33	96
Track-E/O-12	33	33	96	33	33	96
Track-E/O-13	34	30	96	32	33	96
Track-E/O-14	34	30	96	30	34	97
Track-E/O-15	33	33	97	33	33	97
Track-E/O-16	33	33	97	33	33	97
Track-E/O-17	32.5	32.5	96	32.5	32.5	96
Track-E/O-18	32.5	32.5	96	32.5	32.5	96
Track-E/O-19	32.5	33	97	32.5	33	97
Track-E/O-20	32.5	33	97	32.5	33	97

1 kN = 224.8 lbs, 1 N = 0.2248 lbs, 1 mm = 0.0394 in., 1 MPa = 0.145 ksi

Table A8: Stiffener Dimensions (Track-Intermediate-Inside)

Test Designation	Left Hand Stiffener			Right Hand Stiffener		
	flange1 (mm)	flange2 (mm)	web (mm)	flange1 (mm)	flange2 (mm)	web (mm)
Track-I/I-1	32	33	96	32	33	96
Track-I/I-2	32	33	96	32	33	96
Track-I/I-3	33	32	97	32	33	97
Track-I/I-4	32	33	97	32	33	97
Track-I/I-5	33	33	96	32	33	96
Track-I/I-6	32.5	32.5	96	32.5	32.5	96
Track-I/I-7	32	33	96	32	33	96
Track-I/I-8	32	33	96	32	33	96

1 kN = 224.8 lbs, 1 N = 0.2248 lbs, 1 mm = 0.0394 in., 1 MPa = 0.145 ksi

Table A9: Stiffener Dimensions (Track-Intermediate-Outside)

Test Designation	Left Hand Stiffener			Right Hand Stiffener		
	flange1 (mm)	flange2 (mm)	web (mm)	flange1 (mm)	flange2 (mm)	web (mm)
Track-I/O-1	30	33	98	30	33	98
Track-I/O-2	30	33	98	30	33	98
Track-I/O-3	32	33	97	32	33	97
Track-I/O-4	33	33	97	33	33	97
Track-I/O-5	32.5	32.5	96	32	33	96
Track-I/O-6	32.5	32.5	96	32.5	32.5	96
Track-I/O-7	32.5	32.5	97	32.5	32.5	97
Track-I/O-8	32	33	97	32	33	97

1 kN = 224.8 lbs, 1 N = 0.2248 lbs, 1 mm = 0.0394 in., 1 MPa = 0.145 ksi

APPENDIX B:

TESTED CAPACITIES AND CALCULATED PROPERTIES

Table B1: Tested Capacities and Calculated Properties (Stud-End-Inside)

| Test Designation | Avg. Test Load per Stiffener (kN) | Joist | | Stiffener | | | Screw Pattern | Top Screw Location |
		Depth (mm)	Material Number	Material Number	Avg. Gross Area (mm^2)	Avg. Effective Area (mm^2)		
Stud-E/I-1	19.74	203	J1	S3	133.7	75.1	3V	h/4
Stud-E/I-2	20.85	203	J1	S3	135.5	76.9	3V	h/4
Stud-E/I-3	17.57	254	J6	S3	134.0	75.8	3V	h/4
Stud-E/I-4	16.82	254	J6	S3	133.5	75.2	3V	h/4
Stud-E/I-5	22.20	254	J6	S3	135.3	76.2	3V	h/4
Stud-E/I-6	23.43	254	J6	S3	134.6	75.3	3V	h/4
Stud-E/I-7	23.39	254	J6	S3	133.2	75.1	3V	h/4
Stud-E/I-8	23.37	254	J6	S3	132.8	74.9	3V	h/4
Stud-E/I-9	23.10	297	J9	S5	139.6	78.6	3V	h/4
Stud-E/I-10	23.98	297	J9	S5	140.1	79.6	3V	h/4
Stud-E/I-11	21.42	305	J11	S3	133.7	75.7	3V	h/4
Stud-E/I-12	20.28	305	J11	S3	132.4	74.6	3V	h/4
Stud-E/I-13	22.70	305	J11	S5	138.6	81.1	3V	h/4
Stud-E/I-14	23.40	330	J15	S5	137.9	78.8	4V	h/5
Stud-E/I-15	20.89	330	J15	S5	139.0	79.0	4V	h/5
Stud-E/I-16	21.66	356	J16	S3	132.4	74.8	4V	h/5
Stud-E/I-17	21.26	356	J16	S3	132.2	74.5	4V	h/5
Stud-E/I-18	18.89	305	J11	S5	138.6	81.1	3V	h/4
Stud-E/I-19	21.30	254	J6	S1	129.8	70.5	3V	h/4
Stud-E/I-20	20.16	254	J6	S1	129.8	70.5	3V	h/4
Stud-E/I-21	23.13	254	J6	S1	129.8	70.5	3V	h/4
Stud-E/I-22	21.96	254	J6	S1	129.0	71.9	3V	h/4
Stud-E/I-23	19.29	254	J6	S1	129.4	71.2	3V	h/4
Stud-E/I-24	17.32	254	J6	S1	129.0	71.9	3V	h/4
Stud-E/I-25	19.20	254	J6	S1	129.8	70.5	4H	h/4
Stud-E/I-26	24.15	254	J6	S1	129.8	70.5	4H	h/4
Stud-E/I-27	20.79	254	J6	S1	129.8	70.5	4H	h/4
Stud-E/I-28	24.54	254	J6	S1	129.0	71.9	4H	h/4
Stud-E/I-29	19.77	254	J6	S1	129.8	70.5	4H	h/4
Stud-E/I-30	18.03	254	J6	S1	129.0	71.9	4H	h/4
Stud-E/I-31	19.29	203	J2	S1	130.6	72.0	2H	h/2
Stud-E/I-32	19.59	203	J2	S1	130.6	72.0	2H	h/2
Stud-E/I-33	18.27	203	J2	S1	130.6	72.0	2H	h/2
Stud-E/I-34	17.73	203	J2	S1	130.6	72.0	2H	h/2
Stud-E/I-35	17.76	203	J2	S1	130.6	72.0	2H	h/2
Stud-E/I-36	15.72	203	J2	S1	130.6	72.0	2H	h/2
Stud-E/I-37	17.31	203	J2	S1	130.6	72.0	2V	h/4
Stud-E/I-38	18.81	203	J2	S1	130.6	72.0	2V	h/4

Stud-E/I-39	19.74	203	J2	S1	130.6	72.0	2V	h/4
Stud-E/I-40	17.46	203	J2	S1	130.6	72.0	2V	h/4
Stud-E/I-41	17.79	203	J2	S1	130.6	72.0	2V	h/4
Stud-E/I-42	17.58	203	J2	S1	130.6	72.0	2V	h/4
Stud-E/I-43	17.04	203	J2	S1	130.6	72.0	3V	h/4
Stud-E/I-44	20.40	203	J2	S1	130.6	72.0	3V	h/4
Stud-E/I-45	22.11	203	J2	S1	130.2	72.7	3V	h/4
Stud-E/I-46	22.56	203	J2	S1	130.2	72.7	3V	h/4
Stud-E/I-47	22.70	305	J12	S5	217.7	75.3	3V	h/4
Stud-E/I-48	21.19	305	J15	S2	130.2	72.5	2H	h/2
Stud-E/I-49	20.82	305	J16	S3	130.2	71.6	3V	h/4
Stud-E/I-50	33.38	203	J5	S7	179.3	116.9	3V	h/4
Stud-E/I-51	34.35	203	J5	S7	179.3	116.9	3V	h/4
Stud-E/I-52	31.20	254	J8	S7	179.3	116.9	3V	h/4
Stud-E/I-53	32.10	254	J8	S7	179.3	116.9	3V	h/4
Stud-E/I-54	35.70	203	J5	S7	179.3	116.9	3V	h/4
Stud-E/I-55	35.10	203	J5	S7	179.3	116.9	3V	h/4
Stud-E/I-56	37.43	254	J8	S7	179.5	117.5	3V	h/4
Stud-E/I-57	35.78	254	J8	S7	179.3	116.9	3V	h/4
Stud-E/I-58	32.95	305	J14	S7	179.3	116.9	3V	h/4
Stud-E/I-59	32.40	305	J14	S7	179.8	118.1	3V	h/4
Stud-E/I-60	35.70	305	J14	S7	179.5	117.5	3V	h/4
Stud-E/I-61	33.70	305	J14	S7	179.8	118.1	3V	h/4
Stud-E/I-62	56.60	305	J10	S10	240.8	194.1	3V	h/12
Stud-E/I-63	19.30	305	J10	S4	137.8	80.9	3V	h/12
Stud-E/I-64	62.15	305	J10	S10	240.8	194.1	3V	h/6
Stud-E/I-65	18.50	305	J10	S4	137.8	80.9	3V	h/6
Stud-E/I-66	60.20	305	J10	S10	240.8	194.1	3V	h/4
Stud-E/I-67	20.65	305	J10	S4	137.8	80.9	3V	h/4
Stud-E/I-68	58.25	203	J3	S10	240.0	192.6	3V	h/12
Stud-E/I-69	19.70	203	J3	S4	137.8	80.9	3V	h/12
Stud-E/I-70	57.05	203	J3	S10	240.0	192.6	3V	h/6
Stud-E/I-71	17.20	203	J3	S4	137.6	80.6	3V	h/6
Stud-E/I-72	58.45	203	J3	S10	240.8	194.1	3V	h/4
Stud-E/I-73	20.95	203	J3	S4	137.8	80.9	3V	h/4
Stud-E/I-74	56.05	203	J3	S10	240.8	194.2	4H	h/12
Stud-E/I-75	19.25	203	J3	S4	137.8	80.9	4H	h/12
Stud-E/I-76	58.40	203	J3	S10	240.4	193.1	4H	h/6
Stud-E/I-77	18.15	203	J3	S4	137.8	80.9	4H	h/6
Stud-E/I-78	61.85	203	J3	S10	239.3	191.0	4H	h/4
Stud-E/I-79	19.40	203	J3	S4	137.8	80.9	4H	h/4
Stud-E/I-80	60.50	305	J10	S10	241.2	194.9	4H	h/12
Stud-E/I-81	17.85	305	J10	S4	137.8	80.9	4H	h/12

Stud-E/I-82	63.95	305	J10	S10	240.8	194.2	4H	h/6
Stud-E/I-83	19.30	305	J10	S4	137.8	80.9	4H	h/6
Stud-E/I-84	59.35	305	J10	S10	241.2	194.9	4H	h/4
Stud-E/I-85	22.70	305	J10	S4	137.8	80.9	4H	h/4
Stud-E/I-86	55.10	305	J13	S10	240.4	193.4	4H	h/12
Stud-E/I-87	20.30	305	J13	S4	137.8	80.9	4H	h/12
Stud-E/I-88	60.15	305	J13	S10	240.8	194.1	4H	h/6
Stud-E/I-89	19.10	305	J13	S4	137.8	80.9	4H	h/6
Stud-E/I-90	61.45	305	J13	S10	240.8	194.2	4H	h/4
Stud-E/I-91	24.37	305	J13	S4	137.8	80.9	4H	h/4
Stud-E/I-92	59.10	305	J13	S10	240.8	194.1	3V	h/12
Stud-E/I-93	19.65	305	J13	S4	137.4	80.2	3V	h/12
Stud-E/I-94	65.00	305	J13	S10	241.2	194.9	3V	h/6
Stud-E/I-95	18.65	305	J13	S4	137.8	80.9	3V	h/6
Stud-E/I-96	62.85	305	J13	S10	240.4	193.4	3V	h/4
Stud-E/I-97	23.60	305	J13	S4	137.8	80.9	3V	h/4
Stud-E/I-98	54.00	203	J4	S10	239.7	191.8	3V	h/12
Stud-E/I-99	23.40	203	J4	S4	137.8	80.9	3V	h/12
Stud-E/I-100	54.60	203	J4	S10	241.2	194.9	3V	h/6
Stud-E/I-101	21.85	203	J4	S4	137.6	80.5	3V	h/6
Stud-E/I-102	65.60	203	J4	S10	239.3	191.0	3V	h/4
Stud-E/I-103	35.15	203	J4	S4	137.8	80.9	3V	h/4
Stud-E/I-104	58.40	203	J4	S10	241.2	194.9	4H	h/12
Stud-E/I-105	23.70	203	J4	S4	137.8	80.9	4H	h/12
Stud-E/I-106	52.10	203	J4	S10	240.8	194.1	4H	h/6
Stud-E/I-107	22.55	203	J4	S4	137.4	80.2	4H	h/6
Stud-E/I-108	61.40	203	J4	S10	240.8	194.1	4H	h/4
Stud-E/I-109	19.35	203	J4	S4	137.8	80.9	4H	h/4

1 kN = 224.8 lbs, 1 N = 0.2248 lbs, 1 mm = 0.0394 in., 1 MPa = 0.145 ksi

Table B2: Tested Capacities and Calculated Properties (Stud-End-Outside)

Test Designation	Avg. Test Load per Stiffener (kN)	Joist		Stiffener			Screw Pattern	Top Screw Location
		Depth (mm)	Material Number	Material Number	Avg. Gross Area (mm^2)	Avg. Effective Area (mm^2)		
Stud-E/O-1	18.52	203	J1	S3	135.9	75.0	3V	h/4
Stud-E/O-2	18.15	203	J1	S3	135.9	75.0	3V	h/4
Stud-E/O-3	24.57	203	J2	S1	129.8	72.0	3V	h/4
Stud-E/O-4	21.69	203	J2	S1	129.8	72.0	3V	h/4
Stud-E/O-5	29.10	330	J15	S6	169.6	104.3	4V	h/5
Stud-E/O-6	25.50	330	J15	S6	170.0	105.8	4V	h/5
Stud-E/O-7	43.80	356	J16	S8	227.4	172.9	4V	h/5
Stud-E/O-8	43.50	356	J16	S8	227.4	172.9	4V	h/5

Stud-E/O-9	58.20	356	J16	S9	275.0	205.8	4V	h/5
Stud-E/O-10	56.10	356	J16	S9	275.8	207.4	4V	h/5
Stud-E/O-11	62.70	254	J7	S9	277.2	207.6	4V	h/5
Stud-E/O-12	66.30	254	J7	S9	277.2	207.6	4V	h/5
Stud-E/O-13	41.40	203	J5	S7	179.3	116.9	3V	h/4
Stud-E/O-14	43.05	203	J5	S7	179.3	116.9	3V	h/4
Stud-E/O-15	35.03	254	J8	S7	179.8	118.1	3V	h/4
Stud-E/O-16	41.40	254	J8	S7	179.8	118.1	3V	h/4
Stud-E/O-17	40.95	203	J5	S7	179.3	116.9	3V	h/4
Stud-E/O-18	37.58	203	J5	S7	179.3	116.9	3V	h/4
Stud-E/O-19	34.58	254	J8	S7	179.8	118.1	3V	h/4
Stud-E/O-20	38.25	305	J14	S7	179.3	116.9	3V	h/4
Stud-E/O-21	39.25	305	J14	S7	179.8	118.1	3V	h/4

1 kN = 224.8 lbs, 1 N = 0.2248 lbs, 1 mm = 0.0394 in., 1 MPa = 0.145 ksi

Table B3: Tested Capacities and Calculated Properties (Stud-Intermediate-Inside)

| Test Designation | Avg. Test Load per Stiffener (kN) | Joist | | Stiffener | | | Screw Pattern | Top Screw Location |
		Depth (mm)	Material Number	Material Number	Avg. Gross Area (mm^2)	Avg. Effective Area (mm^2)		
Stud-I/I-1	25.02	203	J1	S3	135.9	75.1	3V	h/4
Stud-I/I-2	24.09	203	J1	S3	135.9	75.0	3V	h/4
Stud-I/I-3	24.20	254	J7	S3	134.2	74.8	3V	h/4
Stud-I/I-4	21.57	254	J7	S3	133.8	74.8	3V	h/4
Stud-I/I-5	24.24	305	J11	S3	132.4	74.9	3V	h/4
Stud-I/I-6	20.22	305	J11	S3	133.5	75.0	3V	h/4
Stud-I/I-7	22.73	356	J16	S3	134.6	74.9	3V	h/4
Stud-I/I-8	22.24	356	J16	S3	133.7	75.0	3V	h/4
Stud-I/I-9	20.40	203	J2	S1	129.8	72.0	3V	h/4
Stud-I/I-10	25.32	203	J2	S1	130.2	72.7	3V	h/4
Stud-I/I-11	39.53	203	J5	S7	179.3	116.9	3V	h/4
Stud-I/I-12	47.85	203	J5	S7	179.3	116.9	3V	h/4
Stud-I/I-13	48.53	203	J5	S7	179.3	116.9	3V	h/4
Stud-I/I-14	45.75	203	J5	S7	179.3	116.9	3V	h/4
Stud-I/I-15	59.75	305	J10	S10	240.4	193.3	3V	h/4
Stud-I/I-16	22.00	305	J10	S4	137.8	80.9	3V	h/4
Stud-I/I-17	61.75	305	J10	S10	240.8	194.1	3V	h/4
Stud-I/I-18	22.40	305	J10	S4	137.6	80.6	3V	h/4
Stud-I/I-19	59.90	305	J10	S10	240.8	194.2	3V	h/4
Stud-I/I-20	22.00	305	J10	S4	137.6	80.5	3V	h/4
Stud-I/I-21	61.85	203	J3	S10	241.5	195.7	3V	h/4
Stud-I/I-22	24.25	203	J3	S4	137.8	80.9	3V	h/4

129

Stud-I/I-23	61.05	203	J3	S10	240.4	193.4	3V	h/4
Stud-I/I-24	24.05	203	J3	S4	137.4	80.2	3V	h/4
Stud-I/I-25	59.25	203	J3	S10	240.0	192.6	3V	h/4
Stud-I/I-26	24.30	203	J3	S4	137.6	80.6	3V	h/4
Stud-I/I-27	59.70	203	J3	S10	240.8	194.2	4H	h/4
Stud-I/I-28	22.75	203	J3	S4	137.8	80.9	4H	h/4
Stud-I/I-29	60.00	203	J3	S10	240.8	194.1	4H	h/4
Stud-I/I-30	26.10	203	J3	S4	137.8	80.9	4H	h/4
Stud-I/I-31	58.00	203	J3	S10	240.0	192.6	4H	h/4
Stud-I/I-32	25.20	203	J3	S4	137.8	80.9	4H	h/4
Stud-I/I-33	60.05	305	J10	S10	240.8	194.1	4H	h/4
Stud-I/I-34	23.75	305	J10	S4	137.4	80.2	4H	h/4
Stud-I/I-35	62.80	305	J10	S10	241.2	194.9	4H	h/4
Stud-I/I-36	24.05	305	J10	S4	137.8	80.9	4H	h/4
Stud-I/I-37	64.00	305	J10	S10	240.8	194.1	4H	h/4
Stud-I/I-38	27.20	305	J10	S4	137.8	80.9	4H	h/4
Stud-I/I-39	63.55	305	J13	S10	240.4	193.4	4H	h/4
Stud-I/I-40	27.15	305	J13	S4	137.8	80.9	4H	h/4
Stud-I/I-41	69.90	305	J13	S10	240.8	194.1	4H	h/4
Stud-I/I-42	28.70	305	J13	S4	137.6	80.6	4H	h/4
Stud-I/I-43	68.55	305	J13	S10	241.2	194.9	4H	h/4
Stud-I/I-44	29.25	305	J13	S4	137.6	80.6	4H	h/4
Stud-I/I-45	67.00	305	J13	S10	241.2	194.9	3V	h/4
Stud-I/I-46	26.80	305	J13	S4	137.8	80.9	3V	h/4
Stud-I/I-47	67.40	305	J13	S10	240.8	194.2	3V	h/4
Stud-I/I-48	29.10	305	J13	S4	137.6	80.6	3V	h/4
Stud-I/I-49	69.75	305	J13	S10	240.8	194.2	3V	h/4
Stud-I/I-50	30.00	305	J13	S4	137.4	80.2	3V	h/4
Stud-I/I-51	65.65	203	J4	S10	240.4	193.3	3V	h/4
Stud-I/I-52	34.95	203	J4	S4	137.8	80.9	3V	h/4
Stud-I/I-53	69.55	203	J4	S10	240.8	194.1	3V	h/4
Stud-I/I-54	34.60	203	J4	S4	137.8	80.9	3V	h/4
Stud-I/I-55	57.60	203	J4	S10	239.3	191.0	3V	h/4
Stud-I/I-56	23.05	203	J4	S4	137.8	80.9	3V	h/4
Stud-I/I-57	66.40	203	J4	S10	240.8	193.9	4H	h/4
Stud-I/I-58	38.70	203	J4	S4	137.6	80.6	4H	h/4
Stud-I/I-59	67.40	203	J4	S10	239.7	191.8	4H	h/4
Stud-I/I-60	36.00	203	J4	S4	137.4	80.2	4H	h/4
Stud-I/I-61	69.65	203	J4	S10	241.5	195.7	4H	h/4
Stud-I/I-62	32.60	203	J4	S4	137.8	80.9	4H	h/4
Stud-I/I-63	22.23	336	J2	S1	130.6	72.0	3V	h/4
Stud-I/I-64	29.76	336	J2	S1	130.6	72.0	3V	h/4
Stud-I/I-65	23.58	336	J2	S1	130.6	72.0	3V	h/4

Stud-I/I-66	22.14	336	J2	S1	130.6	72.0	3V	h/4
Stud-I/I-67	22.23	336	J2	S1	130.6	72.0	3V	h/4
Stud-I/I-68	23.73	336	J2	S1	130.6	72.0	3V	h/4

1 kN = 224.8 lbs, 1 N = 0.2248 lbs, 1 mm = 0.0394 in., 1 MPa = 0.145 ksi

Table B4: Tested Capacities and Calculated Properties (Stud-Intermediate-Outside)

| Test Designation | Avg. Test Load per Stiffener (kN) | Joist | | Stiffener | | | Screw Pattern | Top Screw Location |
		Depth (mm)	Material Number	Material Number	Avg. Gross Area (mm^2)	Avg. Effective Area (mm^2)		
Stud-I/O-1	30.60	330	J15	S6	168.7	104.2	4V	h/5
Stud-I/O-2	22.50	330	J15	S6	169.1	105.8	4V	h/5
Stud-I/O-3	73.80	356	J16	S9	276.5	206.0	4V	h/5
Stud-I/O-4	66.60	356	J16	S9	275.0	204.3	4V	h/5
Stud-I/O-5	39.60	203	J5	S7	179.3	116.9	3V	h/4
Stud-I/O-6	37.95	203	J5	S7	179.3	116.9	3V	h/4
Stud-I/O-7	41.93	254	J8	S7	179.8	118.1	3V	h/4
Stud-I/O-8	39.60	254	J8	S7	179.8	118.1	3V	h/4
Stud-I/O-9	38.63	203	J5	S7	179.3	116.9	3V	h/4
Stud-I/O-10	39.75	203	J5	S7	179.3	116.9	3V	h/4
Stud-I/O-11	43.95	254	J8	S7	179.8	118.1	3V	h/4
Stud-I/O-12	43.88	254	J8	S7	179.8	118.1	3V	h/4
Stud-I/O-13	44.95	305	J14	S7	179.8	118.1	3V	h/4
Stud-I/O-14	45.55	305	J14	S7	179.8	118.1	3V	h/4

1 kN = 224.8 lbs, 1 N = 0.2248 lbs, 1 mm = 0.0394 in., 1 MPa = 0.145 ksi

Table B5: Tested Capacities and Calculated Properties (Track-End-Inside)

| Test Designation | Avg. Test Load per Stiffener (kN) | Joist | | Stiffener | | | Screw Pattern | Top Screw Location |
		Depth (mm)	Material Number	Material Number	Avg. Gross Area (mm^2)	Avg. Effective Area (mm^2)		
Track-E/I-1	16.54	203	J1	T2	130.5	45.2	3V	h/4
Track-E/I-2	18.23	203	J1	T2	131.3	45.2	3V	h/4
Track-E/I-3	17.82	254	J1	T2	131.3	45.2	3V	h/4
Track-E/I-4	20.76	254	J1	T2	130.9	45.2	3V	h/4
Track-E/I-5	23.82	254	J1	T2	130.0	45.2	3V	h/4
Track-E/I-6	20.12	254	J6	T2	130.2	45.2	3V	h/4
Track-E/I-7	19.74	254	J6	T2	130.9	45.2	3V	h/4
Track-E/I-8	21.82	279	J9	T3	133.4	45.9	3V	h/4
Track-E/I-9	16.65	279	J9	T3	133.4	45.9	3V	h/4
Track-E/I-10	26.51	305	J11	T2	130.9	45.2	3V	h/4
Track-E/I-11	26.66	305	J11	T2	130.0	45.2	3V	h/4
Track-E/I-12	22.90	330	J15	T3	132.6	45.9	4V	h/5

Test Designation								
Track-E/I-13	23.85	330	J15	T3	133.0	45.9	4V	h/5
Track-E/I-14	23.11	356	J16	T2	130.0	45.2	4V	h/5
Track-E/I-15	21.18	356	J16	T2	129.6	45.2	4V	h/5

1 kN = 224.8 lbs, 1 N = 0.2248 lbs, 1 mm = 0.0394 in., 1 MPa = 0.145 ksi

Table B6: Tested Capacities and Calculated Properties (Track-End-Outside)

Test Designation	Avg. Test Load per Stiffener (kN)	Joist		Stiffener			Screw Pattern	Top Screw Location
		Depth (mm)	Material Number	Material Number	Avg. Gross Area (mm^2)	Avg. Effective Area (mm^2)		
Track-E/O-1	21.51	203	J1	T2	130.0	45.2	3V	h/4
Track-E/O-2	22.57	203	J1	T2	130.5	45.2	3V	h/4
Track-E/O-3	19.41	254	J6	T2	131.7	45.2	3V	h/4
Track-E/O-4	19.92	254	J6	T2	130.0	45.2	3V	h/4
Track-E/O-5	19.80	305	J11	T2	129.8	45.2	3V	h/4
Track-E/O-6	23.67	305	J11	T2	130.5	45.2	3V	h/4
Track-E/O-7	19.81	356	J16	T2	130.2	45.2	4V	h/4
Track-E/O-8	23.24	356	J16	T2	130.5	45.2	4V	h/4
Track-E/O-9	17.10	330	J15	T1	124.2	47.6	4V	h/4
Track-E/O-10	15.00	330	J15	T1	123.8	47.6	4V	h/4
Track-E/O-11	41.40	356	J16	T6	225.4	141.2	4V	h/4
Track-E/O-12	48.90	356	J16	T6	226.2	141.3	4V	h/4
Track-E/O-13	66.90	356	J16	T7	276.9	212.9	4V	h/4
Track-E/O-14	67.80	356	J16	T7	276.9	212.9	4V	h/4
Track-E/O-15	35.25	203	J5	T5	172.7	84.1	3V	h/4
Track-E/O-16	35.33	203	J5	T5	172.7	84.1	3V	h/4
Track-E/O-17	36.98	254	J8	T5	170.6	84.0	3V	h/4
Track-E/O-18	33.53	254	J8	T5	170.6	84.0	3V	h/4
Track-E/O-19	32.35	305	J14	T5	172.2	84.1	3V	h/4
Track-E/O-20	34.20	305	J14	T5	172.2	84.1	3V	h/4

1 kN = 224.8 lbs, 1 N = 0.2248 lbs, 1 mm = 0.0394 in., 1 MPa = 0.145 ksi

Table B7: Tested Capacities and Calculated Properties (Track-Intermediate-Inside)

Test Designation	Avg. Test Load per Stiffener (kN)	Joist		Stiffener			Screw Pattern	Top Screw Location
		Depth (mm)	Material Number	Material Number	Avg. Gross Area (mm^2)	Avg. Effective Area (mm^2)		
Track-I/I-1	33.15	254	J8	T5	170.6	84.0	3V	h/4
Track-I/I-2	37.43	254	J8	T5	170.6	84.0	3V	h/4
Track-I/I-3	31.28	254	J8	T5	171.6	84.0	3V	h/4
Track-I/I-4	36.83	254	J8	T5	171.6	84.0	3V	h/4
Track-I/I-5	34.60	305	J14	T5	171.1	84.0	3V	h/4
Track-I/I-6	33.25	305	J14	T5	170.6	84.0	3V	h/4

| Track-I/I-7 | 35.95 | 305 | J14 | T5 | 170.6 | 84.0 | 3V | h/4 |
| Track-I/I-8 | 35.95 | 305 | J14 | T5 | 170.6 | 84.0 | 3V | h/4 |

1 kN = 224.8 lbs, 1 N = 0.2248 lbs, 1 mm = 0.0394 in., 1 MPa = 0.145 ksi

Table B8: Tested Capacities and Calculated Properties (Track-Intermediate-Outside)

| Test Designation | Avg. Test Load per Stiffener (kN) | Joist | | Stiffener | | | Screw Pattern | Top Screw Location |
		Depth (mm)	Material Number	Material Number	Avg. Gross Area (mm^2)	Avg. Effective Area (mm^2)		
Track-I/O-1	28.80	330	J15	T4	169.0	89.7	4V	h/5
Track-I/O-2	25.20	330	J15	T4	169.0	89.7	4V	h/5
Track-I/O-3	42.08	203	J5	T5	171.6	84.0	3V	h/4
Track-I/O-4	36.83	203	J5	T5	172.7	84.1	3V	h/4
Track-I/O-5	36.68	254	J8	T5	170.6	84.0	3V	h/4
Track-I/O-6	35.18	254	J8	T5	170.6	84.0	3V	h/4
Track-I/O-7	35.85	305	J14	T5	171.6	84.0	3V	h/4
Track-I/O-8	40.45	305	J14	T5	171.6	84.0	3V	h/4

1 kN = 224.8 lbs, 1 N = 0.2248 lbs, 1 mm = 0.0394 in., 1 MPa = 0.145 ksi

APPENDIX C – WEB BUCKLING MEASUREMENTS

Table C1: Measured Deflected Shape at Pre-load = 0.81 kN
Deflections Relative to Unloaded Shape (Dimensions in mm)

		Horizontal Grid Position								
		I	H	G	F	E	D	C	B	A
	0.0	0.3	0.3	0.2	0.2	0.2	0.2	0.2	0.2	0.1
	12.5	0.3	0.3	0.3	0.3	0.2	0.4	0.4	0.5	0.6
	25.0	0.3	0.4	0.3	0.4	0.5	0.6	0.7	0.5	1.0
	37.5	0.4	0.4	0.5	0.5	0.7	0.8	0.9	1.1	1.3
Vertical Position (mm)	**50.0**	0.5	0.5	0.6	0.6	0.9	0.9	1.1	1.3	1.5
	62.5	0.5	0.5	0.7	0.8	0.9	1.1	1.2	1.4	1.7
	75.0	0.5	0.6	0.7	0.8	1.0	1.2	1.3	1.5	1.8
	87.5	0.6	0.7	0.8	1.0	1.1	1.3	1.5	1.8	1.8
	100.0	0.5	0.7	0.8	1.1	1.1	1.3	1.5	1.6	1.8
	112.5	0.6	0.7	0.9	1.0	1.2	1.4	1.5	1.7	1.9
	125.0	0.6	0.8	0.9	1.2	1.2	1.3	1.6	1.8	2.0
	137.5	0.6	0.8	0.9	1.1	1.3	1.5	1.7	1.9	2.1
	150.0	0.7	0.8	1.0	1.1	1.3	1.5	1.7	1.9	2.1

Table C2: Measured Deflected Shape at Load = 11.25 kN
Deflections Relative to Pre-loaded Shape (Dimensions in mm)

		Horizontal Grid Position								
		I	H	G	F	E	D	C	B	A
	0.0	-0.2	-0.1	0.0	0.1	0.4	0.6	0.6	0.7	0.7
	12.5	-0.2	0.0	0.3	0.6	1.2	1.6	1.7	1.9	2.1
	25.0	-0.1	0.2	0.8	1.4	2.2	3.0	3.4	3.7	4.1
	37.5	0.0	0.5	1.2	2.1	3.0	3.9	4.4	4.9	5.4
Vertical Position (mm)	**50.0**	0.1	0.7	1.5	2.5	3.6	4.3	5.1	5.6	6.3
	62.5	0.2	0.8	1.7	2.7	3.7	4.5	5.3	5.9	6.6
	75.0	0.2	0.9	1.8	2.7	3.6	4.5	5.2	5.9	6.6
	87.5	0.1	0.8	1.7	2.6	3.4	4.1	4.6	5.4	6.1
	100.0	-0.1	0.6	1.4	2.1	2.9	3.7	4.1	4.6	5.3
	112.5	-0.2	0.4	1.1	1.8	2.4	2.8	3.3	3.8	4.4
	125.0	-0.4	0.1	0.7	1.2	1.9	2.2	2.7	3.0	3.4
	137.5	-0.6	-0.2	0.3	0.8	1.2	1.5	1.9	2.2	2.7
	150.0	-0.8	-0.5	-0.1	0.4	0.6	0.9	1.2	1.5	1.8

Table C3: Measured Deflected Shape at Load = 22.5 kN

Deflections Relative to Pre-loaded Shape (Dimensions in mm)

		Horizontal Grid Position								
		I	H	G	F	E	D	C	B	A
Vertical Position (mm)	0.0	-0.3	-0.2	-0.1	0.1	0.4	0.5	0.6	0.6	0.8
	12.5	-0.2	0.2	0.5	1.0	1.8	2.5	2.4	2.3	2.4
	25.0	0.1	0.6	1.4	2.3	3.4	4.4	4.7	4.7	4.9
	37.5	0.4	1.2	2.1	3.3	4.5	5.6	6.3	6.7	7.0
	50.0	0.6	1.6	2.7	3.9	5.2	6.1	7.1	7.6	8.3
	62.5	0.7	1.9	3.1	4.2	5.3	6.2	7.1	7.8	8.7
	75.0	0.8	2.0	3.1	4.2	5.2	6.0	6.9	7.6	8.4
	87.5	0.7	1.8	3.0	4.0	4.8	5.5	6.1	6.9	7.7
	100.0	0.5	1.5	2.6	3.3	4.1	4.6	5.2	5.8	6.7
	112.5	0.1	1.1	2.1	2.8	3.4	3.7	4.4	4.9	5.5
	125.0	-0.2	0.6	1.4	1.9	2.6	2.9	3.4	3.7	4.2
	137.5	-0.6	0.1	0.8	1.3	1.7	2.0	2.3	2.7	3.1
	150.0	-1.0	-0.4	0.2	0.7	1.0	1.2	1.8	2.0	2.3

Table C4: Measured Deflected Shape at Load = 33.75 kN

Deflections Relative to Pre-loaded Shape (Dimensions in mm)

		Horizontal Grid Position								
		I	H	G	F	E	D	C	B	A
Vertical Position (mm)	0.0	-0.2	-0.1	0.0	0.2	0.5	0.7	0.7	0.6	0.7
	12.5	0.1	0.4	0.7	1.2	2.1	2.9	2.8	2.5	2.6
	25.0	0.5	1.1	1.8	2.7	4.0	5.0	5.3	5.2	5.3
	37.5	0.9	1.8	2.8	3.9	5.1	6.3	7.0	7.3	7.6
	50.0	1.4	2.4	3.5	4.7	6.0	6.8	7.8	8.3	9.0
	62.5	1.8	2.9	4.0	5.2	6.2	7.1	7.8	8.6	9.4
	75.0	1.9	3.1	4.3	5.3	6.1	6.9	7.6	8.4	9.1
	87.5	2.0	3.2	4.2	5.1	5.9	6.4	6.9	7.6	8.5
	100.0	1.9	3.0	4.0	4.6	5.2	5.6	6.1	6.7	7.3
	112.5	1.6	2.7	3.6	4.1	4.4	4.9	5.1	5.6	6.2
	125.0	1.3	2.3	2.9	3.3	3.8	3.9	4.4	4.6	5.0
	137.5	1.0	1.7	2.4	2.7	2.9	3.0	3.3	3.6	4.0
	150.0	0.5	1.2	1.7	2.0	2.1	2.2	2.6	2.8	3.1

Table C5: Measured Deflected Shape at Failure Load = 41.25 kN

Deflections Relative to Pre-loaded Shape (Dimensions in mm)

Vertical Position (mm)	Horizontal Grid Position								
	I	**H**	**G**	**F**	**E**	**D**	**C**	**B**	**A**
0.0	0.4	0.3	0.4	0.4	0.6	0.6	0.5	0.3	0.3
12.5	1.5	1.7	1.9	2.1	2.9	3.5	3.2	2.8	2.7
25.0	3.2	3.6	4.0	4.8	5.9	6.9	7.0	6.7	6.6
37.5	4.9	5.5	6.3	7.3	8.5	9.6	10.0	10.2	10.4
50.0	6.7	7.5	8.4	9.5	10.7	11.6	12.4	12.9	13.6
62.5	8.2	9.3	10.3	11.4	12.5	13.6	14.7	15.4	16.6
75.0	9.6	10.7	11.8	12.9	14.0	15.2	16.3	17.4	18.5
87.5	10.8	11.9	13.1	14.1	15.3	16.5	17.6	18.8	20.1
100.0	11.7	12.8	14.0	15.0	16.3	17.5	18.8	20.0	21.4
112.5	12.3	13.4	14.7	15.7	16.9	18.1	19.4	20.7	22.1
125.0	12.6	13.4	14.8	15.8	17.5	18.5	19.8	20.9	22.3
137.5	12.6	13.7	14.9	16.0	17.2	18.4	19.5	20.6	22.0
150.0	12.4	13.5	14.6	15.7	16.8	18.1	19.1	20.0	21.4

American Iron and Steel Institute

1140 Connecticut Avenue, NW
Suite 705
Washington, DC 20036

www.steel.org

The New Steel